

Budapest University of Technology and Economics



Department of Networked Systems and Services
Laboratory of Acoustics and Studio Technologies

PhD Thesis

**A Unified Wave Field Synthesis Framework
with Application for Moving Virtual Sources**

Gergely Firtha

October 25, 2017

Gergely Firtha

*A Unified Wave Field Synthesis Framework
with Application for Moving Virtual Sources*
PhD Thesis, October 25, 2017
Supervisor: Peter Fiala

Budapest University of Technology and Economics
Laboratory of Acoustics and Studio Technologies
Department of Networked Systems and Services
Magyar Tudosok korutja 2.
1117 and Budapest

Contents

1 Theory of wave propagation and radiation problems	1
1.1 The wave equation	1
1.1.1 The homogeneous wave equation	2
1.1.2 The inhomogeneous wave equation	3
1.1.3 Boundary conditions	4
1.2 Solution of the homogeneous wave equation	6
1.2.1 Plane wave theory	6
1.2.2 The angular spectrum representation	8
1.2.3 Solution in other geometries	10
1.3 Solution of the inhomogeneous wave equation	11
1.3.1 The Green's function	11
1.3.2 Solution of the general inhomogeneous wave equation	13
1.4 Boundary integral representation of sound fields	15
1.4.1 The Kirchhoff-Helmholtz integral equation	15
1.4.2 The Simple Source Formulation	17
1.4.3 The Rayleigh integrals	19
2 High frequency approximation of wave fields and radiation problems	23
2.1 Local attributes of sound fields	23
2.1.1 The local wavenumber vector	23
2.1.2 The local wavefront curvature	25
2.1.3 High frequency gradient approximation	26
2.2 The Kirchhoff approximation	29
2.3 The stationary phase approximation	31
2.3.1 The integral approximation	32
2.3.2 Asymptotic approximation of boundary integrals	33
2.3.3 Asymptotic approximation of spectral integrals	37
3 Theory of Sound Field Synthesis	43
3.1 Implicit solution: Wave Field Synthesis	44
3.1.1 3D Wave Field Synthesis	44
3.1.2 The 2.5D Kirchhoff approximation	46
3.1.3 2.5D Wave Field Synthesis	48
3.2 Explicit solution: Spectral Division Method	55
3.2.1 3D Spectral Division Method	55
3.2.2 2.5D Spectral Division Method	58
3.2.3 Approximate explicit solution in the spatial domain	60

3.3 Relation of implicit and explicit solutions	66
3.4 Summary	69
Appendices	71
A Appendix A	73
A.1 Derivation of Green's theorem	73
B Appendix B	75
B.1 Notes on the Hessian of the phase function	75
B.1.1 Definition of the principal curvatures and principal directions .	75
B.1.2 Hessian for the SPA applied for the Rayleigh-integral	76
C Appendix C	81
C.1 Wavenumber vector of a point source pair	81
D Appendix D	83
D.1 2.5D Kirchhoff integral for a 3D point source	83
Bibliography	85

Nomenclature

c	Speed of sound
∇_x	Gradient operator. In Descartes-coordinates it is given by $\nabla_x = \frac{\partial}{\partial x} \mathbf{e}_x + \frac{\partial}{\partial y} \mathbf{e}_y + \frac{\partial}{\partial z} \mathbf{e}_z$
∇^2	Laplacian operator. In Descartes-coordinates: $\nabla^2 = \frac{\partial^2}{\partial x^2} + \frac{\partial^2}{\partial y^2} + \frac{\partial^2}{\partial z^2}$
$\nabla_x \cdot$	Divergence operator. In Descartes-coordinates: $\nabla_x \cdot = \frac{\partial}{\partial x} + \frac{\partial}{\partial y} + \frac{\partial}{\partial z}$
$\langle \mathbf{a} \cdot \mathbf{b} \rangle$	Inner product of vector \mathbf{a} and \mathbf{b} , given by $\mathbf{a}^T \mathbf{b}$
ϕ_f	Phase of the complex valued function $f(x) \in \mathbb{C}$, written in a general polar form $f(x) = A_f(x)e^{j\phi_f(x)}$

Temporal Fourier transforms: The forward and inverse temporal Fourier transform is defined as

$$F(\omega) = \mathcal{F}_t \{f(t)\} = \int_{-\infty}^{\infty} f(t)e^{-j\omega t} dt, \quad (0.1)$$

$$f(t) = \mathcal{F}_{\omega}^{-1} \{F(\omega)\} = \frac{1}{2\pi} \int_{-\infty}^{\infty} F(\omega)e^{j\omega t} d\omega. \quad (0.2)$$

Spatial Fourier transforms: Following the convention as given in e.g. [Wil99] the spatial Fourier transformed is defined with reversed exponential for the sake of a consequent physical interpretation, when applied for planar or outgoing spherical waves:

$$F(k_x) = \mathcal{F}_x \{f(x)\} = \int_{-\infty}^{\infty} f(x)e^{jk_x x} dx, \quad (0.3)$$

$$f(x) = \mathcal{F}_{k_x}^{-1} \{F(k_x)\} = \frac{1}{2\pi} \int_{-\infty}^{\infty} F(k_x)e^{-jk_x x} dk_x, \quad (0.4)$$

Theory of wave propagation and radiation problems

In this chapter the theoretical basis of sound radiation is introduced. The section starts with discussing the physics of sound propagation and radiation by deriving the formulation and solution of the governing homogeneous and inhomogeneous wave equations. Various integral representations of sound fields are presented including spectral and boundary integrals.

1.1 The wave equation

Sound is a mechanical disturbance propagating in an elastic fluid, causing an alternation in the fluid's density and pressure, as well as displacement of the medium's particles. The propagation of the disturbance is described by the acoustic wave equation.

Consider a homogeneous, elastic fluid, modeled as an ideal gas with no viscosity. In the aspect of the present thesis it is appropriate to restrict the investigation to sound propagation solely in air at room temperature.

The domain of investigation $\Omega \in \mathbb{R}^n$ where sound waves propagate is termed *sound field* hereinafter. Within this thesis usually 3 dimensional problems are investigated ($n = 3$). The acoustical quantities of the sound field are described by *dynamic field variables* in each point $\mathbf{x} \in \Omega$, at each time instant t : the vector variable *particle velocity* $\mathbf{v}(\mathbf{x}, t)$ and the scalar *instantaneous sound pressure* $p(\mathbf{x}, t)$ superimposed onto the static pressure $P_0 \approx 10^5$ Pa. The medium is quiescent, meaning that on average each particle is at rest with zero particle displacement (thus zero particle velocity) at the static pressure P_0 . The presence of sound waves causes incremental change in the instantaneous pressure and the particle velocity.

In order to apply a linear model for sound propagation two assumptions are made. Since the traveling speed of thermal diffusion is small compared to the speed of sound, it is feasible to assume that heat exchange in the wave due to compression and expansion is negligible: the state changes are modeled as adiabatic. Furthermore the alternation of the instantaneous sound pressure is small compared to the static pressure, so the non-linear adiabatic state-change characteristics can be linearized around P_0 . This latter assumption is fulfilled for pressure magnitudes below the threshold of pain of the human auditory system [GD04; Ahr12].

First the homogeneous wave equation is presented, valid for a *source-free domain*, describing merely the propagation characteristics of acoustic waves. For a more detailed derivation refer to [Ber93; MI68; Wil99; Bla00].

1.1.1 The homogeneous wave equation

The linear homogeneous wave equation may be derived by utilizing two fundamental physical principles.

- *The equation of motion:* By applying Newton's second law for an infinitesimal small volume of the fluid the connection between the particle velocity vector and the pressure field is obtained at each point at each time instant. The resulting *Euler's equation* states that the force acting on the volume due to variation in the spatial pressure distribution causes an acceleration of the volume:

$$\nabla_{\mathbf{x}} p(\mathbf{x}, t) = -\rho_0 \frac{\partial}{\partial t} \mathbf{v}(\mathbf{x}, t), \quad (1.1)$$

where $\nabla_{\mathbf{x}}$ is the gradient operator and ρ_0 is the fluid's ambient density. In room temperature for the above given static pressure $\rho_0 = 1.18 \text{ kg/m}^3$.

- *The gas law:* For adiabatic processes the change of state is governed by the relation

$$PV^\gamma = \text{constant}, \quad (1.2)$$

where $\gamma = C_P/C_V$ is the ratio of specific heats of the fluid with constant pressure and with constant volume. For air it is given as $\gamma = 1.4$. Linearization of (1.2) around the static state P_0, V_0 yields

$$dP = p(\mathbf{x}, t) = -\gamma P_0 \frac{dV}{V_0}. \quad (1.3)$$

where V_0 is the undisturbed volume. The relative change of volume dV/V_0 may be expressed by the *divergence* of the particle displacement $\nabla_{\mathbf{x}} \cdot \mathbf{u}$. Applying the definition of divergence and expressing the equation in terms of particle velocity yields

$$\frac{\partial}{\partial t} p(\mathbf{x}, t) = -\gamma P_0 \nabla_{\mathbf{x}} \cdot \mathbf{v}(\mathbf{x}, t), \quad (1.4)$$

This *continuity equation* states that the net flow of the fluid out of an infinitesimal volume results in decreased density and pressure inside the volume [AW05].

Taking the time derivative of equation (1.4) and the divergence of equation (1.1) the particle velocity may be eliminated. By using the *Laplace operator* $\nabla_{\mathbf{x}} \cdot \nabla_{\mathbf{x}} = \nabla_{\mathbf{x}}^2$ the scalar linear homogeneous wave equation is obtained for the sound pressure

$$\nabla_{\mathbf{x}}^2 p(\mathbf{x}, t) - \frac{1}{c^2} \frac{\partial^2}{\partial t^2} p(\mathbf{x}, t) = 0, \quad (1.5)$$

where $c \equiv \sqrt{\frac{\gamma P_0}{\rho_0}}$ is the speed of sound in the medium. For air in room temperature it is given as $c = 343.1 \text{ m/s}$. The instantaneous pressure may also be eliminated in

a similar manner, resulting in the vector wave equation for each component of the particle velocity

$$\nabla_{\mathbf{x}}^2 \mathbf{v}(\mathbf{x}, t) - \frac{1}{c^2} \frac{\partial^2}{\partial t^2} \mathbf{v}(\mathbf{x}, t) = \mathbf{0}, \quad (1.6)$$

valid in curl-free media, where $\nabla_{\mathbf{x}} (\nabla_{\mathbf{x}} \cdot) = \nabla_{\mathbf{x}}^2$ holds. Besides the pressure and the velocity, acoustic fields are often expressed via the scalar *velocity potential* $\varphi(\mathbf{x}, t)$, for which the acoustic wave equation also holds, and which is related to the other field variables as

$$\mathbf{v}(\mathbf{x}, t) = \nabla_{\mathbf{x}} \varphi(\mathbf{x}, t), \quad p(\mathbf{x}, t) = -\rho_0 \frac{\partial}{\partial t} \varphi(\mathbf{x}, t). \quad (1.7)$$

The wave equations fully describe the properties of acoustic wave propagation as long as the above made assumptions are fulfilled.

Equations (1.1) and (1.5) may be transformed into the angular frequency domain by performing a temporal Fourier transform according to (0.1). Applying the differentiation property of the Fourier transform to (1.1) yields the frequency domain Euler's equation,

$$\nabla_{\mathbf{x}} P(\mathbf{x}, \omega) = -j\omega \rho_0 \mathbf{V}(\mathbf{x}, \omega) \quad (1.8)$$

relating the pressure distribution of a time-harmonic sound field to the harmonic velocity vector field. By taking the Fourier transform of the wave equation (1.5), the *homogeneous Helmholtz equation* is obtained:

$$\nabla_{\mathbf{x}}^2 P(\mathbf{x}, \omega) + k^2 P(\mathbf{x}, \omega) = 0, \quad (1.9)$$

where k is the *acoustic wavenumber*, which is related to the temporal frequency through the linear *dispersion relation* $k = \frac{\omega}{c}$. Equation (1.9) must hold for every physically possible *steady-state* wave form with harmonic time-dependence for a source-free volume. In the aspect of the present thesis the time domain wave equation is rarely solved, therefore the general solution of the Helmholtz equation is presented in the followings.

1.1.2 The inhomogeneous wave equation

So far wave propagation in source-free volumes was investigated. A simple scalar disturbance of the pressure field may be included into the wave equation resulting in the time domain *inhomogeneous wave equation*

$$\nabla_{\mathbf{x}}^2 p(\mathbf{x}, t) - \frac{1}{c^2} \frac{\partial^2}{\partial t^2} p(\mathbf{x}, t) = -s(\mathbf{x}, t), \quad (1.10)$$

and by taking the Fourier transform with respect to time in the *inhomogeneous Helmholtz equation*

$$(\nabla_{\mathbf{x}}^2 + k^2) P(\mathbf{x}, \omega) = -S(\mathbf{x}, \omega). \quad (1.11)$$

Term $s(\mathbf{x}, t)$ is referred to as the *load term*, and it describes the spatial extension and time history of the excitation.

To involve more physical source excitation models additional force source terms may be added to the equation of motion (1.1), or injected mass/volume terms may be included in the continuity equation (1.4). This results in the *general inhomogeneous wave equations* [Pie91; Kin+00; How07]

$$\nabla_{\mathbf{x}}^2 p(\mathbf{x}, t) - \frac{1}{c^2} \frac{\partial^2}{\partial t^2} p(\mathbf{x}, t) = -\rho_0 \frac{\partial}{\partial t} q(\mathbf{x}, t) + \nabla_{\mathbf{x}} \cdot \mathbf{f}(\mathbf{x}, t), \quad (1.12)$$

and

$$(\nabla_{\mathbf{x}}^2 + k^2) P(\mathbf{x}, \omega) = -j\omega \rho_0 Q(\mathbf{x}, \omega) + \nabla_{\mathbf{x}} \cdot \mathbf{F}(\mathbf{x}, \omega). \quad (1.13)$$

in the time and angular frequency domains respectively, where $q(\mathbf{x}, t)$ describes the rate of increase of fluid volume per unit volume¹ and $\mathbf{f}(\mathbf{x}, t)$ represents a body force excitation. The first term is generated by sources that change the fluid volume, e.g. a pulsating sphere or a baffled dynamic loudspeaker. The latter force term is produced by sources moving through the fluid without any change in volume e.g unbaffled loudspeakers. A further third type of excitation term, as introduced by Lighthill, accounts for sounds produced by turbulence resulting in quadrupole sound fields [Lig52; Lig54; Kin+00]. This third term is not investigated in the present thesis.

1.1.3 Boundary conditions

So far wave propagation in free field was considered, i.e. no boundaries were present. In order to obtain a particular solution of the wave equation the wave field must satisfy prescribed boundary conditions. The general geometry is depicted in Figure 1.1. If the domain of interest is the exterior of the enclosing boundary while the sources are inside the volume—or it is the vibrating boundary surface itself—the problem to be solved is termed an *exterior radiation problem*. On the other hand, if the aim is to determine the sound field inside a source-free volume—or the reflected field of a sound source inside a cavity—an *interior problem* must be solved.

The boundary conditions are typically prescribed pressure or particle velocity. Zero pressure or velocity on the boundary surface formulates *homogeneous boundary conditions*. Non-zero field variables on the other hand represent a vibrating surface and are termed *inhomogeneous boundary conditions*.

In the aspect of this thesis two types of boundary conditions are of interest:

- *Dirichlet boundary condition* prescribes the pressure measured on the boundary surface. The homogeneous Dirichlet boundary conditions are thus

$$P(\mathbf{x}, \omega) = 0, \quad \forall \mathbf{x} \in \partial\Omega. \quad (1.14)$$

These types of boundaries are called *sound-soft* or *pressure release* boundaries, and are used to model e.g. the surface of the ocean for a wave propagating in the water [Bla00; Zio95].

¹The volume injection term $q(\mathbf{x}, t)$ can be modeled as a simple disturbance in the velocity potential i.e. satisfies equation $\nabla_{\mathbf{x}}^2 \varphi(\mathbf{x}, t) - \frac{1}{c^2} \frac{\partial^2}{\partial t^2} \varphi(\mathbf{x}, t) = -q(\mathbf{x}, t)$ [Jen+07].

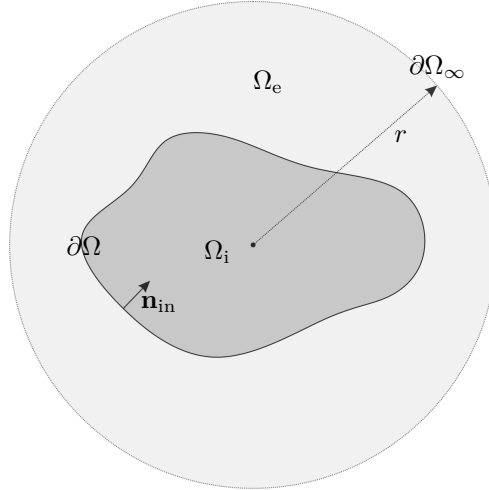


Figure 1.1. Geometry for the boundary conditions in general interior and exterior radiation problems. The Sommerfeld radiation condition can be derived in a mixed interior and exterior radiation problem by prescribing proper boundary conditions on the surface $\partial\Omega_\infty$ besides increasing its radius r to infinity, which ensure that reflection may occur from this outer boundary surface.

The inhomogeneous Dirichlet boundary condition assumes a prescribed pressure value on the boundary surface:

$$P(\mathbf{x}, \omega) = f_D(\mathbf{x}, \omega), \quad \forall \mathbf{x} \in \partial\Omega. \quad (1.15)$$

- *Neumann boundary condition* gives the normal derivative of the pressure on the boundary surface, i.e. prescribes the normal velocity of the surface. Homogeneous Neumann boundary condition are

$$\frac{\partial P(\mathbf{x}, \omega)}{\partial \mathbf{n}} = 0, \quad \forall \mathbf{x} \in \partial\Omega, \quad (1.16)$$

where $\mathbf{n}(\mathbf{x})$ is the interior or exterior normal vector of the boundary surface, and $\frac{\partial}{\partial \mathbf{n}} P(\mathbf{x}, \omega) = \langle \mathbf{n}(\mathbf{x}) \cdot \nabla_{\mathbf{x}} P(\mathbf{x}, \omega) \rangle$. These type of boundaries are termed *sound hard*, or *rigid* boundaries, ensuring that no incident wave can mobilize the boundary surface.

Inhomogeneous Neumann boundary conditions are given by

$$\frac{\partial P(\mathbf{x}, \omega)}{\partial \mathbf{n}} = f_N(\mathbf{x}, \omega), \quad \forall \mathbf{x} \in \partial\Omega. \quad (1.17)$$

Vibrating surfaces—e.g. mounted loudspeakers, or baffled pistons—are most often modeled using these type of boundary conditions.

For radiation problems it is feasible to assume free field conditions, i.e. only outgoing waves are present in the sound field. This is ensured by the *Sommerfeld radiation condition* that excludes the non-physical solutions of the wave equation emerging from infinity. Mathematically it can be formulated by implying boundary condition on $\partial\Omega_\infty$ with r increased to infinity—as shown in Figure 1.1 [Sch92; Wil99]—reading as

$$\lim_{r \rightarrow \infty} r \left(\frac{\partial}{\partial r} P(\mathbf{x}, \omega) \Big|_{\mathbf{x} \in \partial\Omega_\infty} + j \frac{\omega}{c} P(\mathbf{x}, \omega) \right) = 0, \quad \forall \mathbf{x} \in \partial\Omega_\infty. \quad (1.18)$$

1.2 Solution of the homogeneous wave equation

1.2.1 Plane wave theory

Now the general solution of the homogeneous wave equation is discussed in Cartesian coordinate systems, leading to plane wave theory. The Descartes coordinate form of the Laplace-operator is given in the nomenclature. A common method for obtaining the general solution of the Helmholtz equation is the separation of variables [Dev12]: it is supposed that the solution of (1.9) can be written in the form of the product

$$P(\mathbf{x}, \omega) = \hat{P}(\omega)X(x)Y(y)Z(z). \quad (1.19)$$

Substituting it into (1.9) and dividing both sides by $\hat{P}(\omega)X(x)Y(y)Z(z)$ yields

$$\underbrace{\frac{d^2 X(x)}{dx^2}}_{-k_x^2} \frac{1}{X(x)} + \underbrace{\frac{d^2 Y(y)}{dy^2}}_{-k_y^2} \frac{1}{Y(y)} + \underbrace{\frac{d^2 Z(z)}{dz^2}}_{-k_z^2} \frac{1}{Z(z)} = -k^2. \quad (1.20)$$

Since each term contains a total derivative—Independent from any other variable—equality may hold only if each term is constant. These constant are denoted by k_x^2, k_y^2, k_z^2 . Consequently each part of the equation leads to a simple eigenvalue problem, for which the eigenfunction solution is given by exponentials. Written e.g. for the x -variable:

$$\frac{\partial^2 X(x)}{\partial x^2} = -k_x^2 X(x) \quad \rightarrow \quad X(x) = A_1 e^{-jk_x x} + A_2 e^{jk_x x}. \quad (1.21)$$

The solutions may be substituted back into equation (1.19). In order to include every possible solution the general solution for the free field homogeneous Helmholtz equation is yielded by summation over all possible values of $k_x - k_y - k_z$ weighted by arbitrary constants. However, the variables are not independent. For a fixed temporal frequency their relation is described the dispersion relation, resulting from (1.20)

$$k^2 = \left(\frac{\omega}{c} \right)^2 = k_x^2 + k_y^2 + k_z^2. \quad (1.22)$$

As a dependent variable we will use k_y through this thesis, so that

$$k_y^2 = k^2 - k_x^2 - k_z^2 \quad (1.23)$$

holds. With all the foregoing and by denoting the arbitrary weighting constant by $\tilde{P}(k_x, k_z, \omega)$, the general solution of the 3D Helmholtz equation reads as

$$P(\mathbf{x}, \omega) = \frac{1}{(2\pi)^2} \iint_{-\infty}^{\infty} \tilde{P}(k_x, k_z, \omega) e^{-jk_x x + jk_z z} dk_x dk_z. \quad (1.24)$$

Constant $\frac{1}{(2\pi)^2}$ is introduced as a Fourier transform normalization term. The general solution—describing the inverse Fourier transform of $\tilde{P}(k_x, k_z, \omega) e^{-jk_y y}$ —therefore is obtained in the form of a spectral integral, similarly to the case of the temporal

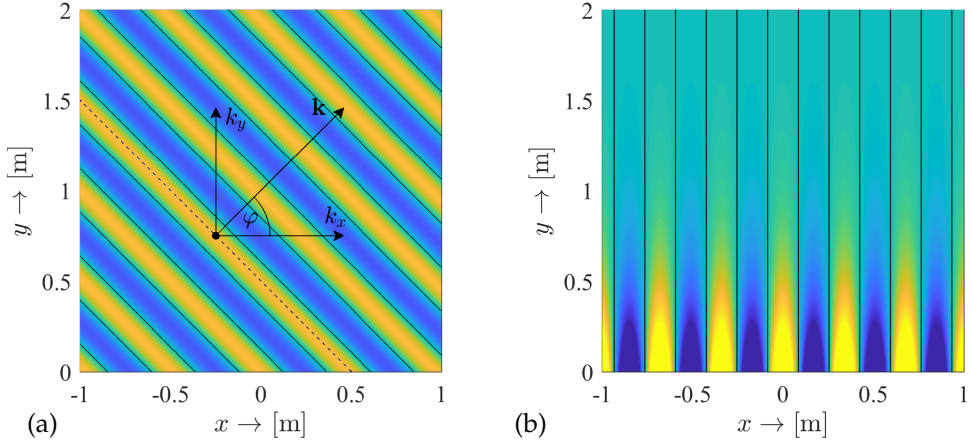


Figure 1.2. Illustration of a traveling plane wave (a) and an evanescent wave (b) with $\omega = 2\pi \cdot 1000 \text{ rad/s}$. In the present case the plane wave travels along the xy -plane, with $k_z = 0$. Variables $k_x = k \cos \varphi$, $k_y = k \sin \varphi$ give the wavenumber components along the x and y directions. For the case of the evanescent wave $k_x > \frac{\omega}{c}$, resulting in exponential decay along the y -coordinate. In a source free region propagating and evanescent waves form a complete, orthonormal basis for the solution of the helmholtz equation.

solution. Obviously, the spectral coefficients are obtained via a suitable forward Fourier transform, as explained in the next section.

One separated solution from the integral is in the form of [Wil99]

$$P(\mathbf{x}, \omega) = \hat{P}(\omega) e^{-j(k_x x + k_y y + k_z z)} = \hat{P}(\omega) e^{-j\langle \mathbf{k} \cdot \mathbf{x} \rangle}, \quad (1.25)$$

where $\mathbf{k} = [k_x, k_y, k_z]^T$ is the *wavenumber vector*, with its length equaling the acoustic wavenumber $k = |\mathbf{k}|$ and pointing into the direction of the maximum phase advance, given by the gradient of the phase function . The solution represents a *plane wave* component with the acoustic wavelength $\lambda = 2\pi/k$, traveling in the direction

$$\mathbf{k} = -\nabla \phi_P(\mathbf{x}, \omega) \quad (1.26)$$

where ϕ_P denotes the phase of function P . The terminology indicates that the surface of constant phase points are lying along an infinite plane, perpendicular to \mathbf{k} . Refer to Figure 1.2 (a) for the illustration of a traveling plane wave.

Since there is no constraint on the values of k_x and k_z , the plane wave equation is satisfied also when $k_x^2 + k_z^2 > k^2$. Resulting from the dispersion relation in these cases k_y becomes complex. In order to ignore the non-physical exponentially increasing solution in the followings we define k'_y as

$$k'_y = \begin{cases} \sqrt{(\frac{\omega}{c})^2 - k_x^2 - k_z^2} & \text{if } k_x^2 + k_z^2 \leq (\frac{\omega}{c})^2 \\ -j\sqrt{k_x^2 + k_z^2 - (\frac{\omega}{c})^2} & \text{if } k_x^2 + k_z^2 > (\frac{\omega}{c})^2. \end{cases} \quad (1.27)$$

Solutions with k'_y given as

$$P(\mathbf{x}, \omega) = \hat{P}(\omega) e^{-k'_y y} e^{-j(k_x x + k_z z)} \quad (1.28)$$

describe plane waves, propagating perpendicular to the y -axis, and exhibiting an exponentially decaying amplitude along the y -direction (see Figure 1.2 (b)): in those cases when one wavelength component is shorter than the acoustic wavelength, the wave can not propagate from the $y = 0$ surface, but an exponentially decaying radiation phenomena occurs. These type of waves are termed *evanescent waves*, opposed to *propagating waves*, when all wavenumber components are real valued.

Evanescence waves are often the results of the difference between the speed of sound in different materials: in solids the propagation speed of flexural bending waves is proportional to the square root of their temporal frequency. As a consequence, in the exemplary case of a vibrating plate higher-order modes will not be radiated into the free-space, since the bending wave's wavelength on the surface may become shorter than the acoustic wavelength would be in air. In these cases air above the surface acts as a hydrodynamic short-circuit. An other example may be the radiation from a cold surface into a warmer half space with a continuous temperature profile, resulting in a continuous sound speed profile. Due to the variation in the speed of sound the wavenumber components of a plane wave also alter continuously resulting in refraction phenomena. As soon as one wavenumber component reaches the evanescent region total internal refraction occurs and only rapidly decaying evanescent waves are present in the further part of the half space.

The evanescent contribution is of central importance in the field of *Nearfield Acoustic Holography*—when one needs a high-resolution image from the velocity distribution on the vibrating object's surface—however their contribution is often neglected in the field of sound field synthesis, when the listener is relatively far from the secondary loudspeaker array, and loudspeaker spacing is higher than the evanescent wavelengths.

1.2.2 The angular spectrum representation

It could be seen that any source-free sound field may be expressed in terms of a double inverse Fourier transform, given by (1.24). This formulation is termed the *angular spectrum representation* [Ahr10; Ahr12; Wil99] or the *plane wave expansion* [Spo05] of the sound field. The meaning of the spectral weighting components $\tilde{P}(k_x, k_z, \omega)$ is obtained by expressing the pressure by (1.24) at the infinite plane $y = 0$: it is revealed, the *angular spectrum*, or *plane wave expansion coefficients* $\tilde{P}(k_x, k_z, \omega)$ is given as the corresponding forward Fourier transform of the pressure distribution at $y = 0$. In the followings, the domain characterized by k_x, k_z is termed the *wavenumber domain*.

Equation (1.24) thus relates the pressure distribution of an arbitrary sound field measured on the plane $y = 0$ to its pressure distribution on an arbitrary parallel plane. In the wavenumber domain the relation reads as

$$\mathcal{F}_x \mathcal{F}_z \{P(\mathbf{x}, \omega)\} = \tilde{P}(k_x, y, k_z, \omega) = \tilde{P}(k_x, 0, k_z, \omega) e^{-jk_y y}, \quad (1.29)$$

with k_y given by (1.27). Since the propagation of a single plane wave component is determined merely by the phase change between the planes of investigation, therefore generally speaking the following equation holds:

$$\tilde{P}(k_x, y, k_z, \omega) = \tilde{P}(k_x, y_0, k_z, \omega) e^{-jk_y(y-y_0)}. \quad (1.30)$$

Furthermore, the y -derivative of the angular spectrum can be expressed by differentiating both sides of (1.30) with respect to the y -coordinate

$$\frac{\partial}{\partial y} \tilde{P}(k_x, y, k_z, \omega) = \frac{\partial}{\partial y} \left(\tilde{P}(k_x, y_0, k_z, \omega) e^{-jk_y(y-y_0)} \right) = -jk_y \tilde{P}(k_x, y, k_z, \omega), \quad (1.31)$$

which is the Fourier transform differentiation theorem for wavefield extrapolation.

These statements lead to two important formulations: equation (1.30) written in the spatial domain yields

$$P(\mathbf{x}, \omega) = \frac{1}{4\pi^2} \iint_{-\infty}^{\infty} \tilde{P}(k_x, y_0, k_z, \omega) e^{-jk_y(y-y_0)} e^{-j(k_x x + k_z z)} dk_x dk_z. \quad (1.32)$$

By expressing $\tilde{P}(k_x, y_0, k_z, \omega)$ in terms of the normal velocity $\tilde{V}_n(k_x, y_0, k_z, \omega)$ using the Euler's equation (1.8), with the normal —i.e. y —derivative at $y = y_0$ calculated by applying the differentiation one obtains

$$P(\mathbf{x}, \omega) = \frac{1}{4\pi^2} \iint_{-\infty}^{\infty} \underbrace{\rho_0 c k \tilde{V}_n(k_x, y_0, k_z, \omega)}_{-\frac{1}{j} \frac{\partial}{\partial y} \tilde{P}(k_x, y_0, k_z, \omega)} \frac{e^{-jk_y(y-y_0)}}{k_y} e^{-j(k_x x + k_z z)} dk_x dk_z. \quad (1.33)$$

These formulations are of central importance in the field of Fourier acoustics. They state that an arbitrary sound field is completely determined by either the pressure, or by the normal velocity component measured along an infinite plane. Wave propagation is calculated by multiplying the measured spectra with an exponential term, referred to as the *pressure propagator* \tilde{G}_p in (1.32) and the *velocity propagator* \tilde{G}_v in (1.33):

$$\tilde{G}_p(k_x, y-y_0, k_z, \omega) = e^{-jk_y(y-y_0)}, \quad \tilde{G}_v(k_x, y-y_0, k_z, \omega) = \rho_0 c k \frac{e^{-jk_y(y-y_0)}}{k_y} \quad (1.34)$$

$$\tilde{P}(k_x, y, k_z, \omega) = \tilde{P}(k_x, y_0, k_z, \omega) \tilde{G}_p(k_x, y-y_0, k_z, \omega) \quad (1.35)$$

$$= \tilde{V}_n(k_x, y_0, k_z, \omega) \tilde{G}_v(k_x, y-y_0, k_z, \omega). \quad (1.36)$$

Wave propagation in source-free volumes therefore can be modeled by 2D linear filtering of the sound field, where the filter transfer characteristics are given by the corresponding propagator. Formulation of the equations in the spatial domain results in 2D spatial convolutions, termed the Rayleigh I. and II. integrals, as it will be further discussed in the latter sections.

1.2.3 Solution in other geometries

Similarly to the presented Cartesian-solution, the general solution of the free field homogeneous Helmholtz equation can be found for spherical and cylindrical coordinate systems. The required representations are given in the form of an infinite series of spherical and cylindrical harmonics respectively, relating the radiated sound at an arbitrary point to the sound field measured on a spherical or an infinite cylindrical surface. These solutions are of great importance when spherical or circular secondary source distributions are applied for sound field reconstruction. Since the present thesis does not include the spectral solution of the reconstruction problem for these geometries, the presentation of the spherical and cylindrical solutions are omitted. For a detailed investigation refer to [Wil99; Zot09; Ahr12].

1.3 Solution of the inhomogeneous wave equation

1.3.1 The Green's function

A common way to obtain the solution for the inhomogeneous wave equation is using the *Green's function*. We define the n -dimensional *Green's function* as the solution for the following equation [GD04; Wil99]

$$\nabla^2 g(\mathbf{x}|\mathbf{x}_0, t) - \frac{1}{c^2} \frac{\partial^2}{\partial t^2} g(\mathbf{x}|\mathbf{x}_0, t) = -\delta(\mathbf{x} - \mathbf{x}_0) \delta(t - t_0), \quad (1.37)$$

with $\mathbf{x}, \mathbf{x}_0 \in \mathbb{R}^n$ and $\delta()$ being the Dirac-delta distribution. The Green's function describes the sound field at \mathbf{x} due to an impulsive disturbance located at \mathbf{x}_0 at the time instant t_0 . The Green's function is often referred to as the *spatio-temporal impulse response* of the domain of interest and its temporal Fourier transform $G(\mathbf{x}|\mathbf{x}_0, \omega)$ as the *spatio-temporal transfer function* of a point source at \mathbf{x}_0 . In the followings we assume free field conditions by implying the Sommerfeld radiation condition. Under these assumptions the *free field Green's function* is translation invariant, denoted by $g(\mathbf{x} - \mathbf{x}_0, t)$. Furthermore, in a stationary isotropic medium the *reciprocity principle* for the Green's function holds due to its symmetry [SH11]

$$g(\mathbf{x}_0|\mathbf{x}, t) = g(\mathbf{x}|\mathbf{x}_0, t) = g(\mathbf{x} - \mathbf{x}_0, t), \quad (1.38)$$

$$\frac{\partial}{\partial \mathbf{x}} g(\mathbf{x}_0|\mathbf{x}, t) = \frac{\partial}{\partial \mathbf{x}} g(\mathbf{x}|\mathbf{x}_0, t), \quad (1.39)$$

stating that a response at \mathbf{x} caused by a unit source at \mathbf{x}_0 is the same as the response at \mathbf{x}_0 due to a unit source at \mathbf{x} .

The motivation behind the use of the Green's function is that assuming an arbitrary linear differential operator $\mathcal{L}_{\mathbf{x}} \{ \cdot \}$ acting on a distribution $p(\mathbf{x})$ with an arbitrary excitation $-s(\mathbf{x})$, the solution of the inhomogeneous differential equation $\mathcal{L}_{\mathbf{x}} \{ p(\mathbf{x}) \} = -s(\mathbf{x})$ may be expressed by the convolution of the Green's function and the load term:²

$$\mathcal{L}_{\mathbf{x}} \{ g(\mathbf{x} - \mathbf{x}_0) \} = -\delta(\mathbf{x} - \mathbf{x}_0) \rightarrow p(\mathbf{x}) = \int_{\Omega} g(\mathbf{x} - \mathbf{x}_0) s(\mathbf{x}_0) d\Omega(\mathbf{x}_0). \quad (1.40)$$

The Green's function is usually obtained by the eigenfunction expansion of the operator in a given geometry with specified boundary conditions. Under free-space assumptions, where harmonic functions give a full orthogonal basis a straightforward method is to perform a Fourier transform to equation (1.37) with $\mathbf{x}_0 = 0$ with respect to space and time, yielding in $\mathbf{x} \in \mathbb{R}^3$

$$\left(-(k_x^2 + k_y^2 + k_z^2) + \left(\frac{\omega}{c} \right)^2 \right) \tilde{G}(\mathbf{k}, \omega) = -1, \quad (1.41)$$

²Multiplying both sides of the left equation of (1.40) by $-s(\mathbf{x}_0)$ and integrating along all dimensions according to \mathbf{x}_0 results in $-\int_{\Omega} s(\mathbf{x}_0) \mathcal{L}_{\mathbf{x}} \{ g(\mathbf{x} - \mathbf{x}_0) \} d\Omega(\mathbf{x}_0) = s(\mathbf{x})$. Since $\mathcal{L}_{\mathbf{x}}$ acts only on \mathbf{x} , the operator may be taken outside of the integration. Expressing the load term by $-\mathcal{L}_{\mathbf{x}} \{ p(\mathbf{x}) \}$ leads to $\mathcal{L}_{\mathbf{x}} \{ \int_{\Omega} s(\mathbf{x}_0) g(\mathbf{x} - \mathbf{x}_0) d\Omega(\mathbf{x}_0) \} = \mathcal{L}_{\mathbf{x}} \{ p(\mathbf{x}) \}$.

with $\mathbf{k} = [k_x, k_y, k_z]^T$. The Green's function in the wavenumber domain is therefore given as [Dev12; Wat15]

$$\tilde{G}(\mathbf{k}, \omega) = -\frac{1}{(\frac{\omega}{c})^2 - k_x^2 - k_y^2 - k_z^2}. \quad (1.42)$$

Applying the Fourier convolution theorem to (1.40) the solution of (1.12) in the wavenumber domain reads as

$$\tilde{P}(\mathbf{k}, \omega) = \tilde{S}(\mathbf{k}, \omega)\tilde{G}(\mathbf{k}, \omega) = -\frac{\tilde{S}(\mathbf{k}, \omega)}{(\frac{\omega}{c})^2 - k_x^2 - k_y^2 - k_z^2}, \quad (1.43)$$

and the solution in the spatio-temporal domain is yielded by the inverse Fourier transform

$$p(\mathbf{x}, t) = \frac{1}{(2\pi)^4} \iiint_{-\infty}^{\infty} -\frac{\tilde{S}(\mathbf{k}, \omega)}{(\frac{\omega}{c})^2 - k_x^2 - k_y^2 - k_z^2} e^{-j((\mathbf{k} \cdot \mathbf{x}) - \omega t)} dk_x dk_y dk_z d\omega. \quad (1.44)$$

The different representations of the free field Green's function may be obtained by the corresponding inverse Fourier transform of (1.42). The resulting formulas are collected in Table 1.1 by taking only the causal solutions into consideration.

Table 1.1. Free field acoustic Green's function representations ($\mathbf{x}_0 = 0$) [Dev12; Duf01; AS10a; Ahr12; Gib08; DeS92]. $\theta()$ denotes the Heaviside step function, $H_0^{(2)}$ () is the zeroth order Hankel function of the second kind and $K_0()$ is the modified Bessel function of the second kind [Olv+10b]. The conditional expressions ensure that evanescent waves are attenuated with increasing distance from the source. For the sake of brevity in the followings Greens function is expressed only in the propagating region, however it should be kept in mind, that evanescent wavenumber components are defined as given in (1.27), resulting in the presented conditional expressions.

	3-dimensional	2-dimensional
$\tilde{G}(k_x, k_y, k_z, \omega)$	$-\frac{1}{(\frac{\omega}{c})^2 - k_x^2 - k_y^2 - k_z^2}$	$-\frac{1}{(\frac{\omega}{c})^2 - k_x^2 - k_y^2} \delta(k_z)$
$\tilde{G}(k_x, k_y, z, \omega)$	$-\frac{j}{2} \frac{e^{-j\sqrt{(\frac{\omega}{c})^2 - k_x^2 - k_y^2} z }}{\sqrt{(\frac{\omega}{c})^2 - k_x^2 - k_y^2}}, \quad \sqrt{k_x^2 + k_y^2} \leq \left \frac{\omega}{c}\right $ $\frac{1}{2} \frac{e^{-\sqrt{k_x^2 + k_y^2 - (\frac{\omega}{c})^2} y }}{\sqrt{k_x^2 + k_y^2 - (\frac{\omega}{c})^2}}, \quad \sqrt{k_x^2 + k_y^2} > \left \frac{\omega}{c}\right $	$-\frac{1}{(\frac{\omega}{c})^2 - k_x^2 - k_y^2}$
$\tilde{G}(k_x, y, z, \omega)$	$-\frac{j}{4} H_0^{(2)} \left(\sqrt{(\frac{\omega}{c})^2 - k_x^2} \sqrt{y^2 + z^2} \right), \quad k_x < \left \frac{\omega}{c}\right $ $\frac{1}{2\pi} K_0 \left(\sqrt{k_x^2 - (\frac{\omega}{c})^2} \sqrt{y^2 + z^2} \right), \quad k_x > \left \frac{\omega}{c}\right $	$-\frac{j}{2} \frac{e^{-j\sqrt{(\frac{\omega}{c})^2 - k_x^2} y }}{\sqrt{(\frac{\omega}{c})^2 - k_x^2}}, \quad k_x \leq \left \frac{\omega}{c}\right $ $\frac{1}{2} \frac{e^{-\sqrt{k_x^2 - (\frac{\omega}{c})^2} y }}{\sqrt{k_x^2 - (\frac{\omega}{c})^2}}, \quad k_x > \left \frac{\omega}{c}\right $
$G(x, y, z, \omega)$	$\frac{1}{4\pi} \frac{e^{-j\frac{\omega}{c}\sqrt{x^2 + y^2 + z^2}}}{\sqrt{x^2 + y^2 + z^2}}$	$-\frac{j}{4} H_0^{(2)} \left(\frac{\omega}{c} \sqrt{x^2 + y^2} \right)$
$g(x, y, z, t)$	$\frac{1}{4\pi} \frac{\delta(t - \sqrt{x^2 + y^2 + z^2}/c)}{\sqrt{x^2 + y^2 + z^2}}$	$\frac{1}{2\pi} \frac{\theta(t - \sqrt{x^2 + y^2}/c)}{\sqrt{t^2 - \left(\frac{\sqrt{x^2 + y^2}}{c}\right)^2}}$

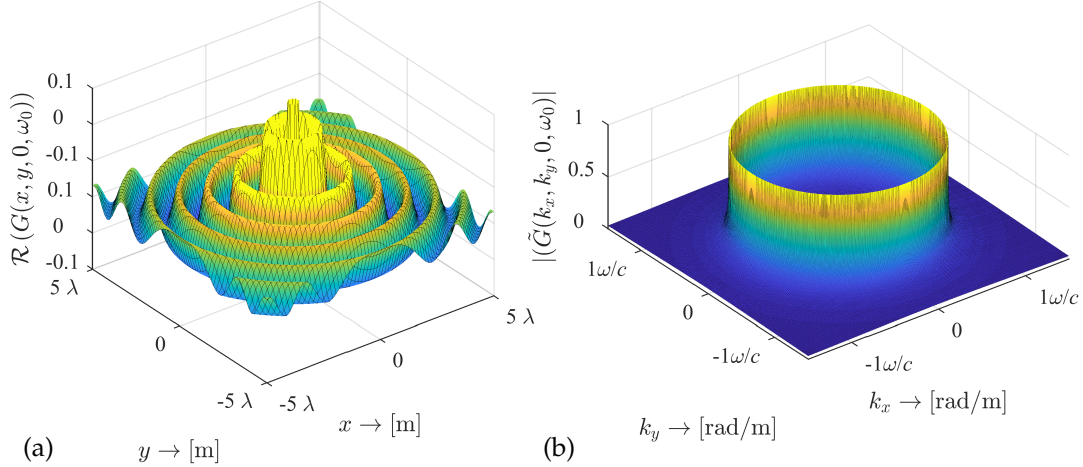


Figure 1.3. Different representations of the 3D free field Green's function in the angular frequency domain $G(x, y, z, \omega)$, with $\lambda = \frac{c}{f} = \frac{2\pi c}{\omega}$ (a) and in the semi-wavenumber domain (i.e. the angular spectrum) $\tilde{G}(k_x, k_y, z, \omega)$ (b) shown at $z = 0$.

Two representations of the 3D Green's function is depicted in Figure 1.3

In 3-dimensions the 2-dimensional Green's function represents the field of an infinite line source along the z -axis, that can be described as a continuous linear distribution of 3D point sources—explaining the infinite tail of the 2D impulse response—, thus the relation between the 3D and 2D Green's functions is given as

$$G_{2D}(x, y, \omega) = \int_{-\infty}^{\infty} G_{3D}(x, y, z, \omega) dz = \mathcal{F}_z \{G_{3D}(x, y, z, \omega)\}|_{k_z=0}, \quad (1.45)$$

obviously holding for any other representation, as it is reflected by the table above.

1.3.2 Solution of the general inhomogeneous wave equation

Now the solution of the general inhomogeneous wave equation, given by (1.13) is presented. From (1.40) the solution in the spatial domain is obtained by the convolution of the source term with the Green's function ³:

$$P(\mathbf{x}, t) = - \int_{\Omega} j\omega \rho_0 Q(\mathbf{x}_0, \omega) G(\mathbf{x} - \mathbf{x}_0, \omega) + \langle \mathbf{F}(\mathbf{x}_0, \omega) \cdot \nabla_{\mathbf{x}} G(\mathbf{x} - \mathbf{x}_0, \omega) \rangle d\Omega(\mathbf{x}_0), \quad (1.46)$$

where $\Omega(\mathbf{x})$ is the domain of interest, containing the source distribution. From the general solution the case of point-like disturbances are of special interest, with the distribution function described by a Dirac distribution:

- supposing, that $Q(\mathbf{x}_0, \omega) = \hat{Q}(\omega) \delta(\mathbf{x})$ one obtains the field response to a point-like volume injection

$$P_m(\mathbf{x}, \omega) = - \frac{j\omega \rho_0 \hat{Q}(\omega)}{4\pi} \frac{e^{-j\frac{\omega}{c}|\mathbf{x} - \mathbf{x}_0|}}{|\mathbf{x} - \mathbf{x}_0|}. \quad (1.47)$$

³The second term can be obtained by integration by parts: $\int \nabla \cdot \mathbf{F}(\mathbf{x}_0) G(\mathbf{x} - \mathbf{x}_0) d\mathbf{x}_0 = \int \nabla \cdot (\mathbf{F}(\mathbf{x}_0) G(\mathbf{x} - \mathbf{x}_0)) d\mathbf{x}_0 - \int \langle \nabla G(\mathbf{x} - \mathbf{x}_0) \cdot \mathbf{F}(\mathbf{x}_0) \rangle d\mathbf{x}_0$. Applying the Gauss theorem and invoking the Sommerfeld radiation condition reveals, that the first term of the right handside vanishes.

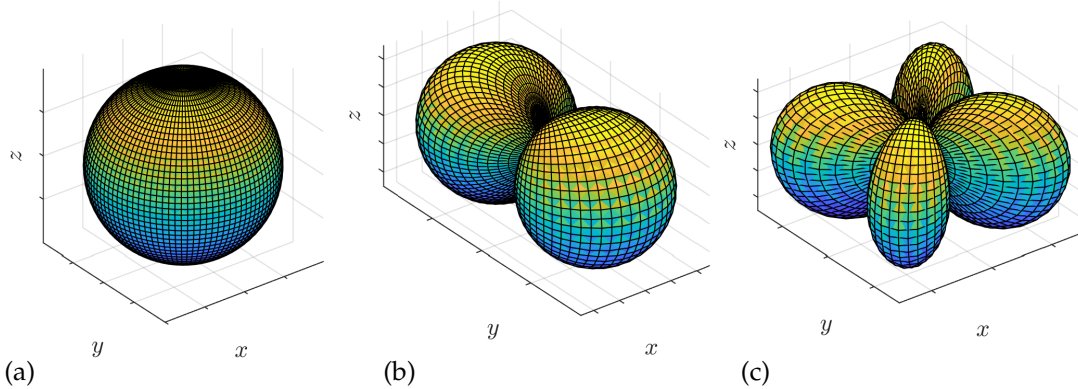


Figure 1.4. Directivity characteristics of a monopole (a), a dipole with the dipole axis being the y axis (b) and a horizontal quadrupole constructed from two opposing dipoles in the horizontal plane (c). All multipoles are solutions to the wave equation due to its linearity.

This is the field of an *acoustic monopole*, which is defined as a pulsating sphere, with its radius decreased to infinitesimal while the total volume velocity held constant [How07]. $\hat{Q}(\omega)$ is often referred to as *monopole strength*. Monopoles constitute a good far-field approximation of sources in the velocity field, e.g. a dynamical loudspeaker.

- assuming a point-like force excitation, described by $\mathbf{F}(\mathbf{x}, \omega) = \mathbf{f}\hat{F}(\omega)\delta(\mathbf{x})$, where the unit vector \mathbf{f} denotes the direction of the force the solution for the inhomogeneous wave equation is given by

$$P_d(\mathbf{x}, \omega) = -\hat{F}(\omega) \langle \mathbf{f} \cdot \nabla_{\mathbf{x}} G(\mathbf{x}, \omega) \rangle. \quad (1.48)$$

The expression describes the field generated by an *acoustic dipole*, with vector $\hat{F}(\omega)\mathbf{f}$ denoting the *dipole moment*. The terminology reflects that an acoustic dipole can be constructed by two antiphase point sources positioned infinitesimally close to each other⁴. By expressing the gradient of the Green's function the full form of a dipole field is given as

$$P_d(\mathbf{x}, \omega) = \hat{F}(\omega) \cos \theta \left(\frac{1}{|\mathbf{x} - \mathbf{x}_0|} + j \frac{\omega}{c} \right) \frac{1}{4\pi} \frac{e^{-j\frac{\omega}{c}|\mathbf{x} - \mathbf{x}_0|}}{|\mathbf{x} - \mathbf{x}_0|}. \quad (1.49)$$

with $\cos \theta = \frac{\langle \mathbf{f} \cdot (\mathbf{x} - \mathbf{x}_0) \rangle}{|\mathbf{x} - \mathbf{x}_0|}$. Unlike monopoles, dipoles are directive sources, with the directivity characteristics described by $\cos \theta$. Dipoles give a good model for e.g. unbaffled loudspeakers, moving freely in the fluid, radiating maximally into the direction of motion \mathbf{f} often termed the *dipole axis*, and without any lateral radiation.

The importance of monopoles and dipoles along with higher order *multipoles* lies in the far-field approximation of the field of extended sources, where a complex radiation pattern may be expanded into series of weighted multipole fields, termed *multipole expansion*. Figure 1.4 presents the directivity pattern of multipoles up to the third order.

⁴Such a distribution can be described by the directional gradient of a Dirac distribution $s(\mathbf{x}, \omega) = \langle \mathbf{f} \cdot \nabla \delta(\mathbf{x}) \rangle$.

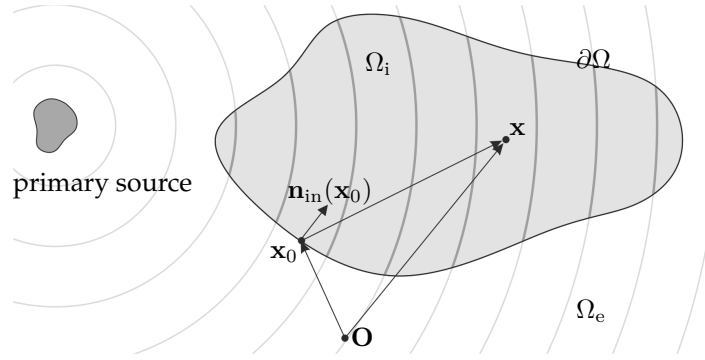


Figure 1.5. Geometry for the interior Kirchhoff-Helmholtz integral, representing the sound field inside an enclosure Ω_i generated by an exterior sound source in the form of a surface integral along $\partial\Omega$. For 2D problems the boundary degenerates to a closed contour, enclosing the area Ω_i .

Furthermore, comparison of $\tilde{G}(k_x, y, k_z, \omega)$ in Table 1.1 with the pressure and velocity propagators (1.34) and by applying the Fourier differentiation theorem (1.31) reveals that

$$\tilde{G}_p(k_x, y, k_z, \omega) = 2jk_y \tilde{G}(k_x, y, k_z, \omega) \rightarrow G_p(\mathbf{x}, \omega) = -2 \frac{\partial}{\partial y} G(\mathbf{x}, \omega) = 2P_d(\mathbf{x}, \omega), \quad (1.50)$$

$$\tilde{G}_v(k_x, y, k_z, \omega) = 2j\omega\rho_0 \tilde{G}(k_x, y, k_z, \omega) \rightarrow G_v(\mathbf{x}, \omega) = 2j\omega\rho_0 G(\mathbf{x}, \omega) = -2P_m(\mathbf{x}, \omega), \quad (1.51)$$

i.e. the pressure and velocity propagators are given by dipoles and monopoles respectively. This finding will be further discussed in the section, dealing with the Rayleigh integral formulation.

1.4 Boundary integral representation of sound fields

1.4.1 The Kirchhoff-Helmholtz integral equation

Any sound field obeying the homogeneous Helmholtz equation may be written in the form of a surface integral above an enclosing surface, termed the *Kirchhoff-Helmholtz integral equation*. This integral formulation, solving the homogeneous wave equation with inhomogeneous boundary conditions is of central importance in the field of acoustics, e.g. forming the backbone of the Boundary Element Method [Kir07; MN08], SVD-based Conformal Nearfield Acoustic Holography [Wil99; Bai92; Wu10], and sound field synthesis.

In this section the integral formulation of interior problems in source-free volumes is introduced. The effect of direct sources inside the enclosure may be straightforwardly included in the following results by the proper addition of the solution of the inhomogeneous Helmholtz equation [Spo05].

Let Ω_i be an n -dimensional enclosure, bounded by the surface $\partial\Omega$ with arbitrary position vectors $\mathbf{x}_0, \mathbf{x} \in \mathbb{R}^n$. Refer to Figure 1.5 for the geometry. For two continuous,

differentiable scalar valued functions $\Phi(\mathbf{x}_0), \Psi(\mathbf{x}_0)$ the Green's theorem reads (see A.1 for the derivation)

$$\begin{aligned} \int_{\Omega} \left(\Phi(\mathbf{x}_0) \nabla_{\mathbf{x}}^2 \Psi(\mathbf{x}_0) - \Psi(\mathbf{x}_0) \nabla_{\mathbf{x}}^2 \Phi(\mathbf{x}_0) \right) d\Omega_i(\mathbf{x}_0) = \\ = \oint_{\partial\Omega} \left(\Psi(\mathbf{x}_0) \frac{\partial \Phi(\mathbf{x}_0)}{\partial \mathbf{n}_{in}} - \Phi(\mathbf{x}_0) \frac{\partial \Psi(\mathbf{x}_0)}{\partial \mathbf{n}_{in}} \right) d\partial\Omega(\mathbf{x}_0), \quad (1.52) \end{aligned}$$

with $\frac{\partial}{\partial \mathbf{n}_{in}}$ denoting the inward normal derivative $\langle \mathbf{n}_{in}(\mathbf{x}_0) \cdot \nabla_{\mathbf{x}} \Phi(\mathbf{x})|_{\mathbf{x}=\mathbf{x}_0} \rangle$. Let Φ be the pressure field inside the enclosure satisfying the homogeneous Helmholtz equation and let Ψ be the Green's function located at \mathbf{x} ⁵—with its actual form depending on the problem dimensionality—, therefore equations

$$(\nabla^2 + k^2)P(\mathbf{x}_0, \omega) = 0, \quad (\nabla^2 + k^2)G(\mathbf{x}_0|\mathbf{x}, \omega) = -\delta(\mathbf{x}_0 - \mathbf{x}) \quad (1.53)$$

hold. Substituting into the Green's theorem leads to

$$-\int_{\Omega_i} P(\mathbf{x}_0, \omega) \delta(\mathbf{x}_0 - \mathbf{x}) d\Omega_i(\mathbf{x}_0) = \oint_{\partial\Omega} \left(G(\mathbf{x}_0|\mathbf{x}, \omega) \frac{\partial P(\mathbf{x}_0, \omega)}{\partial \mathbf{n}_{in}} - P(\mathbf{x}_0, \omega) \frac{\partial G(\mathbf{x}_0|\mathbf{x}, \omega)}{\partial \mathbf{n}_{in}} \right) d\partial\Omega(\mathbf{x}_0). \quad (1.54)$$

The sifting property of the Dirac-delta may be exploited by taking into account that the singularity is located in the enclosure: if \mathbf{x} lies outside the volume the integral is identically zero, while if it is on the surface it is assumed, that "only half of the Dirac-impulse is in the volume". For a rigorous derivation refer to [Wil99]. Finally, by exploiting the symmetry and translation invariancy of the free field Green's function (1.38) the *Kirchhoff-Helmholtz integral equation* (KHIE) is obtained:

$$\alpha P(\mathbf{x}, \omega) = \oint_{\partial\Omega} - \left(\frac{\partial P(\mathbf{x}_0, \omega)}{\partial \mathbf{n}_{in}} G(\mathbf{x} - \mathbf{x}_0, \omega) - P(\mathbf{x}_0, \omega) \frac{\partial G(\mathbf{x} - \mathbf{x}_0, \omega)}{\partial \mathbf{n}_{in}} \right) d\partial\Omega(\mathbf{x}_0), \quad (1.55)$$

with

$$\alpha = \begin{cases} 1 & \forall \mathbf{x} \in \Omega_i \\ \frac{1}{2} & \forall \mathbf{x} \in \partial\Omega \\ 0 & \forall \mathbf{x} \in \Omega_e. \end{cases}$$

The equation states that the pressure field inside an enclosure is completely determined by the boundary conditions for the pressure and normal velocity on the boundary surface. The interior KHIE describes the pressure field only inside the volume of investigation, outside the volume the left hand side is identically zero. For exterior radiation problems the exterior KHIE can be derived in a similar manner, describing the pressure field outside the volume and ensuring zero left hand side inside [Wil99]. In both cases the approach is capable of dealing only with *forward propagation problems* i.e. capable to describe the effects of a source distribution based on the radiated field measured on a surface, but unable to describe the source properties from these data.

⁵Although the continuity requirement is not fulfilled for the Green's function, with proper mathematical workaround the singularity at \mathbf{x} may be excluded from the enclosure [Wil99].

This latter scenario is called an acoustic *inverse problem*, forming the basis of Acoustic Holography and Sound Field Synthesis⁶.

A frequently used form of the KHIE—utilizing the Euler’s equation (1.8) to express the normal derivative of the pressure in terms of the normal velocity on the surface—is given as

$$\alpha P(\mathbf{x}, \omega) = \oint_{\partial\Omega} \left(V_n(\mathbf{x}_0, \omega) \underbrace{j\rho_0 \omega G(\mathbf{x} - \mathbf{x}_0, \omega)}_{-P_m(\mathbf{x} - \mathbf{x}_0, \omega)} + P(\mathbf{x}_0, \omega) \underbrace{\frac{\partial G(\mathbf{x} - \mathbf{x}_0, \omega)}{\partial \mathbf{n}_{in}}}_{-P_d(\mathbf{x} - \mathbf{x}_0, \omega)} \right) d\partial\Omega(\mathbf{x}_0), \quad (1.56)$$

where the weighting factors containing the Green’s function can be recognized as the fields of monopoles and dipoles, functioning as velocity and pressure propagators analogously to the angular spectrum approach. KHIE therefore consists of two integral components, termed the *single layer potential* and the *double layer potential*: single layer potential describes the field as the weighted sum of a single layer of point sources, characterized by $G(\mathbf{x}|\mathbf{x}_0)$, while the double layer potential describes the field of an ensemble of dipole point sources, described by $\frac{\partial G(\mathbf{x}|\mathbf{x}_0, \omega)}{\partial \mathbf{n}_{in}}$, realized by two anti-phase point sources: by a double layer.

One drawback of interior HIE is that it overspecifies the problem in order to ensure zero pressure and velocity outside the domain of interest. In the aspect of sound field synthesis the presence of both single and double layer potentials is infeasible. By letting the sound field be non-zero outside the enclosure it is possible to completely describe the sound field in the region of interest in terms of only single or double layer potentials by either modifying the Green’s function in order to satisfy Dirichlet or Neumann boundary conditions, or to impose these boundary conditions on the sound field $P(\mathbf{x}_0, \omega)$ itself in an equivalent scattering problem. In the following sections these approaches are applied for the simplification of the KHIE.

1.4.2 The Simple Source Formulation

The simple source formulation is derived from the KHIE by the construction of a separate exterior and interior radiation problem with prescribing the same inhomogeneous Dirichlet boundary condition for both fields on the boundary surface $\partial\Omega$ [Cop68].

Assume an exterior sound field $P_e(\mathbf{x}, \omega)$ in the geometry depicted in Figure 1.5, satisfying the homogeneous Helmholtz equation at $\mathbf{x} \in \Omega_e$, meaning that all sources are located within the enclosure. The exterior wave field is the combination of radiating, or diverging waves. On the other hand assume an interior sound field $P_i(\mathbf{x}, \omega)$ inside the enclosure $\mathbf{x} \in \Omega_i$, induced by a sound source located outside the volume of investigation. The interior field constructed by a set of incoming or converging waves also satisfies the homogeneous Helmholtz equation in the interior domain. The two

⁶Actually, the KHIE may be made able to solve inverse problems, by replacing the forward propagating Green’s function by the backward propagating Green’s function [WB89]

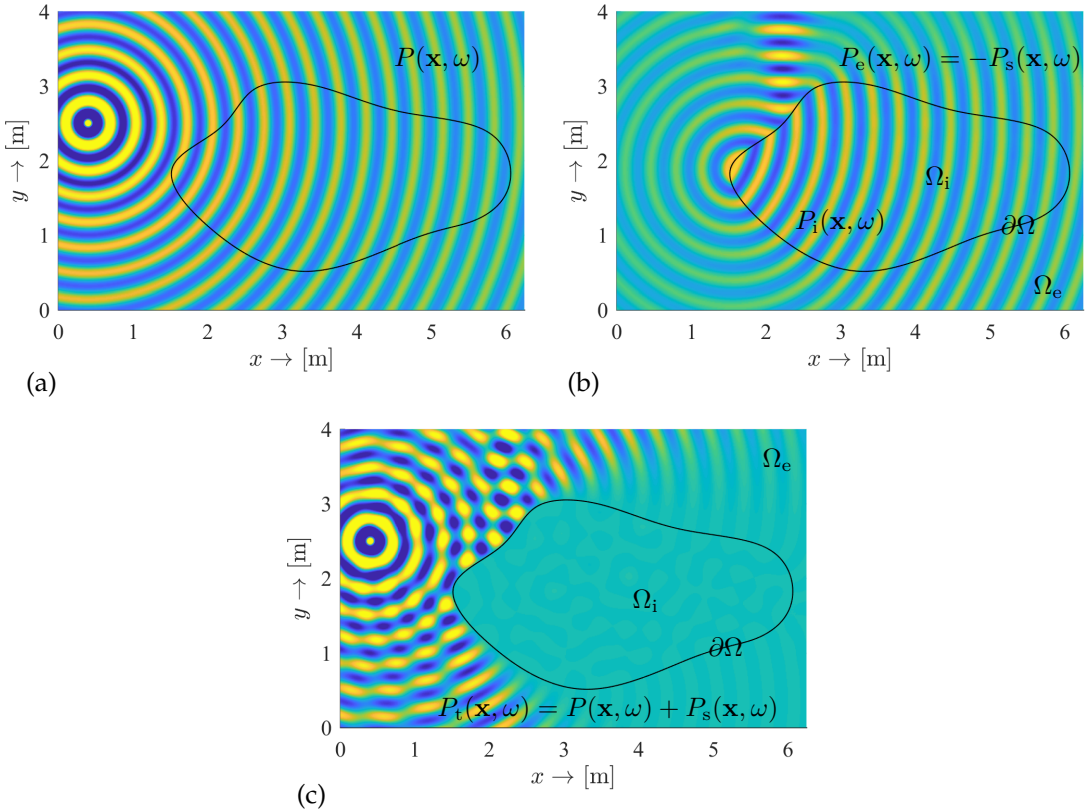


Figure 1.6. Illustration of simple source formulation in a 2D problem ($\Omega \subset \mathbb{R}^2$). Figures show the incident/target sound field (a), the field given by the simple source formulation (b) and the scattering of the incident field from a sound soft boundary (c). The incident field is the field of a 2D point source (i.e. a line source) at $\mathbf{x}_s = [-0.4, 2.5]^T$ oscillating at $\omega = 2\pi \cdot 1$ krad/sec. Equation (1.58) was evaluated numerically using an open source C++ Boundary Element software [FR14]. The figures demonstrate, how simple source formulation expresses the incident field inside Ω_i , and the (-1) times the scattered field at Ω_e in an equivalent sound soft scattering problem. Figure (c) showing the difference between the incident field and the simple source field ((a)-(b)) therefore illustrates the total scattering in the exterior.

spatially disjunct problems are connected through the following boundary condition written onto the boundary surface

$$P_e(\mathbf{x}_0, \omega) = P_i(\mathbf{x}_0, \omega), \quad \mathbf{x}_0 \in \partial\Omega. \quad (1.57)$$

Both fields may be expressed in terms of an exterior and an interior KHIE respectively, for the exterior KHIE expressed in terms of the inward normals refer to [Wil99, eq. 8.30]. By adding the exterior and interior KHIEs—due to the coupled boundary condition—terms, weighted by the pressure on the boundary vanish and the following integral expression is obtained [CH62; Kel67; Wil99]

$$\oint_{\partial\Omega} G(\mathbf{x}|\mathbf{x}_0, \omega) \left(\frac{\partial P_e(\mathbf{x}_0, \omega)}{\partial \mathbf{n}_{\text{in}}} - \frac{\partial P_i(\mathbf{x}_0, \omega)}{\partial \mathbf{n}_{\text{in}}} \right) d\partial\Omega(\mathbf{x}_0) = \begin{cases} P_e(\mathbf{x}, \omega) & \forall \mathbf{x} \in \Omega_e \\ P_e = P_i & \forall \mathbf{x} \in \partial\Omega \\ P_i(\mathbf{x}, \omega) & \forall \mathbf{x} \in \Omega_i. \end{cases} \quad (1.58)$$

The equation states that either the interior or the exterior sound field, satisfying the homogeneous Helmholtz equation may be represented as a single layer potential. The

single layer strength function is given in the integral (1.58) implicitly. The discontinuity in the pressure gradient is termed the *jump relation*, expressing the fact that the sound field generated by the single layer potential is continuous in pressure on the boundary $\partial\Omega$, while the gradient changes sign i.e. *jumps*.

As pointed out in [FN13; Faz10; SS14; ZS13] the following physical interpretation can be assigned to the simple source formulation: Assume that the surface $\partial\Omega$ represents the boundary of a sound soft scattering object! In acoustic scattering problems it is assumed, that an the *incident sound field* $P(\mathbf{x}, \omega)$ that is reflected by the scattering object, generating the *scattered field* $P_s(\mathbf{x}, \omega)$ is known a priori. The field measured in the presence of the obstacle is termed the *total field* $P_t(\mathbf{x}, \omega)$, given by the sum of the incident and scattered fields. The scattered field is the solution of the exterior radiation problem, so that the total field obeys homogeneous boundary conditions on the sound soft scatterer surface, i.e. $P_s(\mathbf{x}_0, \omega) = -P(\mathbf{x}_0, \omega) = -P_e(\mathbf{x}_0, \omega)$, $\mathbf{x}_0 \in \partial\Omega$. Comparing this result with the simple source formulation it is clear, that the single layer strength function is the derivative of (-1) times the total field on the boundary. See Figure 1.6 for an illustration of the simple source formulation and for its interpretation as an equivalent scattering problem. In the presented general 2D scenario the single layer weighting factors were calculated numerically for an arbitrary enclosing reflecting surface.

1.4.3 The Rayleigh integrals

The Rayleigh integrals formulate the sound field based on the pressure field or the normal velocity measured on an infinite plane utilizing the Neumann or Dirichlet Green's functions.

In order to derive the Rayleigh integrals an interior problem is considered by writing the KHIE on a simply joint boundary consisting of a disc $\partial\Omega_P$ and hemisphere $\partial\Omega_S$, as shown in Figure 1.7. With the radius of the hemisphere increased to infinity ($r \rightarrow \infty$) the Sommerfeld-radiation condition is invoked and the contribution of the hemisphere vanishes: the radiated field is described by a surface integral written on an infinite plane, termed here the *Rayleigh plane*. For the sake of simplicity the plane is located at $y = 0$ with its normal given by $\mathbf{n}_{in} = [0, 1, 0]^T$ and all the primary sources of sound are located at $y < 0$. In this geometry the KHIE (1.55) describing the field at $\mathbf{x} = [x, y > 0, z]^T$ degenerates to

$$P(\mathbf{x}, \omega) = \lim_{r \rightarrow \infty} \left(\int_{\partial\Omega_P} d\partial\Omega_P + \int_{\partial\Omega_S} d\partial\Omega_S \right) = \\ \int_{\partial\Omega_P} \left(P(\mathbf{x}_0, \omega) \frac{\partial G(\mathbf{x}_0 | \mathbf{x}, \omega)}{\partial y_0} \Big|_{y_0=0} - \frac{\partial P(\mathbf{x}_0 | \mathbf{x}, \omega)}{\partial y_0} \Big|_{y_0=0} G(\mathbf{x}_0 | \mathbf{x}, \omega) \right) d\partial\Omega_P(\mathbf{x}_0). \quad (1.59)$$

Obviously, any homogeneous solution of the Helmholtz equation may be added to the Green's function, the inhomogeneous wave equation and the Kirchhoff-Helmholtz integral still holds. Generally, this property can be in order to solve the inhomogeneous wave equation in the presence of boundaries, by taking the reflected field into consideration. In the following this fact is exploited in order to eliminate either the

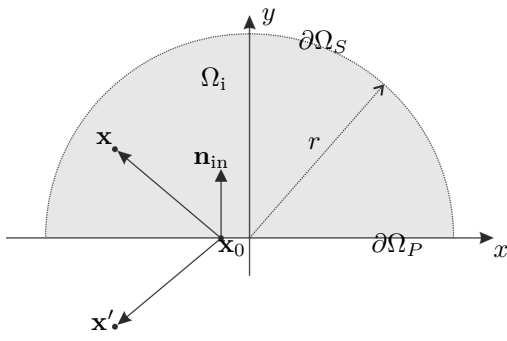


Figure 1.7. Geometry for deriving the Rayleigh integrals. The radius of the hemisphere $\partial\Omega_S$ is increased to infinity, therefore only the Rayleigh plane $\partial\Omega_P$ contributes to the radiated field at $y > 0$. For this special geometry the required Neumann and Dirichlet Green's functions are given by the sum of a point source at the evaluation point x and a point source, positioned at x' , obtained by mirroring x to the Rayleigh plane.

single or the double layer potential in the integral (1.59) by finding a proper additive term to the Green's function:

- The *Neumann Green's function* eliminates the double layer potential by describing Neumann boundary conditions for the Green's function along the infinite plane:

$$G_N(\mathbf{x}_0, \omega) = G(\mathbf{x}_0|\mathbf{x}, \omega) + G'_N(\mathbf{x}_0, \omega), \quad (1.60)$$

$$\frac{\partial G_N(\mathbf{x}_0, \omega)}{\partial \mathbf{n}_{in}} = \frac{\partial G_N(\mathbf{x}_0, \omega)}{\partial y_0} = 0, \quad \forall \mathbf{x}_0 \in \partial\Omega_P. \quad (1.61)$$

- The *Dirichlet Green's function* eliminates the double layer potential by describing Dirichlet boundary conditions for the Green's function, given by

$$G_D(\mathbf{x}_0, \omega) = G(\mathbf{x}_0|\mathbf{x}, \omega) + G'_D(\mathbf{x}_0, \omega) = 0, \quad \forall \mathbf{x}_0 \in \partial\Omega_P. \quad (1.62)$$

In the general case of an arbitrary shaped enclosing surface the Neumann and Dirichlet Green's functions are given by the scattered field of a point source positioned at \mathbf{x} , reflected from a rigid or a sound soft boundary respectively. Their actual form therefore would depend on the evaluation point \mathbf{x} . In the present geometry the scattered field of a point source from a rigid or sound soft infinite plane can be easily obtained by mirroring the in-phase or anti-phase source to the scatterer plane, and the required Green's functions are given as

$$G_N(\mathbf{x}_0, \omega) = G(\mathbf{x}_0|\mathbf{x}, \omega) + G(\mathbf{x}_0|\mathbf{x}', \omega) \quad (1.63)$$

$$G_D(\mathbf{x}_0, \omega) = G(\mathbf{x}_0|\mathbf{x}, \omega) - G(\mathbf{x}_0|\mathbf{x}', \omega) \quad (1.64)$$

with $\mathbf{x}' = [x, -y, z]^T$.

Substituting them into the integral (1.59) yields the Rayleigh I and II integrals respectively [Ber84]:

$$P_N(\mathbf{x}, \omega) = \int_{\partial\Omega_P} -2 \frac{\partial P(\mathbf{x}, \omega)}{\partial y_0} \Big|_{y_0=0} G(\mathbf{x} - \mathbf{x}_0, \omega) d\partial\Omega_P(\mathbf{x}_0) \quad (1.65)$$

$$P_D(\mathbf{x}, \omega) = \int_{\partial\Omega_P} 2P(\mathbf{x}_0, \omega) \frac{\partial G(\mathbf{x} - \mathbf{x}_0, \omega)}{\partial y_0} \Big|_{y_0=0} d\partial\Omega_P(\mathbf{x}_0). \quad (1.66)$$

Obviously, the Rayleigh integrals do not ensure a zero sound field behind the Rayleigh plane at $y < 0$. In this region the Rayleigh I integral expresses the field of the primary source distribution, reflected from an infinite rigid plane, while the Rayleigh II integral gives that from a sound soft planar boundary.

The Rayleigh integrals are of major importance in the theory of diffraction from finite aperture. In the present treatise the Rayleigh I integral is of special importance, being a single layer potential. This formulation is used extensively for the calculation of radiated fields from finite radiators mounted in infinite walls, e.g. the field of loudspeakers. It states that the radiated field from a rigid vibrating plane can be calculated by summing the field of point sources on the surface, driven by the normal velocity distribution, or mathematically speaking by convolving the Green's function with the velocity distribution over the infinite surface.

Besides the presented methodology involving the Neumann and Dirichlet Green's function the Rayleigh integral can be deduced directly using the equivalent scattering interpretation of the simple source approach: for a planar reflecting surface the reflected field can be obtained by mirroring the incident field to the scatterer, resulting in the same formulation. Another straightforward way to obtain the Rayleigh integrals stems from the direct inverse Fourier transform of the angular spectrum representations (1.32) and (1.33) by applying the Fourier transform convolution theorem and applying that the pressure and velocity propagators are given by the field of dipoles and monopoles, as it was stated in section 1.3.2. Obviously, the fact, that all the presented three approaches lead to the same solution stems from the uniqueness single layer problem for a planar boundary.

High frequency approximation of wave fields and radiation problems

The boundary integral representations introduced in the previous section already give the possibility for solving the sound field synthesis problem for special geometries, or at the expense of great computational complexity. In order to derive integral representations more suitable for general sound field synthesis, the application of approximate solutions are inevitable. This chapter presents several high-frequency asymptotic approximations of sound fields and their integral representations. These approximations will be of crucial interest for finding the driving functions for general loudspeaker contours in the latter sections.

The presented local/asymptotic description of wave fields are not unknown in the fields of acoustics: with minor modifications they are massively used concepts in ray tracing and geometrical optics/acoustics. However, their application for sound field synthesis problems has been unprecedented so far.

2.1 Local attributes of sound fields

2.1.1 The local wavenumber vector

Consider an arbitrary steady state harmonic sound field in $\mathbf{x} \in \mathbb{R}^3$ written in a general polar form with $A^P(\mathbf{x}, \omega), \phi^P(\mathbf{x}, \omega) \in \mathbb{R}$

$$P(\mathbf{x}, \omega) = A^P(\mathbf{x}, \omega)e^{j\phi^P(\mathbf{x}, \omega)}, \quad (2.1)$$

with a suppressed temporal dependency $e^{j\omega t}$. The dynamics of wave propagation is described by the phase of the sound field. From ray-tracing/geometrical optics theory the following quantitiy is introduced[BG04; Roe05]:

$$\mathbf{k}^P(\mathbf{x}) = [k_x^P(\mathbf{x}), k_y^P(\mathbf{x}), k_z^P(\mathbf{x})]^T = -\nabla_{\mathbf{x}} \phi^P(\mathbf{x}, \omega), \quad (2.2)$$

termed the *local wavenumber vector* of sound field P , being obviously the generalization of the plane wave wavenumber vector introduced in equation (1.26). In the followings the existence of the superscript distinguishes local properties from the global ones, e.g. local wavenumber components of spectral decomposition. The wavenumber vector, defined as the negative gradient of the phase function points in the direction of

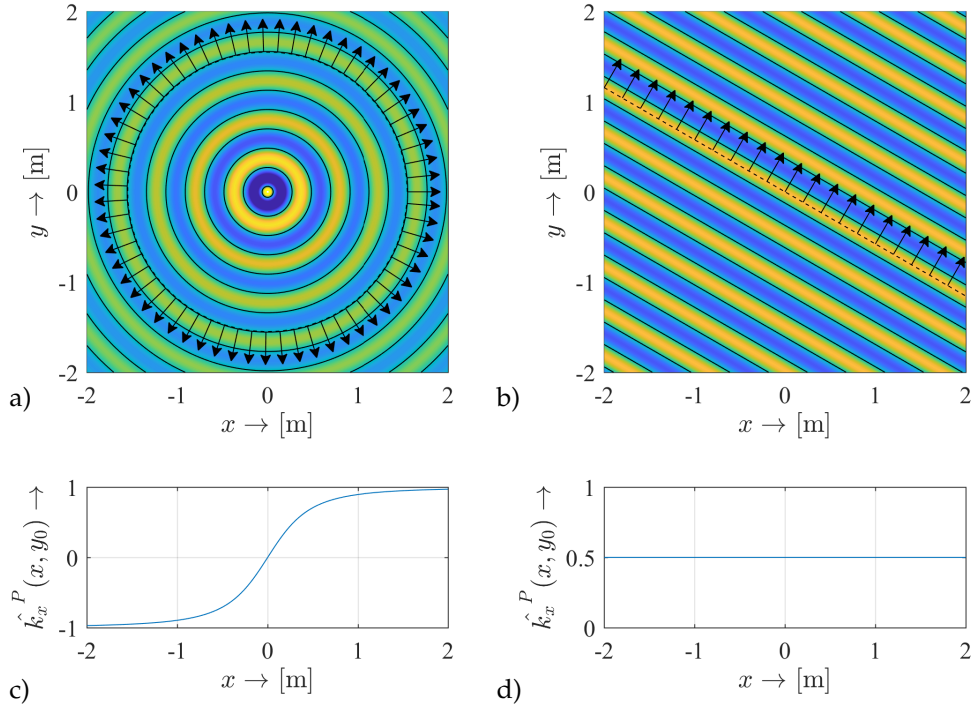


Figure 2.1. Illustration of the local wavenumber vector for a 2D acoustic point source (a,c) and a 2D plane wave (b,d). (a-b) show an arbitrarily chosen contour of constant phase (isochronous contour), along with the wavenumber vector on this contour. (c-d) show the local normalized $\hat{k}_x^P(x, y_0)$ component along the line $y_0 = 0.5$ m.

maximal phase advance, i.e. it is perpendicular to the wavefront in any position. For an isotropic medium, where the propagation speed is constant, the phase velocity and the group velocity coincide, and the wavenumber vector points in the direction of the wave's energy flow, thus in the local wave propagation direction¹.

Introducing the general formulation (2.1) into the Helmholtz equation (1.9) and expressing the Laplace operator explicitly yields (for the sake of transparency with suppressed function arguments)

$$\left(\frac{\nabla_{\mathbf{x}}^2 A^P}{A^P} - |\nabla_{\mathbf{x}} \phi^P|^2 + j \left(\nabla_{\mathbf{x}}^2 \phi^P + 2 \frac{\langle \nabla_{\mathbf{x}} \phi^P \cdot \nabla_{\mathbf{x}} A^P \rangle}{A^P} \right) + \left(\frac{\omega}{c} \right)^2 \right) P(\mathbf{x}, \omega) = 0. \quad (2.3)$$

In order to have the equality satisfied for an arbitrary sound field both real and imaginary parts of the bracketed term have to vanish, resulting in the following equations:

$$\frac{\nabla_{\mathbf{x}}^2 A^P}{A^P} - |\nabla_{\mathbf{x}} \phi^P|^2 + \left(\frac{\omega}{c} \right)^2 = 0, \quad (2.4)$$

$$\nabla_{\mathbf{x}}^2 \phi^P + 2 \frac{\langle \nabla_{\mathbf{x}} \phi^P \cdot \nabla_{\mathbf{x}} A^P \rangle}{A^P} = 0. \quad (2.5)$$

¹This statement holds exclusively for isotropic media. Although the wavenumber vector is always perpendicular to the wavefront, in anisotropic media the energy of a wave not necessarily travels along the path as the wavefront normals [Pol77].

Assuming high frequency conditions, where the phase changes rapidly compared to the amplitude, $\frac{\nabla_x^2 A^P}{A^P} \ll |\nabla_x \phi^P|^2$ holds and by applying the definition of the local wavenumber vector equation (2.4) leads to the *local dispersion relation*

$$|\mathbf{k}^P(\mathbf{x})|^2 = k_x^P(\mathbf{x})^2 + k_y^P(\mathbf{x})^2 + k_z^P(\mathbf{x})^2 = \left(\frac{\omega}{c}\right)^2 = k^2. \quad (2.6)$$

The equation holds trivially for simple sound fields: for plane waves, point sources and line sources excluding the singular point², however fails in the presence of strong interference phenomena, due to which the amplitude distribution varies heavily. It is important to note that the present form of the local dispersion relation is only valid for a stationary sound field in isotropic medium. In latter sections the theory will be extended to non-stationary fields, with the example of the sound field generated by a moving harmonic source.

Applying the local dispersion relation the *normalized wavenumber vector* can be defined for a stationary sound field as

$$\hat{\mathbf{k}}^P(\mathbf{x}) = \frac{\mathbf{k}^P(\mathbf{x})}{|\mathbf{k}^P(\mathbf{x})|} = \frac{\mathbf{k}^P(\mathbf{x})}{\omega/c}, \quad (2.7)$$

being a vector of unit length, pointing in the local propagation direction of the sound field. The normalized wavenumber vector, i.e. the normalized phase change of wave fields, is a basic concept in ray tracing, massively used for solving wave propagation problems in anisotropic media. In the field of ray tracing, expression $\Gamma(\mathbf{x}) = \frac{\phi^P(\mathbf{x}, \omega)}{k}$ is termed the *eikonal*, whose gradient defines the local propagation direction of the wave field: $\nabla \Gamma(\mathbf{x}) = \hat{\mathbf{k}}(\mathbf{x})$. In that context, the local dispersion relation in the form of (2.4) is termed the *eikonal equation* [Kin+00; Pie91], having to be solved for the eikonal at space-variant sound speeds resulting in the phase of sound rays. The second basic ray tracing equation termed the *transport equation* is given by (2.5), with its solution providing the intensity change of sound rays.

2.1.2 The local wavefront curvature

Applying the local wavenumber vector concept the *local wavefront curvature* of arbitrary sound fields can be introduced in order to distinguish *divergent* and *convergent* wavefronts. A wave field is termed *divergent* with a convex wavefront propagating away from a source distribution and *convergent* or *focused*, if a concave wavefront propagates towards a focal point. Mathematically the local vergence of the wave field may be described by the *principal curvatures* of the wavefront, or in a looser sense by the *mean curvature* of the wavefront.

The principal curvature components $\kappa_1^P(\mathbf{x}), \kappa_2^P(\mathbf{x})$ are defined geometrically as the reciprocal of the principal radii $\rho_1^P(\mathbf{x}), \rho_2^P(\mathbf{x})$, being the maximal and minimal radii of osculating circles at a point on the wavefront, as illustrated in Figure 2.2. Mathematically if the local dispersion relation holds, the principal curvatures are given by the two

²Since for isotropic media the Green's function's amplitude factor serves as the Green's function for the Laplace equation, satisfying $\nabla_x^2 \frac{1}{4\pi} \frac{1}{|\mathbf{x} - \mathbf{x}_0|} = -\delta(\mathbf{x} - \mathbf{x}_0)$.

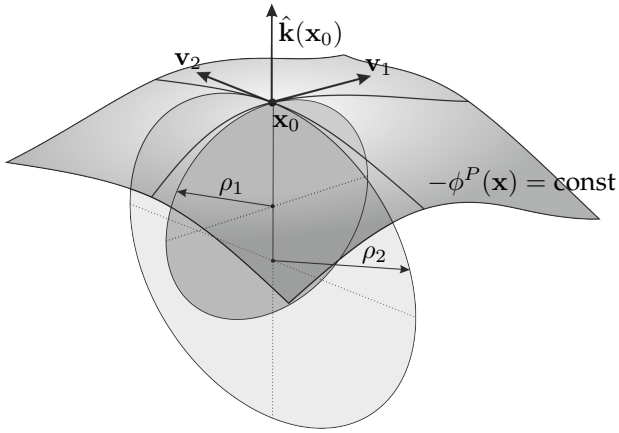


Figure 2.2. Illustration of the principal radii and principal curvatures at x_0 of an arbitrary smooth wavefront, satisfying the local dispersion relation. The principal radii are denoted by ρ_1 and ρ_2 , with the corresponding tangent vectors v_1 and v_2 respectively. The principal curvatures are given by the reciprocal of the principal radii. In the present treatise non-converging wave fields are discussed with both principal curvatures being non-negative.

non-zeros eigenvalues of the phase function's negative Hessian, normalized by ω/c [Har99; Har01]. A wave field is then divergent with both principal curvatures being positive [AB86; Ble84; PT92]. A more detailed treatise on the wavefront curvatures and the Hessian of the phase function is given in section B.1.

The *mean curvature* of the wavefront—generally defined as the divergence of the surface normal [Gol05]—is given by the negative divergence of the normalized local wavenumber vector, or the trace of the Hessian:

$$\bar{\kappa}^P(\mathbf{x}) = \nabla_{\mathbf{x}} \cdot \hat{\mathbf{k}}^P(\mathbf{x}) = -\frac{1}{k} \nabla_{\mathbf{x}}^2 \phi^P(\mathbf{x}, \omega) = -\frac{1}{k} (\phi_{xx}^{P''}(\mathbf{x}) + \phi_{yy}^{P''}(\mathbf{x}) + \phi_{zz}^{P''}(\mathbf{x})), \quad (2.8)$$

with $k = \frac{\omega}{c}$ being the physical wavenumber. Note, that employing the transport equation (2.5) the divergence of the local wavenumber vector can be expressed as

$$\bar{\kappa}^P(\mathbf{x}) = -2 \left\langle \hat{\mathbf{k}}^P(\mathbf{x}) \cdot \frac{\nabla_{\mathbf{x}} A^P(\mathbf{x}, \omega)}{A^P(\mathbf{x}, \omega)} \right\rangle, \quad (2.9)$$

resulting in a formal definition for the vergence of the sound field in a mean sense: a field is divergent if it's amplitude decreases in the local propagation direction and convergent if the intensity is focused towards the propagation direction.

Since the mean and the principle curvatures are related as $\bar{\kappa}^P(\mathbf{x}) = \frac{1}{2} (\kappa_1(\mathbf{x})^P + \kappa_2(\mathbf{x})^P)$, wave fields may be classified as

$$\kappa_1^P(\mathbf{x}), \kappa_2^P(\mathbf{x}), \bar{\kappa}^P(\mathbf{x}) \begin{cases} > 0 & \text{for a locally diverging/non-focused wave field} \\ = 0 & \text{for a plane-wave} \\ < 0 & \text{for a locally converging/focused wave field.} \end{cases} \quad (2.10)$$

Furthermore, it can be proven (by expressing the diagonal elements of the Hessian using (B.3)), that the inequalities also hold for the second partial derivatives in (2.8) separately.

2.1.3 High frequency gradient approximation

As a further approximation in the high-frequency domain, the gradient of an arbitrary sound field may be expressed in a simplified form in terms of the local

wavenumber vector. By applying the product rule of differentiation, the gradient of an arbitrary polar form sound field, described by (2.1) reads

$$\nabla_{\mathbf{x}} P(\mathbf{x}, \omega) = \left(\frac{\nabla_{\mathbf{x}} A^P(\mathbf{x}, \omega)}{A^P(\mathbf{x}, \omega)} + j \nabla_{\mathbf{x}} \phi^P(\mathbf{x}, \omega) \right) P(\mathbf{x}, \omega) = \left(\frac{\nabla_{\mathbf{x}} A^P(\mathbf{x}, \omega)}{A^P(\mathbf{x}, \omega)} - j \mathbf{k}^P(\mathbf{x}) \right) P(\mathbf{x}, \omega). \quad (2.11)$$

In the high frequency region $|\mathbf{k}^P(\mathbf{x})| \approx (\frac{\omega}{c}) \gg \left| \frac{\nabla_{\mathbf{x}} A^P(\mathbf{x}, \omega)}{A^P(\mathbf{x}, \omega)} \right|$ holds, and the gradient can be approximated as

$$\nabla_{\mathbf{x}} P(\mathbf{x}, \omega) \approx -j \mathbf{k}^P(\mathbf{x}) P(\mathbf{x}, \omega). \quad (2.12)$$

For the interpretation of the local wavenumber concept and the high-frequency gradient approximation the first order Taylor-expansion of the phase function may be expressed around an arbitrary point \mathbf{x}_0 in the space

$$\phi^P(\mathbf{x}, \omega) \approx \phi^P(\mathbf{x}_0, \omega) + \langle (\mathbf{x} - \mathbf{x}_0) \cdot \nabla_{\mathbf{x}} \phi^P(\mathbf{x}_0, \omega) \rangle. \quad (2.13)$$

By substitution into (2.1), with a slowly varying amplitude function—i.e. $A^P(\mathbf{x})$ is approximated by the first order Taylor expansion coefficient—in the proximity of \mathbf{x}_0 the sound field is approximated as

$$P(\mathbf{x}, \omega) \approx P(\mathbf{x}_0, \omega) e^{-j \langle \mathbf{k}^P(\mathbf{x}_0) \cdot (\mathbf{x} - \mathbf{x}_0) \rangle}. \quad (2.14)$$

Therefore each point of an arbitrary sound field is approximated as a local elementary plane wave, with the wavenumber and angular frequency given by $\mathbf{k}^P(\mathbf{x})$ and ω , respectively.

Furthermore expressing the gradient of the local plane wave representation (2.14) leads to the high-frequency gradient approximation (2.12), which is therefore obviously the gradient of locally plane wave fields.

Application example: Stereophony

As a simple application example for the local wavenumber vector concept the resultant sound field of two 3D point sources is investigated, modeling a stereo loudspeaker pair.

The point sources are positioned at a $\mathbf{x}_1 = [x_1, y_1, z_1 = 0]^T$, $\mathbf{x}_2 = [-x_1, y_1, z_1 = 0]^T$ in a standard stereo ensemble with the stereo axis being the y -axis, illustrated in Figure 2.3 [Hav+08]. In the case of *amplitude panning* the sources are driven in-phase, with only their frequency independent amplitude factor A_1, A_2 differing. The resultant sound field reads

$$P(\mathbf{x}, \omega) = \frac{A_1}{4\pi} \frac{e^{-j\frac{\omega}{c}|\mathbf{x}-\mathbf{x}_1|}}{|\mathbf{x}-\mathbf{x}_1|} + \frac{A_2}{4\pi} \frac{e^{-j\frac{\omega}{c}|\mathbf{x}-\mathbf{x}_2|}}{|\mathbf{x}-\mathbf{x}_2|}. \quad (2.15)$$

Generally the phase of the resultant field and the local wavenumber vector is described by a complex formula, derived in C.1. From the aspect of stereophonic applications only the investigation of the local propagation direction on the stereo axis

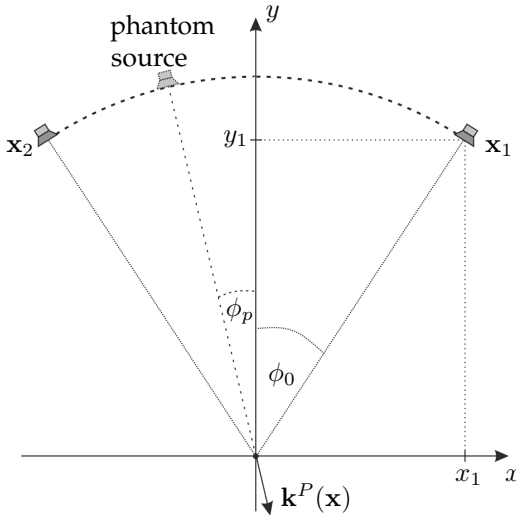


Figure 2.3. General two-channel stereophonic geometry consisting of two point sources positioned symmetrically to the y -axis, termed the *stereo axis*. The *aperture angle* is usually set to $2\phi_0 = 60^\circ$ and the listener's position is at the origin [Rum01]. Simple amplitude panning techniques apply an intensity difference between the loudspeaker pair, so that the listener perceives the illusion of a single sound source placed on the *active arc*, between the two loudspeakers, termed the *phantom source*.

is of importance at the plane of the sources (i.e. $z = 0$), since the listener's position is assumed to be at the origin. On the stereo axis $x = 0$ the local wavenumber vector simplifies to

$$\mathbf{k}^P(0, y, 0) = -\nabla_{\mathbf{x}} \phi^P(\mathbf{x}, \omega) \Big|_{x=0, z=0} = k \begin{bmatrix} \frac{A_1 - A_2}{A_1 + A_2} \frac{x - x_1}{|\mathbf{x} - \mathbf{x}_1|} \\ \frac{y - y_1}{|\mathbf{x} - \mathbf{x}_1|} \\ \frac{z - z_1}{|\mathbf{x} - \mathbf{x}_1|} = 0 \end{bmatrix}. \quad (2.16)$$

Hence, the local wavenumber vector and the position of the phantom source can be steered in the listener's position by applying proper frequency independent gains to the point source pair. The local wavenumber vector for a general stereophonic scenario is illustrated in Figure 2.4

From (2.16) the gain factors may be expressed assuming that the position of the phantom source or the target propagation direction angle measured from the stereo axis is known, denoted by ϕ_p in Figure (2.3). The local propagation angle of the resultant field at the origin $\mathbf{0}$ can be expressed from the local wavenumber components as

$$\tan \phi_p = \frac{k_x^P(\mathbf{0})}{k_y^P(\mathbf{0})} = \frac{A_1 - A_2}{A_1 + A_2} \frac{x_1}{y_1}. \quad (2.17)$$

Exploiting, that $\tan \phi_0 = \frac{x_1}{y_1}$ leads to the formula

$$\frac{A_1 - A_2}{A_1 + A_2} = \frac{\tan \phi_p}{\tan \phi_0}, \quad (2.18)$$

which is identical to the well-known *tangent law* of stereophony [Ben+08; Pul97; Pul01a; Pul01b], originally derived using different considerations [Ben+85]. The tangent law therefore ensures the matching of the local propagation directions of the target field and the produced wavefronts in the proximity of the listener's position.

Obviously the tangent law only expresses the relationship between A_1 and A_2 , the exact gain factors can be calculated by applying some type of normalizing strategy [Moo90]. A frequently used strategy is keeping the power at a constant value by requiring $A_1^2 + A_2^2 = \text{constant}$. Alternatively it may be exploited, that the amplitude of

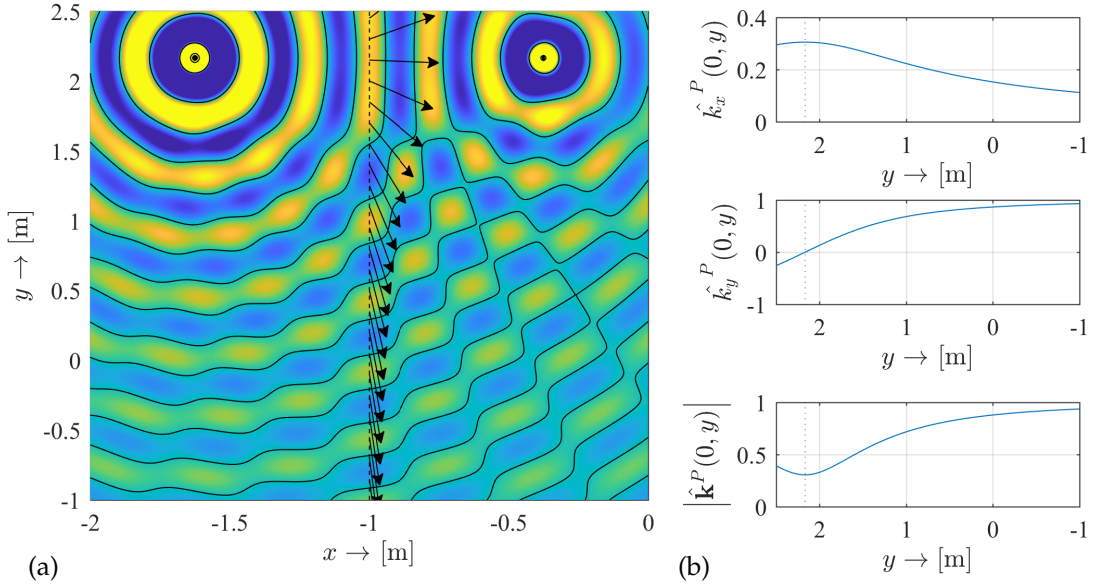


Figure 2.4. Sound field generated in a typical stereo setup. The point sources are positioned with a base angle of $\phi_0 = 30^\circ$ with their distance from the origin being $R_0 = 2.5$ m. The gain factors A_1, A_2 were selected so that the angle of the local wavenumber vector at the origin would equal to $\phi_p = 10^\circ$. In figure (a) contour lines indicate iso-phase surfaces, with the normalized local wavenumber vector displayed along the stereo axis. Figure (b) shows the normalized wavenumber components along $x = 0$. Note, that due to enhanced interference phenomena the amplitude changes rapidly, and the local dispersion relation (2.6) does not hold. The length of the wavenumber vector therefore decreases between the sources, where standing waves may occur, and increases to infinity on the parts where the amplitude vanishes and the phase changes rapidly due to destructive interference.

the resultant field on the stereo axis is given by $\frac{1}{4\pi} \frac{A_1+A_2}{|\mathbf{x}-\mathbf{x}_1|}$ (as given by (C.10)) in order to match the amplitude to that of e.g. a phantom point source.

2.2 The Kirchhoff approximation

The Kirchhoff approximation is an important high-frequency asymptotic approximation of the Kirchhoff-Helmholtz integral. Based on the equivalent scattering interpretation, the simple source formulation may be simplified in the high-frequency region using the *Kirchhoff/Physical optics approximation*, applied frequently to estimate scattering from random surfaces [Tsa+00; Vor99].

In order to approximate the scattered field—and its normal derivative on the scatterer surface—two approximations are applied:

- As a first simplification, the *tangent plane approximation* is applied on the illuminated region. It is assumed, that there exists a local relation between the incident and the scattered field at each point on the surface. By assuming that the incident wave is reflected locally according to the Snell's law [Vor07]—its amplitude changes according to the local *reflection index*, with the angle of incidence equaling the angle of reflection measured from the local normal—the

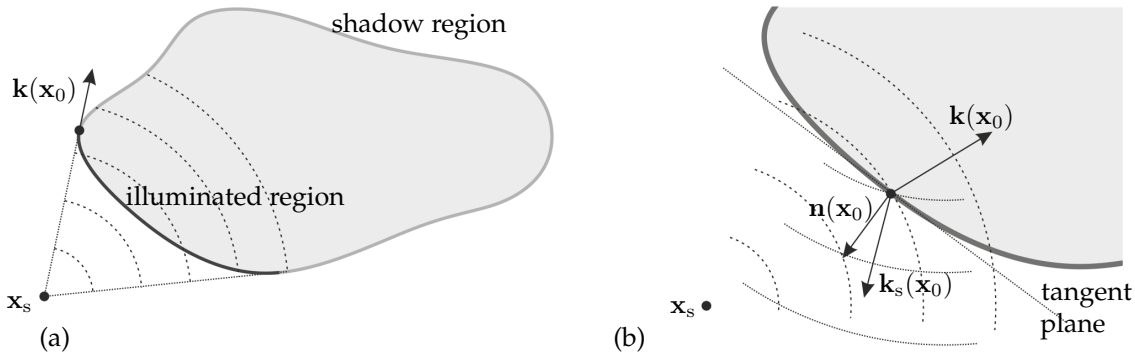


Figure 2.5. Illustration of the geometrical optics approximation (a) and the tangent plane approximation (b)

following relations are yielded for a sound soft scatterer [Ble84; Ble+00; PS02] (see Figure 2.5 (b))

$$P_s(x_0, \omega) = -P(x_0, \omega), \quad \frac{\partial}{\partial n_{in}} P_s(x_0, \omega) = -\frac{\partial}{\partial n_{out}} P(x_0, \omega), \quad x_0 \in \partial\Omega. \quad (2.19)$$

The approximation therefore calculates the reflected wave field by modeling each point on the scatterer with a tangential infinite plane. Obviously, the method also neglects the secondary reflections due to locally reacting assumptions. Furthermore, for low-frequencies and non-smooth boundaries the surface can not be considered locally planar, introducing further artifacts. In order to overcome these limitations several curvature correctional and iterative approaches exist [EG04].

- According to *geometrical optics* or *ray acoustics* the scatterer surface is divided into an *illuminated* and a *shadow region*: only those parts of the scatterer surface contribute to the scattered field that are directly illuminated by the primary source, i.e. where the local propagation directions of the incident and the scattered field—determined locally by the scatterer surface normal—coincide. In the field of high-frequency boundary element method this is termed as *determining the visible elements* on the boundary [Her+03]. Mathematically this requirement is formulated as weighting the integral, describing the scattered field by the windowing function

$$w(x_0) = \begin{cases} 1, & \forall \langle k(x_0) \cdot n_i(x_0) \rangle > 0 \\ 0 & \text{elsewhere,} \end{cases} \quad (2.20)$$

where $k(x_0)$ denotes the local wavenumber vector of the incident sound field at x_0 and $n_i(x_0)$ is the inward normal of the surface elements. For an illustration see Figure 2.5 (a). This windowing means the neglection of both diffracting waves around the scattering object (as well as so-called *creeping rays* [Ble84]) and reflections from one part of the scatterer to an other [Pig+15]. Due to this latter restriction the Kirchhoff approximation may be applied only to convex surfaces, free of secondary reflections.

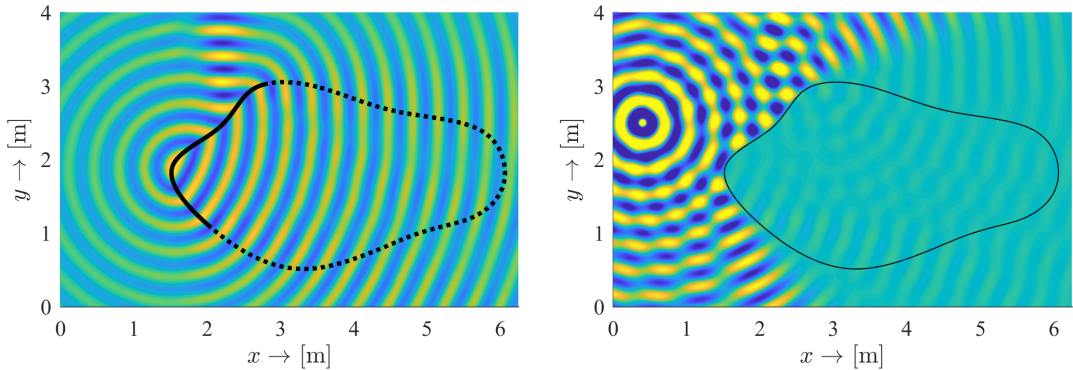


Figure 2.6. Illustration of Kirchhoff approximation in a 2D problem ($\Omega \subset \mathbb{R}^2$). In (a) the illuminated/active part of the scatterer contour is denoted by solid black line, whilst the shadow region by dotted line.

Introducing the window function and (2.19) written in terms of the inward normal vector into the simple source formulation, one obtains the Kirchhoff-approximation of the KHIE

$$\oint_{\partial\Omega} -2w(\mathbf{x}_0) \frac{\partial P(\mathbf{x}_0, \omega)}{\partial \mathbf{n}_{in}} G(\mathbf{x}|\mathbf{x}_0, \omega) d\partial\Omega(\mathbf{x}_0) \approx \begin{cases} P(\mathbf{x}, \omega) & \forall \mathbf{x} \in \Omega_i \\ P = -P_s & \forall \mathbf{x} \in \partial\Omega \\ -P_s(\mathbf{x}, \omega) & \forall \mathbf{x} \in \Omega_e, \end{cases} \quad (2.21)$$

giving a fair approximation for smooth, convex surfaces in the high frequency region, where the wavelength is significantly smaller, than the dimensions of the scattering object³. For the result of applying the approximation for the previous 2D example see Figure 2.6. Note, that the lack of diffractive waves around the enclosure gives rise to artifacts on parts of the space, where the local propagation direction of the incident field is approximately parallel to the contour.

2.3 The stationary phase approximation

The section introduces a basic tool of asymptotic analysis, the *stationary phase approximation (SPA)*. The method is applied to evaluate complex integrals by considering the greatest contribution stemming from critical points in the integral path. In the following chapters the SPA allows to extract asymptotic, local solutions from the global ones for radiation and reproduction problems written in terms of either boundary or spectral integrals.

³According to [BH75, Eq.(2.7.12)] the approximation holds when $k\rho_i \gg 1$, where ρ_i are the principal radii of the curved scatterer locally, and k is the wavenumber.

2.3.1 The integral approximation

Generally speaking the SPA yields approximate solutions of complex integrals of the form

$$I_{1D} = \int_{-\infty}^{\infty} F(z) e^{j\phi(z)} dz, \quad I_{nD} = \int_{\partial\Omega} F(\mathbf{x}) e^{j\phi(\mathbf{x})} d\partial\Omega(\mathbf{x}) \quad (2.22)$$

in one and n dimensions, respectively, with $\mathbf{x} \in \mathbb{R}^n$, when $e^{j\phi(\mathbf{x})}$ is highly oscillating and $F(\mathbf{x})$ is comparably slowly varying.

For the 1D case a rigorous derivation of the SPA based on integration by parts is given in [Ble84; BH75; Wil99]. More informally the method relies on the second order truncated Taylor series of the exponent around z^* , where $\phi'_z(z^*) = 0$ and $\phi''_{zz}(z^*) \neq 0$, with $\phi'_z(z)$ denoting the derivative with respect to z :

$$\phi(z) \approx \phi(z^*) + \frac{1}{2}\phi''_{zz}(z^*)(z - z^*)^2. \quad (2.23)$$

Point z^* is termed the *stationary point*. Supposing that $F(z)$ is a slowly varying smooth function compared to $\phi(z)$, it is assumed, that where the phase varies, i.e. $\phi'_z(z) \neq 0$, the integral of rapid oscillation cancels out, thus the greatest contribution to the total integral comes from the immediate surroundings of the stationary point. Moreover in the proximity of the stationary point $F(z)$ can be regarded as constant with the value $F(z^*)$. With these considerations the integral becomes

$$I_{1D} \approx F(z^*) e^{+j\phi(z^*)} \int_{-\infty}^{\infty} e^{+j\frac{1}{2}\phi''_{zz}(z^*)(z-z^*)^2} dz. \quad (2.24)$$

The remaining integral can be evaluated and the SPA of (2.22) becomes [BH75, Ch. 2.8]

$$I_{1D} \approx \sqrt{\frac{2\pi}{|\phi''_{zz}(z^*)|}} F(z^*) e^{+j\phi(z^*) + j\frac{\pi}{4} \operatorname{sgn}(\phi''_{zz}(z^*))}. \quad (2.25)$$

Similarly, in higher dimensions the stationary point \mathbf{x}^* (or more precisely a *simple stationary point*) is defined as

$$\begin{aligned} \nabla_{\mathbf{x}} \phi(\mathbf{x})|_{\mathbf{x}=\mathbf{x}^*} &= 0, \\ \det H(\mathbf{x}^*) &\neq 0, \quad H_{ij}(\mathbf{x}^*) = \left[\frac{\partial^2 \phi(\mathbf{x})}{\partial x_i \partial x_j} \right]_{\mathbf{x}=\mathbf{x}^*}, \quad i, j = 1, 2, \dots, n, \end{aligned} \quad (2.26)$$

with H being the Hessian matrix of the phase function. The multidimensional formula for the integral value reads

$$I_{nD} \approx \sqrt{\frac{(2\pi)^n}{|\det H(\mathbf{x}^*)|}} F(\mathbf{x}^*) e^{j\phi(\mathbf{x}^*) + j\frac{\pi}{4} \operatorname{sgn}(H(\mathbf{x}^*))}, \quad (2.27)$$

where $\text{sgn}(H(\mathbf{x}^*))$ is the signature of the Hessian: the number of positive eigenvalues minus the number of negative eigenvalues [Ble+00].

In the followings the physical interpretation of the SPA is discussed when applied to boundary and spectral integrals of sound fields, and simple examples are given for its application. The conclusions of the presented examples will be further utilized in the following chapters.

2.3.2 Asymptotic approximation of boundary integrals

For the sake of simplicity first the physical interpretation of the stationary position is discussed for the case when the SPA is applied for boundary integrals trough the example of the Rayleigh I integral.

Assume, that the Rayleigh integral describes an arbitrary sound field at $y > y_0$ in terms of the boundary integral along the plane $\mathbf{x}_0 = [x_0, y = y_0, z_0]^T$ according to (1.65): Since for the application of the SPA high-frequency conditions are standard prerequisites, therefore the high-frequency gradient approximation (2.12) may be applied, resulting in the high-frequency Rayleigh integral

$$P(\mathbf{x}, \omega) = 2 \iint_{-\infty}^{\infty} j k_y^P(\mathbf{x}_0) P(\mathbf{x}_0, \omega) G(\mathbf{x} - \mathbf{x}_0, \omega) d\mathbf{x}_0 dz_0. \quad (2.28)$$

Suppose that the Rayleigh integral is to be evaluated applying the SPA at a given receiver position \mathbf{x} . The involved functions written in polar form read

$$P(\mathbf{x}, \omega) = -2 \iint_{-\infty}^{\infty} \phi_y^{P'}(\mathbf{x}_0, \omega) A^P(\mathbf{x}_0, \omega) A^G(\mathbf{x} - \mathbf{x}_0, \omega) e^{j(\phi^P(\mathbf{x}_0, \omega) + \phi^G(\mathbf{x} - \mathbf{x}_0, \omega) + \frac{\pi}{4})} d\mathbf{x}_0 dz_0. \quad (2.29)$$

By definition, the stationary position for the integral is found where the phase gradient vanishes. Exploiting that the constant phase shift $\frac{\pi}{4}$ vanishes due to differentiation and applying the chain rule, the stationary position for a given receiver position $\mathbf{x}_0^*(\mathbf{x})$ is found, where

$$\begin{aligned} \left[\begin{array}{c} \frac{\partial}{\partial x_0} \\ \frac{\partial}{\partial z_0} \end{array} \right] \phi^P(\mathbf{x}_0^*(\mathbf{x}), \omega) &= - \left[\begin{array}{c} \frac{\partial}{\partial x_0} \\ \frac{\partial}{\partial z_0} \end{array} \right] \phi^G(\mathbf{x} - \mathbf{x}_0^*(\mathbf{x}), \omega) \\ k_x^P(\mathbf{x}_0^*(\mathbf{x})) &= k_x^G(\mathbf{x} - \mathbf{x}_0^*(\mathbf{x})) \\ k_z^P(\mathbf{x}_0^*(\mathbf{x})) &= k_z^G(\mathbf{x} - \mathbf{x}_0^*(\mathbf{x})) \end{aligned} \quad (2.30)$$

holds. Assuming that the local dispersion relation holds—valid under high-frequency conditions and for simple sound fields, e.g. for the Green's function—two components completely determine the local wavenumber vector. In the stationary position therefore

$$\mathbf{k}^P(\mathbf{x}_0^*(\mathbf{x})) = \mathbf{k}^G(\mathbf{x} - \mathbf{x}_0^*(\mathbf{x})) = -\mathbf{k}^G(\mathbf{x}_0^*(\mathbf{x}) - \mathbf{x}) \quad (2.31)$$

satisfies. Note, that in the right hand side the reciprocity of the Green's function was exploited.

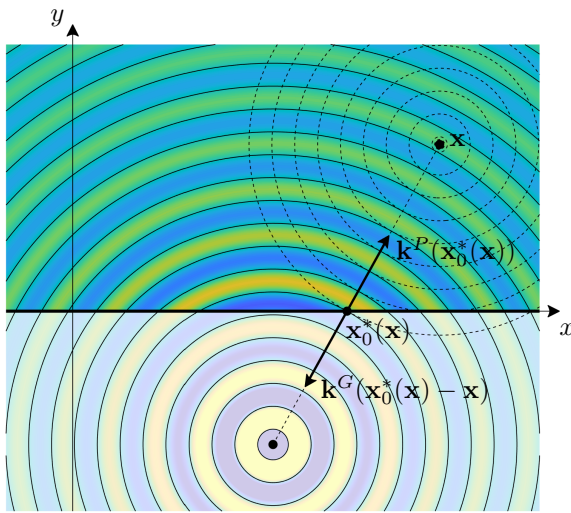


Figure 2.7. 2D Geometry for the physical interpretation of the stationary position for the Rayleigh integral. The stationary position is found along the integral surface/line where the local propagation direction—and the local wavenumber vector—of the described wave field and the spherical field of a point source positioned at \mathbf{x} coincide. Equivalently, it means, that the local propagation direction of the described field at $\mathbf{x}_0^*(\mathbf{x})$ equals with that of the Green's function positioned at $\mathbf{x}_0^*(\mathbf{x})$, measured at the receiver position \mathbf{x} .

Hence, the SPA ‘compares’ the propagation direction/wavefronts of the described field and the Green’s function along the integral path. The stationary position for a given receiver position is then given by that point $\mathbf{x}_0^*(\mathbf{x})$, where the local propagation direction of the described wave field coincides with that of a point source positioned at the receiver position \mathbf{x} . Obviously, by placing back the 3D Green’s function into the $\mathbf{x}_0^*(\mathbf{x})$, its wavenumber vector at \mathbf{x} will coincide with the described field’s wavenumber vector. In other words, since the Rayleigh integral describes an arbitrary sound field as the resultant field of point sources, for a given receiver point that point source will have the greatest contribution, that’s sound field propagates into the same direction as the target sound field in the receiver point.

This interpretation is illustrated in Figure 2.7 via the example of a 2D point source described by the 2D Rayleigh integral. In the 2D case $k_z^P(\mathbf{x}) = k_z^G(\mathbf{x} - \mathbf{x}_0) \equiv 0$ and the stationary point is found where $k_x^P(\mathbf{x}_0^*(\mathbf{x})) = k_x^G(\mathbf{x} - \mathbf{x}_0^*(\mathbf{x}))$ holds. For the case of a point source at \mathbf{x}_s the stationary position is found at the intersection of vector $\mathbf{x} - \mathbf{x}_s$ and the integration path.

Application example #1: Asymptotic evaluation of the Rayleigh integral

As an application example for the stationary phase approximation the evaluation of the Rayleigh integral written onto the $y = y_0$ plane, around the stationary point is investigated in further details. In the present case a general non-convergent primary sound field is assumed, with all the sources of sound located behind the Rayleigh plane, i.e. at the $y < y_0$ half-space.

As discussed in the foregoing the stationary position for the Rayleigh integral is found, where

$$\mathbf{k}^P(\mathbf{x}_0^*(\mathbf{x})) = \mathbf{k}^G(\mathbf{x} - \mathbf{x}_0^*(\mathbf{x})) \quad (2.32)$$

is satisfied. As a simple example, if the primary field is a spherical one, the stationary point is found at the intersection of the Rayleigh plane and the vector pointing from the source into the evaluation position.

In order to evaluate integral (2.28) around the stationary position according to (2.27) with $n = 2$, the signature and the determinant of the Hessian is required, defined by the quadratic form

$$H = \begin{bmatrix} \frac{\partial}{\partial x_0} \\ \frac{\partial}{\partial z_0} \end{bmatrix} \left[\phi^P(\mathbf{x}_0) + \phi^G(\mathbf{x} - \mathbf{x}_0) \right] \begin{bmatrix} \frac{\partial}{\partial x_0} \\ \frac{\partial}{\partial z_0} \end{bmatrix}^T. \quad (2.33)$$

At the stationary point the Hessian can be expressed in terms of the principal curvatures of the described sound field κ_1^P, κ_2^P and the Green's function κ_1^G, κ_2^G as discussed in details in B.1:

$$H = -k\mathbf{V} \begin{bmatrix} \kappa_1^P(\mathbf{x}_0^*(\mathbf{x})) + \kappa_1^G(\mathbf{x} - \mathbf{x}_0^*(\mathbf{x})) & 0 \\ 0 & \kappa_2^P(\mathbf{x}_0^*(\mathbf{x})) + \kappa_2^G(\mathbf{x} - \mathbf{x}_0^*(\mathbf{x})) \end{bmatrix} \mathbf{V}^T, \quad (2.34)$$

with $\mathbf{V} = \begin{bmatrix} v_{1x} & v_{2x} \\ v_{1z} & v_{2z} \end{bmatrix}$ are the components of the principal directions corresponding to κ_1 and κ_2 . Since the determinant is multiplicative, the determinant of the 2D Hessian reads as

$$\det H = k^2 \left(\kappa_1^P(\mathbf{x}_0^*(\mathbf{x})) + \kappa_1^G(\mathbf{x} - \mathbf{x}_0^*(\mathbf{x})) \right) \left(\kappa_2^P(\mathbf{x}_0^*(\mathbf{x})) + \kappa_2^G(\mathbf{x} - \mathbf{x}_0^*(\mathbf{x})) \right) \underbrace{(v_{1x}v_{2z} - v_{2x}v_{1z})^2}_{\hat{k}_y^P(\mathbf{x}_0^*(\mathbf{x}))^2}, \quad (2.35)$$

where the underbraced part is—by the definition of the cross product—the y -coordinate of a vector being perpendicular to \mathbf{v}_1 and \mathbf{v}_2 , i.e. of the normalized local wavenumber vector.

By considering, that for a divergent field both curvatures of the wavefront are positive and the signature of the Hessian equals (-2), the SPA of the Rayleigh integral reads as

$$P(\mathbf{x}, \omega) = 4\pi \frac{1}{\sqrt{(\kappa_1^P(\mathbf{x}_0^*(\mathbf{x})) + \kappa_1^G(\mathbf{x} - \mathbf{x}_0^*(\mathbf{x})))} \sqrt{(\kappa_2^P(\mathbf{x}_0^*(\mathbf{x})) + \kappa_2^G(\mathbf{x} - \mathbf{x}_0^*(\mathbf{x})))}} P(\mathbf{x}_0^*(\mathbf{x}), \omega) G(\mathbf{x} - \mathbf{x}_0^*(\mathbf{x}), \omega). \quad (2.36)$$

Expressing the correction factor in terms of the principal radii, expressing the Green's function by its explicit formula and exploiting, that $\kappa_1^G(\mathbf{x} - \mathbf{x}_0^*(\mathbf{x})) = \kappa_2^G(\mathbf{x} - \mathbf{x}_0^*(\mathbf{x})) = |\mathbf{x} - \mathbf{x}_0^*(\mathbf{x})|$ the asymptotic Rayleigh integral reads as

$$P(\mathbf{x}, \omega) = \sqrt{\frac{\rho_1^P(\mathbf{x}_0^*(\mathbf{x})) \rho_2^P(\mathbf{x}_0^*(\mathbf{x}))}{(\rho_1^P(\mathbf{x}_0^*(\mathbf{x})) + |\mathbf{x} - \mathbf{x}_0^*(\mathbf{x})|) (\rho_2^P(\mathbf{x}_0^*(\mathbf{x})) + |\mathbf{x} - \mathbf{x}_0^*(\mathbf{x})|)}} P(\mathbf{x}_0^*(\mathbf{x}), \omega) e^{-jk|\mathbf{x} - \mathbf{x}_0^*(\mathbf{x})|}. \quad (2.37)$$

Finally, by applying that according to (B.24) $\rho_i^P(\mathbf{x}) = \rho_i^P(\mathbf{x}_0^*(\mathbf{x})) + |\mathbf{x} - \mathbf{x}_0^*(\mathbf{x})|$ holds, the asymptotic formula takes the form.

$$P(\mathbf{x}, \omega) = \sqrt{\frac{\rho_1^P(\mathbf{x}_0^*(\mathbf{x})) \cdot \rho_2^P(\mathbf{x}_0^*(\mathbf{x}))}{\rho_1^P(\mathbf{x}) \cdot \rho_2^P(\mathbf{x})}} P(\mathbf{x}_0^*(\mathbf{x}), \omega) e^{-j\omega \frac{|\mathbf{x} - \mathbf{x}_0^*(\mathbf{x})|}{c}}, \quad (2.38)$$

where $\rho_1^P \cdot \rho_2^P$ is the reciprocal of the Gaussian curvature of the wavefront. The equation reflects the fact, that the intensity of a 3D wave field is proportional to the Gaussian curvature of the wavefront, being a well-known fact in the field of optics [BW70, Sec. 3.1], [Bou+97, Sec. 1.3]. Thus, in a ray-tracing manner the wave field is approximated locally by its value at the stationary position: the numerator of the amplitude factor approximates the pressure field amplitude in the source position, attenuated by the denominator—describing the attenuation factor for the source-to-receiver position—, given by (3.76), while a simple phase shift term corresponds to the propagation time delay.

Application example #2: The Kirchhoff approximation

As a further application for the stationary phase method for boundary integrals an alternative derivation of the Kirchhoff-approximation is presented. Suppose, that an interior radiation problem is described by the Kirchhoff-Helmholtz integral inside an enclosure Ω , bounded by $\partial\Omega$. The field is given by

$$P(\mathbf{x}, \omega) = \oint_{\partial\Omega} - \left(\frac{\partial P(\mathbf{x}_0, \omega)}{\partial \mathbf{n}_{in}} G(\mathbf{x} - \mathbf{x}_0, \omega) - P(\mathbf{x}_0, \omega) \frac{\partial G(\mathbf{x} - \mathbf{x}_0, \omega)}{\partial \mathbf{n}_{in}} \right) d\partial\Omega(\mathbf{x}_0). \quad (2.39)$$

Assuming high-frequency conditions both the sound field and the Green's function normal derivatives may be approximated using the high-frequency gradient approximation, resulting in

$$P(\mathbf{x}, \omega) = \oint_{\partial\Omega} \left(jk_n^P(\mathbf{x}_0) + jk_n^G(\mathbf{x} - \mathbf{x}_0) \right) P(\mathbf{x}_0, \omega) G(\mathbf{x} - \mathbf{x}_0, \omega) d\partial\Omega(\mathbf{x}_0). \quad (2.40)$$

Again, it can be assumed that for a given receiver position \mathbf{x} most part of the integral cancels out, and the field is dominated by one particular point on the surface, i.e. by the stationary point. Obviously, the stationary point is found on $\partial\Omega$ where the phase gradient vanishes, i.e. where the local wavenumber vector/local propagation direction of the described sound field, and the Green's function positioned at \mathbf{x} coincide: $\mathbf{k}^P(\mathbf{x}_0) = -\mathbf{k}^G(\mathbf{x}_0 - \mathbf{x})$. This interpretation is illustrated in Figure 2.8 in case of a primary point source.

As an approximation therefore the amplitude factor of the integral can be substituted by its value at the stationary point, i.e. with $k_n^G(\mathbf{x} - \mathbf{x}_0) = k_n^P(\mathbf{x}_0)$. Furthermore, only that part of the integral path contributes to the total sound field, that serves as a stationary point for any receiver position inside the enclosure, resulting in the windowing function (2.20) and the KHIE may be further simplified towards

$$P(\mathbf{x}, \omega) = \oint_{\partial\Omega} 2w(\mathbf{x}_0) jk_n^P(\mathbf{x}_0) P(\mathbf{x}_0, \omega) G(\mathbf{x} - \mathbf{x}_0, \omega) d\partial\Omega(\mathbf{x}_0). \quad (2.41)$$

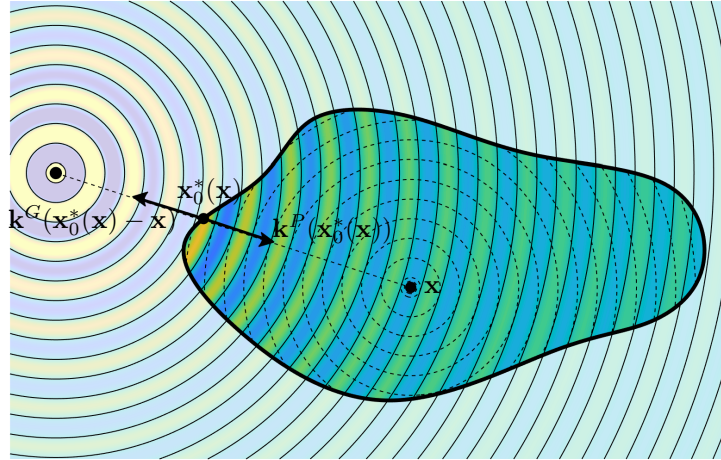


Figure 2.8. 2D Geometry for the illustration of the stationary position for the Kirchhoff-Helmholtz integral.

This is obviously—since high-frequency assumptions must hold—equivalent to the Kirchhoff-approximation (2.21), derived by physically motivated considerations from the simple source formulation.

2.3.3 Asymptotic approximation of spectral integrals

Clearly, there is a strong relationship between the local wavenumber vector concept and the plane wave decomposition/angular spectrum of sound fields. The relation is established by the SPA. Consider the forward and inverse Fourier transform of a general polar form sound field $P(\mathbf{x}, \omega)$ given by (2.1)

$$\tilde{P}(k_x, y, k_z, \omega) = \iint_{-\infty}^{\infty} A^P(\mathbf{x}, \omega) e^{j\phi^P(\mathbf{x}, \omega)} e^{jk_x x} e^{jk_z z} dx dz, \quad (2.42)$$

$$P(\mathbf{x}, \omega) = \frac{1}{(2\pi)^2} \iint_{-\infty}^{\infty} A^{\tilde{P}}(k_x, y, k_z, \omega) e^{j\Phi^{\tilde{P}}(k_x, y, k_z, \omega)} e^{-jk_x x} e^{-jk_z z} dk_x dk_z, \quad (2.43)$$

with $\tilde{P}(k_x, y, k_z, \omega) = A^{\tilde{P}}(k_x, y, k_z, \omega) e^{j\Phi^{\tilde{P}}(k_x, y, k_z, \omega)}$. The forward and inverse transforms describe projecting and composing the sound field P to and from *spectral plane waves*, that's propagation direction i.e. wavenumber components are completely determined by k_x and k_z along with the physical wavenumber k via the dispersion relation.

Supposing that the sound field fulfills the SPA requirements—i.e. high frequency assumptions—the forward transform (2.42) may be evaluated asymptotically applying the stationary phase method [Arn95; TM05]. The stationary point $\mathbf{x}^*(k_x, k_z)$ is found for a given k_x and k_z , where the gradient of the exponent is zero, thus where

$$\frac{\partial}{\partial x} \phi^P(\mathbf{x}^*(k_x, k_z), \omega) + k_x = 0 \rightarrow k_x^P(\mathbf{x}^*(k_x, k_z)) = k_x, \quad (2.44)$$

$$\frac{\partial}{\partial z} \phi^P(\mathbf{x}^*(k_x, k_z), \omega) + k_z = 0 \rightarrow k_z^P(\mathbf{x}^*(k_x, k_z)) = k_z \quad (2.45)$$

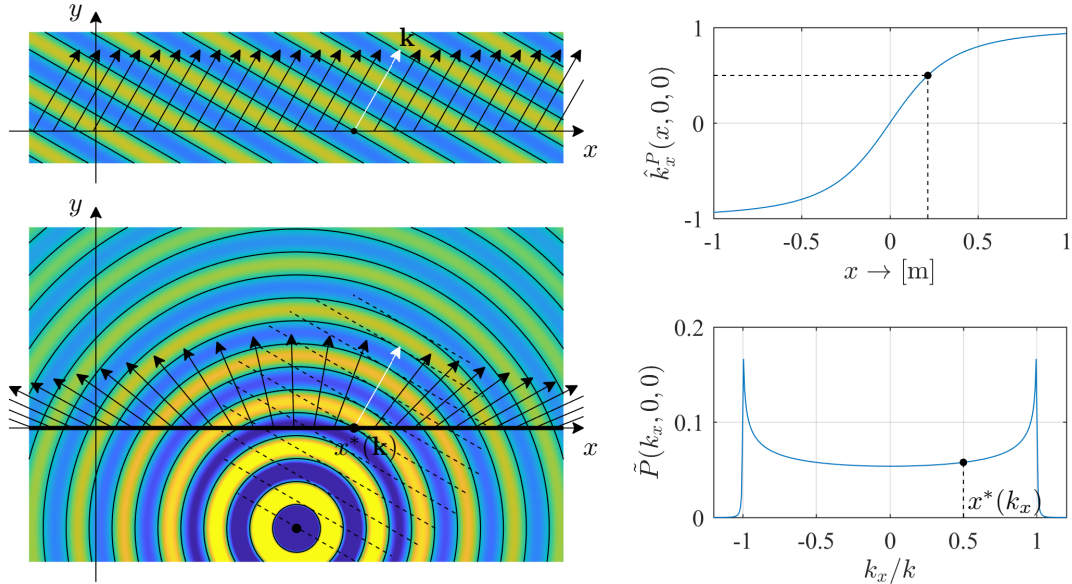


Figure 2.9. Illustration of the stationary phase approximation of the Fourier transform in case of a 3D point source with its one-dimensional Fourier-transform evaluated along the x -axis. Upper part of Figure (a) presents a spectral basis function (i.e. a plane wave), which is at this example chosen as $k_x = 0.5k$. For this spectral component the stationary phase point at the field of the point source is found, where the local propagation direction of the point source coincides with that of the plane wave—indicated by white arrow—. Coincidence of local propagation directions is ensured by the assumption, that in the plane of investigation $k_z^G(x, y, 0) \equiv 0$, and the spectral plane wave is assumed to propagate with $k_z = 0$. The spectrum, shown in Figure (c), given in Table (1.1) around $k_x = 0.5k$ will be dominated by this stationary position, denoted by $x^*(k_x)$ in Figure (b).

holds. Again, assuming that the local dispersion relation holds, two local wavenumber components completely define the local wavenumber vector and the stationary position for the spectral integral is found where $\mathbf{k}^P(\mathbf{x}^*(\mathbf{k})) = \mathbf{k}$ is satisfied, with \mathbf{k} being the wavenumber vector of the spectral plane wave.

This finding states, that each point in the plane wave spectrum of a sound field is dominated by the parts of the space, where the local propagation direction coincides with the corresponding spectral plane wave's propagation direction. The local wavenumber components therefore may be also defined as the stationary points of (2.42) as a function of space⁴. The interpretation of the asymptotic approximation of the Fourier transform is illustrated in Figure 2.9 for the transformation of a point source.

The counterpart of this statement is that the greatest contribution to the inverse transform (2.43) is associated to those plane waves—the stationary phase of the inverse integral for given \mathbf{x} —, whose wave number vector coincide with the local wavenumber components of the sound field at \mathbf{x} .

Note, that here it is assumed, that in the region of investigation (an infinite plane or line, depending on the transform dimensionality) the stationary phase position and thus each propagation direction is unique. This trivially does not hold for the case of e.g. a plane wave, or complex acoustic fields. The SPA however can be extended

⁴This definition is often termed *Lagrange submanifolds* and play a central role in phase space representation of sound fields [Arn95; TM05; SM93]

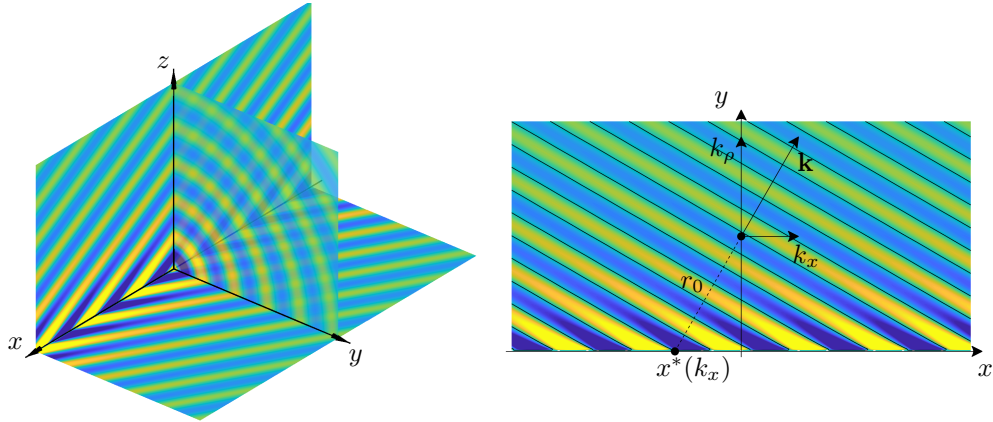


Figure 2.10. Illustration for the interpretation of the Green's function's spectrum as the field of a line source with harmonic spatial distribution described by wavenumber k_x , evaluated at $x = 0$. Such a source radiates a cylindrical symmetric sound field, with a radial wavenumber k_ρ and the longitudinal wavenumber k_x so that $k = \sqrt{k_x^2 + k_\rho^2}$ satisfies. For the case of $k_x = 0$ this equals to the field of the 2D Green's function. Using this interpretation an alternative geometric interpretation may be found for the stationary position of the integral definition (2.46): for a given wavenumber k_x and for a given $\mathbf{x} = [x = 0, y, z]^T$ that part of the x -axis will be a stationary point from which the emerging wavefront coincides with that of a plane wave with k_x in \mathbf{x} . From simple geometric considerations it is found at $x^*(k_x) = r_0 \frac{k_x}{k_\rho}$

for multiple stationary positions, and the result of the approximation is obtained by summing the SPA contributions over the stationary positions [Ble+00, p. 129]. In the present treatise this limitation is not investigated further, since the results involving the SPA of the Fourier transform hold without any modification for a virtual plane wave as a limiting case.

Application example #1: 1D spectrum of the Green's function

As a simple example consider the 1D Fourier transform of the field of a 3D point source. For the sake of simplicity the source is located at the origin, and the transform is taken along the x -dimension. The exact solution for the problem is available analytically, given by the second order Hankel function.

$$\tilde{P}(k_x, y, z, \omega) = \frac{1}{4\pi} \int_{-\infty}^{\infty} \frac{e^{-jk\sqrt{x^2+y^2+z^2}}}{\sqrt{x^2+y^2+z^2}} e^{jk_x x} dx = -\frac{j}{4} H_0^{(2)} \left(\sqrt{k^2 - k_x^2} \sqrt{y^2 + z^2} \right). \quad (2.46)$$

In this simple case, the stationary positions can be found explicitly for a given wavenumber component, and the SPA of the Fourier transform can be evaluated analytically. By definition, the stationary position for an arbitrary spectral wavenumber k_x is found, where the x -derivative of the phase function vanishes i.e. $x^*(k_x)$ satisfies

$$k \frac{x^*(k_x)}{\sqrt{x^*(k_x)^2 + y^2 + z^2}} = k_x \quad \rightarrow \quad x^*(k_x) = \sqrt{y^2 + z^2} \frac{k_x}{\sqrt{k^2 - k_x^2}} = r_0 \frac{k_x}{k_\rho}, \quad (2.47)$$

with $r_0 = \sqrt{y^2 + z^2}$ being the distance from the x -axis and $k_\rho = \sqrt{k^2 - k_x^2}$ being the corresponding radial wavenumber. For the geometric interpretation of the stationary point refer to Figure 2.9. At the stationary point the phase of the integrand and its second derivative reads

$$\phi^G(\mathbf{x}^*(k_x)) = -k\sqrt{x^*(k_x)^2 + y^2 + z^2} + k_x x^*(k_x) = -r_0 k_\rho, \quad (2.48)$$

$$\phi''_{xx}^G(\mathbf{x}^*(k_x)) = -k \frac{y^2 + z^2}{\sqrt{x^*(k_x)^2 + y^2 + z^2}^3} = -\frac{k_\rho^3}{k^2 r_0}. \quad (2.49)$$

Substitution into the SPA (2.25) with $\sqrt{x^*(k_x)^2 + y^2 + z^2} = r_0 \frac{k}{\sqrt{k^2 - k_x^2}}$ and taking the negative sign of the second derivative into account yields the asymptotic form of the 3D point source spectrum

$$\tilde{P}(k_x, y, z, \omega) = -\frac{j}{4} H_0^{(2)}(k_\rho r_0) \approx \frac{1}{\sqrt{8\pi j}} \frac{e^{-jr_0 k_\rho}}{\sqrt{r_0 k_\rho}}. \quad (2.50)$$

This result is the Hankel function's well-known asymptotic expansion for large arguments [Olv+10a, p. 10.17.6]

$$H_0^{(2)}(z) \approx \sqrt{\frac{2j}{\pi z}} e^{-jz}. \quad (2.51)$$

Furthermore, the DC ($k_x = 0$) component of the spectrum of the 3D Green's function describes the sound field generated by an infinite line source along the x -axis, i.e. the approximation of the 2D Green's function which therefore stems from the direct asymptotic approximation of (1.45) by the SPA [Wil99, p. 118]

$$G_{2D}(\mathbf{x}, \omega) \approx \frac{1}{\sqrt{8\pi j}} \frac{e^{-jk|\mathbf{x}|}}{\sqrt{k|\mathbf{x}|}} = \sqrt{\frac{2\pi|\mathbf{x}|}{jk}} G_{3D}(\mathbf{x}, \omega), \quad (2.52)$$

with $\mathbf{x} = [y, z]^T$. This result also verifies, that the 2D Green's function and the 3D Green's function's phase—and thus their local wavenumber vector—approximately equal in the high frequency region, with the 3D distances substituted with the 2D ones.

In case $k_x \neq 0$ equation (2.46) describes the sound field of an infinite line source with a harmonic spatial distribution, evaluated at $x = 0$. Obviously, this special statement only holds because the function to be Fourier transformed is the Green's function itself. Such a line source radiates attenuating plane wavefronts propagating radially away from the x -axis with the local wavenumber vector given by $\mathbf{k}^P(\mathbf{x}) = [k_x, k_\rho]^T$, illustrated in 2.10. For this special case the stationary position defined by (2.47) gains a simple geometrical interpretation, as presented in Figure 2.10.

Application example #2: 2D spectrum of the Green's function

As a second, brief example the 2D Fourier transform of the Green's function, positioned at the origin is discussed. The Fourier transform reads as

$$\tilde{P}(k_y, y, k_z) = \iint_{-\infty}^{\infty} G(x, y, z) e^{jk_x x} e^{jk_z z} dx dz. \quad (2.53)$$

The stationary point for the integral is found on a fixed $y = \text{const}$ plane, where the local propagation direction of the spherical coincides with that of the spectral plane wave, described by k_x, k_z , i.e. where

$$k_x^G(x^*(k_x), y, z^*(k_z)) = k_x, \rightarrow k \frac{x^*(k_x)}{|x^*(k_x, k_z)|} = k_x \quad (2.54)$$

$$k_z^G(x^*(k_x), y, z^*(k_z)) = k_z, \rightarrow k \frac{z^*(k_z)}{|x^*(k_x, k_z)|} = k_z \quad (2.55)$$

$$\mathbf{k}^G(\mathbf{x}^*(k_x, k_z)) = \mathbf{k}, \rightarrow k \frac{y}{|x^*(k_x, k_z)|} = k_y \quad (2.56)$$

holds. As discussed in B.1 the determinant under consideration is given terms of the principal curvatures, known analytically for the Green's function. Also around the stationary position $k_y^G(\mathbf{x}^*(k_x, k_z)) = k_y$ holds, and the determinant reads as

$$\det H = k^2 \kappa_1^G(\mathbf{x}^*(k_x, k_z)) \kappa_2^G(\mathbf{x}^*(k_x, k_z)) \hat{k}^G(\mathbf{x}^*(k_x, k_z))^2 = \frac{k_y^2}{|\mathbf{x}^*(k_x, k_z)|^2}. \quad (2.57)$$

With taking the positive curvatures into consideration the signature of the Hessian equals (-2) and the 2D Fourier transform can be approximated by the 2D SPA as

$$\tilde{P}(k_y, y, k_z) = \frac{2\pi}{\sqrt{|\det H|}} \frac{1}{4\pi} \frac{e^{-jk|\mathbf{x}^*(k_x, k_z)|}}{|\mathbf{x}^*(k_x, k_z)|} e^{jk_x x^*(k_x)} e^{jk_z z^*(k_z)} e^{-j\frac{\pi}{2}}, \quad (2.58)$$

Substituting the determinant, and expressing the stationary positions by (2.54) leads finally to

$$\tilde{P}(k_y, y, k_z) = -\frac{j}{2} \frac{e^{-jk_y y}}{k_y} = -\frac{j}{2} \frac{e^{-j\sqrt{(\frac{\omega}{c})^2 - k_x^2 - k_z^2} y}}{\sqrt{(\frac{\omega}{c})^2 - k_x^2 - k_z^2}}. \quad (2.59)$$

Comparison with Table (1.1) reveals, that in this special case the 2D SPA yields the exact spectrum of the Green's function.

3

Theory of Sound Field Synthesis

In the followings the general Sound Field Synthesis problem is formulated. Consider a source-free volume $\Omega \subset \mathbb{R}^n$, bounded by a continuous set of acoustic sources forming the boundary surface $\partial\Omega$. The enclosing source ensemble is termed the *secondary source distribution (SSD)*. The general geometry is depicted in Figure 3.1. For the sake of simplicity we assume that the boundary is acoustically transparent and the secondary sources are acoustic point sources, i.e. described by the n -dimensional free field Green's function. Unless it is denoted otherwise, $G(\mathbf{x}, \omega)$ refers to the 3D Green's function in the followings. Since dynamic loudspeakers can be modeled as 3D monopoles in the low-frequency region, this choice of SSD elements is feasible.

With these assumptions the pressure at any $\mathbf{x} \in \Omega$ is given by the sum of the individual SSD elements, written as a single layer potential [Ahr12; Ahr10; Wie14; SS14]:

$$P(\mathbf{x}, \omega) = \oint_{\partial\Omega} D(\mathbf{x}_0, \omega) G(\mathbf{x} - \mathbf{x}_0, \omega) d\partial\Omega(\mathbf{x}_0). \quad (3.1)$$

The weighting factor $D(\mathbf{x}_0, \omega)$ is termed the *driving function* for the given SSD. The Sound Field Synthesis problem can be formulated as the following: Given a *target sound field*, or the sound field of a *virtual source* $P(\mathbf{x}, \omega)$, our aim is to solve the integral equation for $D(\mathbf{x}_0, \omega)$, so that the weighted sum of the SSD's sound field—i.e. the *synthesized field*—equals to the target sound field. The problem is therefore an inverse problem and has a unique solution for general enclosures.

Comparing the general SFS formulation (3.1) with the Kirchhoff-Helmholtz integral (1.55) it becomes clear that SFS with a single layer SSD is not able to ensure identically

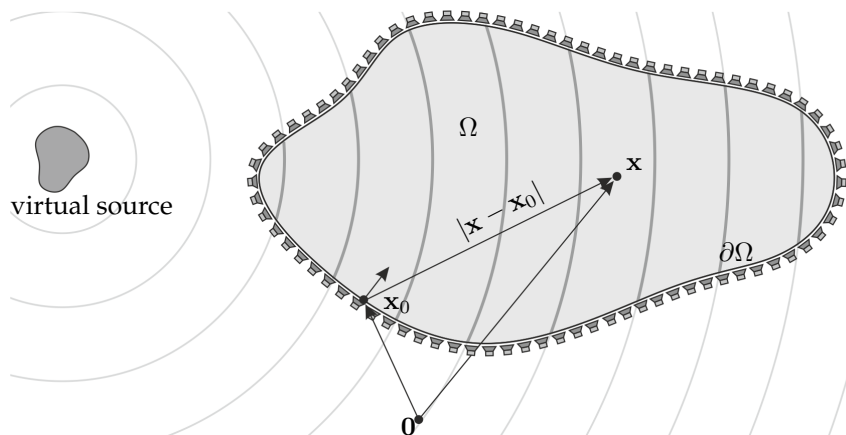


Figure 3.1. Geometry for the general Sound Field Synthesis problem

zero sound field outside the enclosure. Practically, the dipole sources that would cancel the field of the monopoles outside the volume are removed from the surface. In the present thesis free-field conditions are assumed: the exterior sound field satisfies the Sommerfeld radiation condition, thus the effect of the listening environment in practical applications is not considered. For the inclusion of room effects to the SFS problem refer to [Spo05].

So far only the general 3D SFS setup has been discussed. This requires an enclosing surface or an infinite planar distribution of 3D point sources, making practical implementations hardly realizable. In practice it is often sufficient to restrict the reproduction to the plane containing the 2D contour of secondary sources. This *synthesis plane* can be chosen at $z = 0$ without loss of generality. This reproduction scenario is termed *2.5D synthesis*, referring to the fact, that although the problem dimensionality is reduced to $n = 2$, still the 2D SSD contour consists of 3D point source elements. In this geometry the general 2.5D synthesis problem is formulated as

$$P(\mathbf{x}, \omega) = \oint_C D(x_0, y_0, 0, \omega) G(x - x_0, y - y_0, 0, \omega) ds(\mathbf{x}_0), \quad (3.2)$$

where $C(x_0, y_0)$ is the SSD contour and ds is the arc length. Obviously, neither 2D nor 3D sound fields can be perfectly synthesized in this geometry due to dimensionality inconsistency between the target field and the SSD. Overcoming the artifacts of this *dimensionality mismatch* is the central question of practical sound field synthesis and the main topic of the present chapter.

This chapter presents approaches to solve the 3D and 2.5D SFS problem including physically based implicit and particularly mathematical explicit solutions.

3.1 Implicit solution: Wave Field Synthesis

3.1.1 3D Wave Field Synthesis

Generally speaking, the implicit solution for the SFS problem aims at the derivation of an appropriate single layer potential representation of the target sound field, containing the required SSD driving functions implicitly. In case of a 3D SFS problem obtaining the implicit solution is straightforward, based on the boundary integral representations discussed in the previous chapters.

Assume a general enclosing 3D SSD surface consisting of 3D point sources. Comparing the Kirchhoff approximation of the Kirchhoff-Helmholtz integral (2.21) or (2.41) with the general SFS equation (3.1) reveals, that the Kirchhoff approximation implicitly contains the driving functions for a general enclosing SSD, and the driving function is given by

$$D(\mathbf{x}_0, \omega) = -2w(\mathbf{x}_0) \frac{\partial P(\mathbf{x}_0, \omega)}{\partial \mathbf{n}_{\text{in}}}, \quad (3.3)$$

or making use of the high-frequency gradient approximation

$$D(\mathbf{x}_0, \omega) = 2w(\mathbf{x}_0)jk_n^P(\mathbf{x}_0)P(\mathbf{x}_0, \omega) \quad (3.4)$$

with $k_n^P(\mathbf{x}_0)$ being the normal component of the target field's local wavenumber vector taken on the SSD and $w(\mathbf{x}_0)$ being the window function, as introduced in the previous chapter:

$$w(\mathbf{x}_0) = \begin{cases} 1, & \forall \langle \mathbf{k}(\mathbf{x}_0) \cdot \mathbf{n}_{in}(\mathbf{x}_0) \rangle > 0 \\ 0 & \text{elsewhere.} \end{cases} \quad (3.5)$$

The driving function (3.4) is a common generalization of the 3D WFS driving function given by [ZS13, Eq. 20.] for a virtual point source. Both formulations are valid in the high-frequency region, for convex SSDs within the validity of the Kirchhoff approximation: in the far-field of the virtual source distribution generating the virtual sound field—i.e. where the local plane wave approximation of the virtual field holds—. In the context of WFS the windowing is termed *secondary source selection criterion* [Spo07; Spo], selecting the *active secondary sources* contributing to the synthesized field.

In the special case of an infinite planar SSD surface located along the plane $y = 0$, the Kirchhoff-Helmholtz integral simplifies to the Neumann Rayleigh integral representing the field of any source distribution located at $y < 0$, as discussed in 1.4.3. Therefore—as comparison of the general SFS equation (3.1) with the Rayleigh integral (1.65) reveals—the driving function (3.3) is capable of the perfect synthesis of an arbitrary virtual sound field over the listening half-space $y > 0$ without any approximations involved. In this case no windowing is required, i.e. $w(\mathbf{x}_0) \equiv 1$ and the normal derivative is simply given by the y -derivative of the target/virtual sound field.

Application example: 3D synthesis of a virtual point source

As a simple example the 3D WFS of a virtual point source is discussed. Assume a 3D point source located at $\mathbf{x}_s = [x_s, y_s, z_s]^T$. Substituting the Green's function into (3.4) yields the point source specific 3D WFS driving function

$$D(\mathbf{x}_0, \omega) = w(\mathbf{x}_0) \frac{jk}{2\pi} \frac{\langle \mathbf{x}_0 - \mathbf{x}_s \cdot \mathbf{n}(\mathbf{x}_0) \rangle}{|\mathbf{x}_0 - \mathbf{x}_s|} \frac{e^{-jk|\mathbf{x}_0 - \mathbf{x}_s|}}{|\mathbf{x}_0 - \mathbf{x}_s|}, \quad (3.6)$$

begin equivalent to [ZS13, Eq. 20.] and [Spo+08, Eq. 19.].

The result of synthesis is depicted in Figure 3.2 for the special case of an SSD surface, being independent of the z -coordinate, as illustrated by Figure 3.3 in the following section. As it can be seen, the driving functions ensure amplitude correct synthesis within the validity of the Kirchhoff-approximation: amplitude errors arise

- in the proximity of SSD elements with large local curvature of the SSD surface, due to the local failure of the tangent plane approximation
- in the proximity of SSD elements where the normal component of the local wavenumber vector is small—i.e. parts off the SSD, nearly parallel to the local

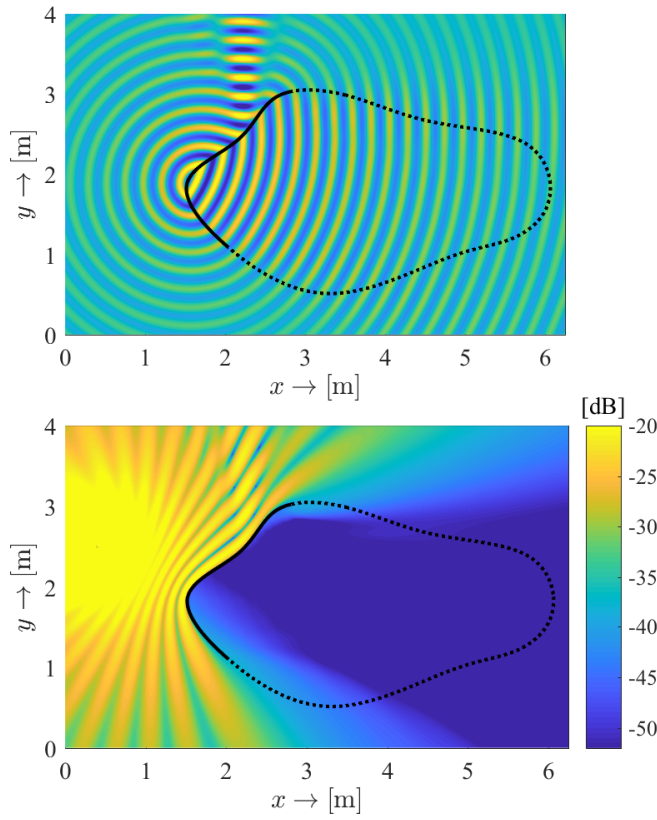


Figure 3.2. 3D synthesis of a 3D point source located at $\mathbf{x}_s = [0.4, 2.5, 0]^T$, radiating at $\omega_0 = 2\pi \cdot 1.5 \text{ krad/s}$. The SSD surface is chosen to be independent of z -coordinate, i.e. as illustrated in 3.3. Obviously, instead of a vertically infinite SSD, the SSD was truncated and tapered along the vertical dimension by choosing parameters, so that the diffraction effects due the truncation are not considerable in the simulation results. Figure (a) depicts the real part of the synthesized field, (b) presents the absolute error of synthesis (i.e. the discrepancy between the synthesized and the target sound field) in a logarithmic scale measured in the horizontal plane, containing the virtual point source. The active arc of the SSD is denoted by solid black line, and the inactive part with dotted by black line.

virtual field propagation direction—, since at these positions the high-frequency gradient approximation fails, with also the lack of diffractive waves causing amplitude errors.

- at space regimes for which the above described SSD elements serve as a stationary position as discussed in .

3.1.2 The 2.5D Kirchhoff approximation

Before dealing with the question of 2.5D Wave Field Synthesis a further simplification of the Kirchhoff approximation is introduced. This simplification reduces the 3D Kirchhoff integral into a 2D contour integral describing a 3D sound field with the integral kernel being the 3D Green's function. The approximation is therefore referred to as the *2.5D Kirchhoff integral*, frequently occurring in the field of seismic migration and inversion problems. The dimensionality reduction is performed by applying the stationary phase method to the Kirchhoff integral along the vertical dimension.

Assume a 3D interior radiation problem, with the sound field under consideration described by the Kirchhoff integral (2.41) written on a surface, being independent of the z -coordinate. The problem geometry is depicted in Figure 3.3. In the followings the receiver position is assumed to be at $z = 0$ inside the enclosure, i.e. $\mathbf{x} = [x, y, 0]^T \in \Omega$. In this special geometry the integral variables are separable and the Kirchhoff integral can be written as

$$P(\mathbf{x}, \omega) = \oint_C \int_{-\infty}^{\infty} 2w(\mathbf{x}_0) j k_n^P(\mathbf{x}_0) P(\mathbf{x}_0, \omega) G(\mathbf{x} - \mathbf{x}_0, \omega) dz_0 ds, \quad (3.7)$$

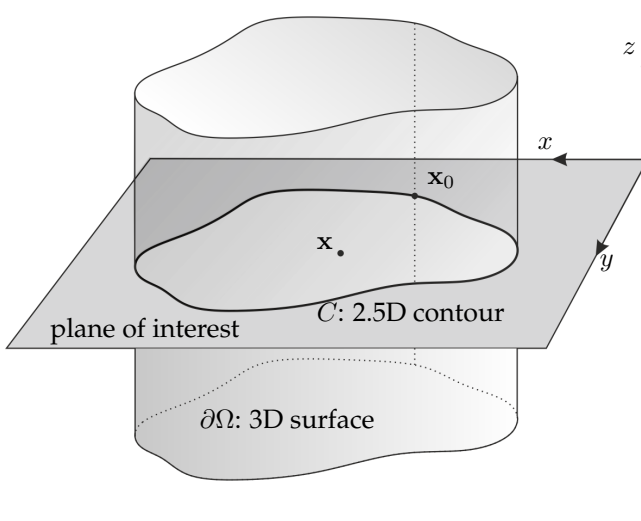


Figure 3.3. Geometry for the derivation of 2.5D Kirchhoff integral. The enclosing surface $\partial\Omega = f(x_0, y_0)$ is chosen to be independent of the z -coordinate in order to be able to evaluate the Kirchhoff integral with respect to z_0 using the SPA. If the sound field to be described is a 2D one, propagating in the direction parallel to the listening plane, then the surface can be interpreted as a continuous set of infinite vertical line sources along C (described by the 2D Green's function), capable of the perfect description of a 2D field inside the enclosure by a 2D contour integral.

with the integral variable ds being the arc length along the contour $C = f(x_0, y_0, 0)$.

The integral is approximated applying the stationary phase approximation along the z_0 -dimension. Since the contour of integration is chosen to lie at the $z = 0$ plane, therefore the vertical stationary position has to be found at $z_0^* = 0$. Based on the foregoing this requirement can be formulated as

$$k_z^P(x_0, y_0, 0) = -k_z^G(x - x_0, y - y_0, 0) = 0, \quad (3.8)$$

stating the trivial fact, that a sound field can be described by a 2.5 dimensional contour integral only in the plane where all the sound sources are located, and which plane the emerging waves propagate parallel with. In the plane of investigation $k_z^P(x, y, 0) \equiv 0$ holds, being valid for 3D sources located at the plane of investigation and for 2D sources being invariant along the vertical dimension.

Having the vertical stationary position fixed to $z_0^* = 0$ the vertical integral can be approximated by the SPA. Application of the 1D SPA formulation (2.25) requires the sign of the phase function's second derivative at the stationary position reading

$$\phi''_{zz}(x_0, y_0, 0) = \phi''_{zz}^P(x_0, y_0, 0) + \phi''_{zz}^G(x - x_0, y - y_0, 0) = -(\kappa_2^P(\mathbf{x}_0) + \kappa_2^G(\mathbf{x} - \mathbf{x}_0)), \quad (3.9)$$

which in the present case is the negative sum of the principal curvatures of sound field P and the Green's function as discussed in appendix B.1 in details. By definition, for an arbitrary diverging sound field the principal curvatures are positive. For a converging wavefront the signature of the resultant curvature depends on the receiver position \mathbf{x} : in regions of the receiver plane where sound field P locally converges the resultant curvature is negative, while in regions where the sound field diverges, e.g. after passing a focal point the resultant curvature is positive. In the present thesis only locally diverging wave fields are discussed, ensuring that $\text{sign}(\phi''_{zz}(x_0, y_0, 0)) = -1$ holds.

With these considerations application of the SPA to (3.7) results in the *2.5D Kirchhoff integral*, reading as

$$P(\mathbf{x}, \omega) = \oint_C 2w(\mathbf{x}_0) \sqrt{\frac{2\pi}{j|\phi_{zz}^{P''}(\mathbf{x}_0) + \phi_{zz}^{G''}(\mathbf{x} - \mathbf{x}_0)|}} \underbrace{j k_n^P(\mathbf{x}_0) P(\mathbf{x}_0, \omega)}_{-\frac{\partial P(\mathbf{x}_0, \omega)}{\partial \mathbf{n}_{in}}} G(\mathbf{x} - \mathbf{x}_0, \omega) ds, \quad (3.10)$$

with both $\mathbf{x} = [x, y, 0]^T$ and $\mathbf{x}_0 = [x_0, y_0, 0]^T$ now denoting in-plane positions.

3.1.3 2.5D Wave Field Synthesis

The 2.5D Kirchhoff integral implicitly contains the 2.5D WFS driving functions for a convex continuous contour of 3D point sources at the $z = 0$ plane. The resulting driving functions are however still dependent on the listener position through the argument of $\phi_{zz}^{G''}(\mathbf{x} - \mathbf{x}_0)$, which dependency may be avoided by fixing the listener position. This strategy would only allow the synthesis of the virtual field, optimized to a single, fixed receiver position termed the *reference point*, while in other points in the listening plane amplitude errors would be present. In the followings it is presented how these driving functions can be further manipulated in order to ensure correct synthesis along an arbitrary receiver curve, termed the *reference curve* within the validity of the stationary phase approximation, resulting in the *unified 2.5D WFS theory*.

As it was stated in section 3.1.1, for any receiver position \mathbf{x} the Kirchhoff integral is dominated by that stationary contour element $\mathbf{x}_0^*(\mathbf{x})$, from which the emerging spherical wavefronts locally coincide with the the target field wavefront, i.e. where $\mathbf{k}^P(\mathbf{x}_0^*(\mathbf{x})) = \mathbf{k}^G(\mathbf{x} - \mathbf{x}_0^*(\mathbf{x}))$ is satisfied. As a consequence, the 2.5D Kirchhoff integral may be further approximated by expressing the amplitude factor with its value at the stationary position as

$$P(\mathbf{x}, \omega) = \oint_C -2w(\mathbf{x}_0) \sqrt{\frac{2\pi}{j|\phi_{zz}^{P''}(\mathbf{x}_0) + \phi_{zz}^{G''}(\mathbf{x} - \mathbf{x}_0^*(\mathbf{x}))|}} j k_n^P(\mathbf{x}_0) P(\mathbf{x}_0, \omega) G(\mathbf{x} - \mathbf{x}_0, \omega) ds, \quad (3.11)$$

where $\mathbf{x}_0^*(\mathbf{x})$ is defined by the implicit relationship above.

The statement can be expressed by reversing causality, forming the main idea of 2.5D WFS: every point \mathbf{x}_0 on the secondary distribution contributes to the total sound field at the set of positions $\mathbf{x}(\mathbf{x}_0)$ where the local propagation direction of a point source positioned at \mathbf{x}_0 coincides with that of the target field, i.e. where their local wavenumber vectors coincide. Hence \mathbf{x} and \mathbf{x}_0 are *stationary point pairs*, mutually determining each other. By reversing the causality, i.e. choosing \mathbf{x}_0 as an independent parameter, the 2.5D WFS driving functions can be extracted from (3.11) resulting in the *unified 2.5D Wave Field Synthesis driving functions*

$$D(\mathbf{x}_0, \omega) = -w(\mathbf{x}_0) \sqrt{\frac{8\pi}{jk}} \sqrt{d_{ref}(\mathbf{x}_0)} j k_n^P(\mathbf{x}_0) P(\mathbf{x}_0, \omega), \quad (3.12)$$

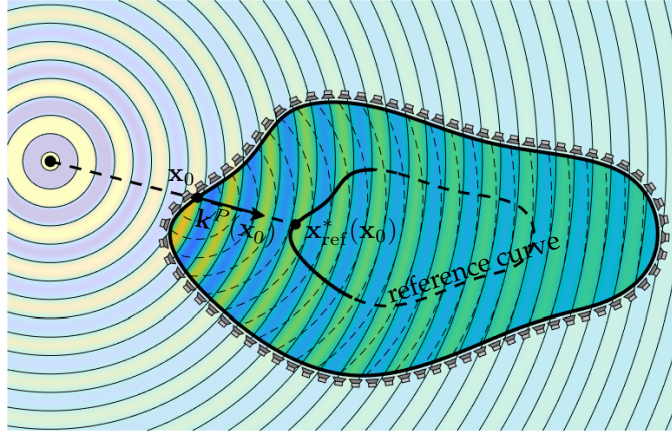


Figure 3.4. Illustration for the location of the reference position for an SSD element located in \mathbf{x}_0 . Due to the phase characteristics of the Green's function, as a simple geometrical consideration, the reference position $\mathbf{x}_{\text{ref}}^*(\mathbf{x}_0)$ for an arbitrary SSD element can be found at the intersection of the reference curve and the line emerging from \mathbf{x}_0 pointing into the local wavenumber vector of the virtual field $\mathbf{k}^P(\mathbf{x}_0)$. The location of the arbitrarily chosen reference curve is denoted by dashed black line, with solid line indicating the positions, for which a stationary SSD position can be found. Amplitude correct synthesis may be only achieved along this part of the reference curve.

with the term $d_{\text{ref}}(\mathbf{x}_0)$ denoting the *referencing function*, defined as

$$d_{\text{ref}}(\mathbf{x}_0) = \frac{k}{|\phi_{zz}^{P''}(\mathbf{x}_0) + \phi_{zz}^{G''}(\mathbf{x}_{\text{ref}}(\mathbf{x}_0) - \mathbf{x}_0)|}. \quad (3.13)$$

Position $\mathbf{x}_{\text{ref}}(\mathbf{x}_0)$ is a point on a pre-defined *reference curve* C_{ref} , for which \mathbf{x}_0 is a stationary position on the SSD, thus defined by

$$\mathbf{k}^P(\mathbf{x}_0) = \mathbf{k}^G(\mathbf{x}_{\text{ref}}(\mathbf{x}_0) - \mathbf{x}_0), \quad (3.14)$$

with $\mathbf{x}_{\text{ref}}(\mathbf{x}_0) \in C_{\text{ref}}$. The reference curve must be a smooth convex curve inside the listening region, ensuring that each reference point has a unique stationary point pair. Once the reference position $\mathbf{x}_{\text{ref}}(\mathbf{x}_0)$ is known for each SSD element the WFS driving functions (3.12) can be evaluated. Referencing the WFS driving function is therefore done by prescribing a unique reference point for each SSD element, so that the set of these reference points form the continuous reference curve. The resulting driving functions will result in amplitude correct synthesis over the reference curve within the validity of integral formulation (3.11).

By substituting the explicit expression for the Green's function's wavenumber ($\mathbf{k}^G(\mathbf{x}) = k \frac{\mathbf{x}}{|\mathbf{x}|}$) into (3.14), the set of positions for which a given \mathbf{x}_0 serves as stationary point reads as

$$\mathbf{x} = \mathbf{x}_0 + \hat{\mathbf{k}}^P(\mathbf{x}_0) |\mathbf{x} - \mathbf{x}_0|. \quad (3.15)$$

The equation describes straight lines passing through \mathbf{x}_0 , being parallel to the local wavenumber vector of the target sound field $\mathbf{k}^P(\mathbf{x}_0)$. Each SSD element therefore dominates the synthesized field towards the direction of the virtual field's local propagation direction at the SSD position. Along this straight line inside the SSD the virtual field wavefront matches the actual SSD element's wavefront, and the reference

position for the actual SSD element is found at the intersection of this straight line and the reference curve. The location of the reference position for a given SSD element is illustrated in Figure 3.4 for the case of a virtual point source. Once the reference position is expressed for each SSD element, the driving functions can be evaluated.

In order to gain a physical interpretation on the structure of the resulting driving functions, the referencing function can be expressed in terms of the principal radii of the virtual field and the Green's function. This results in the driving function expression

$$D(\mathbf{x}_0, \omega) = \underbrace{\sqrt{\frac{2\pi\rho^G(\mathbf{x}_{\text{ref}}(\mathbf{x}_0) - \mathbf{x}_0)}{jk}}}_{\text{SSD compensation}} \underbrace{\sqrt{\frac{\rho^P(\mathbf{x}_0)}{\rho^P(\mathbf{x}_0) + \rho^G(\mathbf{x}_{\text{ref}}(\mathbf{x}_0) - \mathbf{x}_0)}}}_{\text{virtual source compensation}} \underbrace{(-2) w(\mathbf{x}_0) j k_n^P(\mathbf{x}_0) P(\mathbf{x}_0, \omega)}_{\substack{\text{2D} \\ \text{driving function}}} \quad (3.16)$$

where ρ^P and ρ^G are the principal radii of the virtual field and the Green's function along the vertical direction normalized by k , with the absolute value operation omitted due to their positive sign for diverging virtual fields. As it is later verified in (3.76) furthermore $\rho^P(\mathbf{x}) = \rho^P(\mathbf{x}_0) + \rho^G(\mathbf{x}_{\text{ref}}(\mathbf{x}_0) - \mathbf{x}_0)$ holds.

The terms in the driving function can be identified as compensation factors for the *dimensionality mismatch*, present in the 2.5D Kirchhoff integral. According to the 2D Kirchhoff approximation given by (2.21), an arbitrary 2D sound field may be described in the area of investigation by a contour integral. The enclosing boundary can be interpreted as the continuous distribution of two dimensional secondary point sources described by the 2D Green's function, being infinite vertical line sources in three dimensions. The 2D Green's function is weighted by the normal derivative of the 2D sound field, taken on the SSD contour.

Application of the 2.5D WFS driving functions aims to describe a 3D sound field in terms of a 2D contour integral with the kernel being the 3D Green's function, weighted by the normal derivative of the 3D sound field. This results in a dimensionality mismatch for both the virtual field and the secondary source elements. The interpretation of the compensation factors in the driving function is then the following:

- Term $\sqrt{\frac{2\pi|\mathbf{x}_{\text{ref}}(\mathbf{x}_0) - \mathbf{x}_0|}{jk}}$ is the compensation factor for the *secondary source dimensionality mismatch*, by expressing the principal radius for the 2D and 3D Green's function as $\rho^G(\mathbf{x}_{\text{ref}}(\mathbf{x}_0) - \mathbf{x}_0) = |\mathbf{x}_{\text{ref}}(\mathbf{x}_0) - \mathbf{x}_0|$. Comparison with (2.52) indicates, that the compensation factor approximates the frequency response and attenuation factor of the 2D Green's function in terms of the 3D Green's function. Obviously, the attenuation factors can be matched only at a particular position of the space for a given SSD element, chosen to be at the reference position \mathbf{x}_{ref} .
- The virtual source compensation factor resolves the *virtual source dimensionality mismatch*, correcting the virtual source attenuation factor. In case of a virtual point source, located at \mathbf{x}_s the principal radius is given by $\rho^P(\mathbf{x}_0) = |\mathbf{x}_0 - \mathbf{x}_s|$ and around the horizontal stationary point $\rho^P(\mathbf{x}_0) + \rho^G(\mathbf{x}_{\text{ref}}(\mathbf{x}_0) - \mathbf{x}_0) = |\mathbf{x}_{\text{ref}}(\mathbf{x}_0) - \mathbf{x}_s|$ holds. The numerator of the correction factor then corrects the 3D driving function to an ideal 2D one, while the denominator ensures the correct attenuation of the virtual field at the reference position, as described in details in

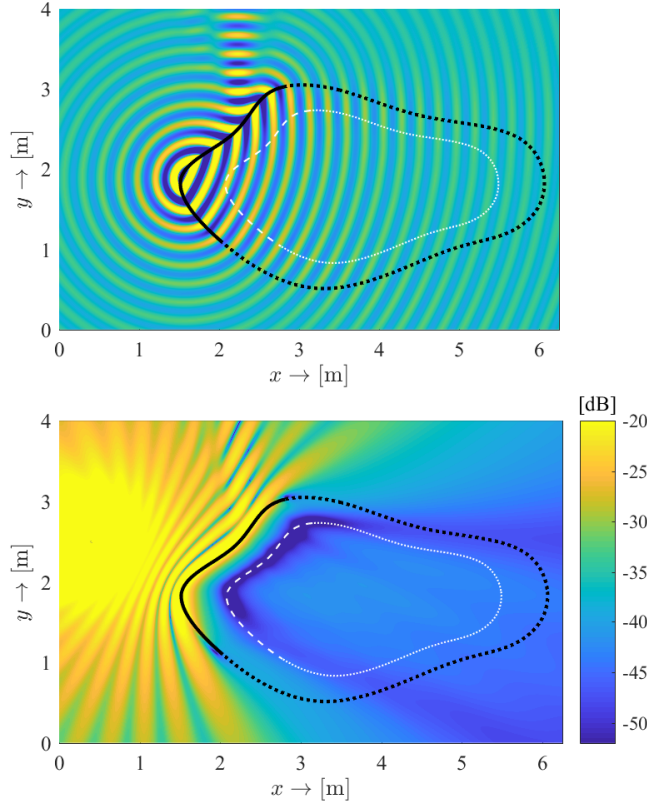


Figure 3.5. 2.5D synthesis of a 3D point source located at $\mathbf{x}_s = [0.4, 2.5, 0]^T$, radiating at $\omega_0 = 2\pi \cdot 1.5 \text{ krad/s}$ in order to ensure high-frequency conditions. Figure (a) depicts the real part of the synthesized field, (b) presents the absolute error of synthesis in a logarithmic scale. The reference curve is derived by rescaling the SSD contour. The active arc of the SSD is denoted by solid black line, and the inactive part with dotted by black line. The reference position on the reference curve for each active SSD element is evaluated numerically. Obviously in the present geometry there exist SSD elements, for which no unique reference position can be found. In order to ensure smooth driving functions and avoid truncation artifacts for these SSD positions, the referencing function is extrapolated.

appendix D.1. Formulating the correction factors in terms of the principal radii is a straightforward generalization of the foregoing towards general 3D virtual fields.

Referencing the synthesis therefore can be interpreted physically by adjusting both attenuation correction factors for each SSD element to be amplitude correct on the reference curve.

The introduced driving function is capable of the synthesis of arbitrary sound fields applying arbitrary shaped convex SSDs, referencing the synthesis to an arbitrary reference curve. The result of such a general 2.5D WFS scenario is presented in Figure 3.5. As the image depicting the synthesis error indicates: on those part of the reference curve for which a stationary point pair can be found on the SSD amplitude correct synthesis is ensured, as the error exhibits a minimum.

If a parametrization of the SSD contour and the reference curve is known, the referencing function can be expressed analytically, resulting closed form driving functions specific to the SSD and the referencing contour. The following two examples are presented in order to demonstrate the analytical application of the presented driving functions.

The presented referencing approach is not only capable of deriving referencing functions for arbitrary SSD-reference curve geometries, but also allows the analysis of former WFS approaches in the aspect of the positions of amplitude correct synthesis. These former approaches include traditional WFS, which references the synthesis of a point source to a reference line as discussed via the following example [Ber+93; Sta97; Ver97], and revisited WFS formulation, which applies a target field independent con-

stant referencing function without taking the virtual source dimensionality mismatch into consideration [Spo+08]. The further analysis of the latter approach is not included in the present thesis, a thorough discussion of the topic can be found in [Fir+17].

Application example: Synthesis of a 3D point source applying a linear SSD

As a first example assume an infinite linear SSD located at $\mathbf{x}_0 = [x_0, 0, 0]^T$. The reference contour is set to be an infinite line parallel to the SSD, located at $\mathbf{x}_{\text{ref}} = [x_{\text{ref}}, y_{\text{ref}}, 0]^T$. This geometry has a distinctive role in the field of sound field synthesis, being the arrangement for which traditional WFS was first formulated. Since the driving functions may be derived directly by applying the SPA to the Rayleigh integral describing an arbitrary sound field perfectly in terms of a planar integral, therefore application of a linear SSD involves the least approximations avoiding errors due to the application of the Kirchhoff approximation. Choosing a reference line parallel to the SSD also ensures a unique reference position for each SSD element. As a consequence amplitude correct synthesis may be ensured on the entire reference line. Furthermore, explicit solution can be found for this special geometry as described in the following section.

Evaluation of the 2.5D WFS driving functions (3.12) requires determining the distance of the reference position on the reference line from the corresponding SSD elements, i.e. equation

$$\mathbf{x}_{\text{ref}}(\mathbf{x}_0) = \mathbf{x}_0 + \hat{\mathbf{k}}^P(\mathbf{x}_0)|\mathbf{x}_{\text{ref}}(\mathbf{x}_0) - \mathbf{x}_0| \quad (3.17)$$

has to be solved for $|\mathbf{x}_{\text{ref}}(\mathbf{x}_0) - \mathbf{x}_0|$ termed the *reference distance*. The terminology indicates that it denotes the distance measured from the SSD elements at which the synthesis is optimized. For a 2D virtual field, for which $\phi''_{zz}(\mathbf{x}) = 0$ the reference distance is the referencing function itself.

In the present geometry equation (3.17) has to be solved so that both \mathbf{x}_0 and \mathbf{x}_{ref} are lying along infinite parallel lines. As a general case assume that the direction of the SSD and reference line are described by the unit vector \mathbf{v} and their normal vector is given by \mathbf{n} , with the distance between them being d . From simple geometrical considerations the reference position for a given SSD position

$$\mathbf{x}_{\text{ref}}(\mathbf{x}_0) = \mathbf{x}_0 + d\mathbf{n} + \mathbf{v} \left\langle |\mathbf{x}_{\text{ref}}(\mathbf{x}_0) - \mathbf{x}_0| \hat{\mathbf{k}}^P(\mathbf{x}_0) \cdot \mathbf{v} \right\rangle \quad (3.18)$$

must hold. The reference distance therefor can be expressed by solving

$$\hat{\mathbf{k}}^P(\mathbf{x}_0)|\mathbf{x}_{\text{ref}}(\mathbf{x}_0) - \mathbf{x}_0| = d\mathbf{n} + \mathbf{v} \left\langle |\mathbf{x}_{\text{ref}}(\mathbf{x}_0) - \mathbf{x}_0| \hat{\mathbf{k}}^P(\mathbf{x}_0) \cdot \mathbf{v} \right\rangle \quad (3.19)$$

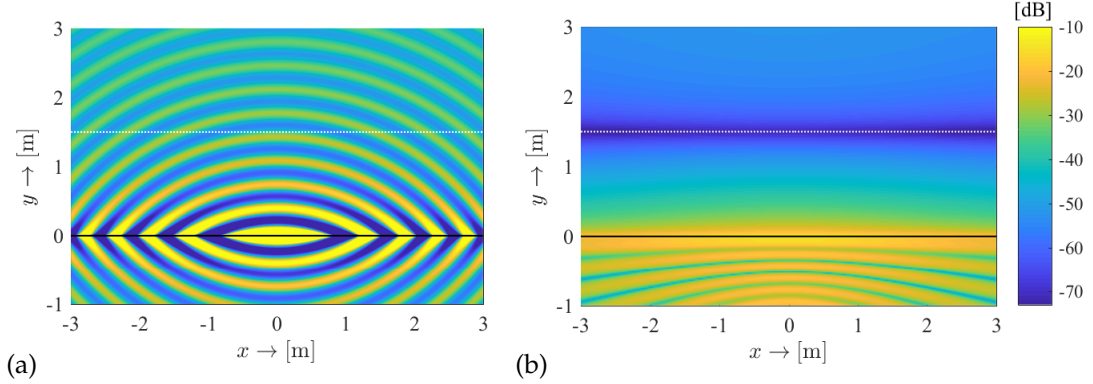


Figure 3.6. 2.5D synthesis of a 3D point source located at $\mathbf{x}_s = [0, -2, 0]^T$, radiating at $\omega_0 = 2\pi \cdot 1 \text{ krad/s}$ with the reference line set at $y_{\text{ref}} = 1.5 \text{ m}$. Figure (a) depicts the real part of the synthesized field, (b) shows the error of synthesis. Based on the equivalent scattering interpretation of the synthesis the discrepancy between the synthesized field and the virtual field at $y < 0$ can be interpreted as the field of a point source reflected from a planar scatterer surface. Due to the problem symmetry the scattered field is given amplitude correctly along $y = -y_{\text{ref}}$.

for $|\mathbf{x}_{\text{ref}}(\mathbf{x}_0) - \mathbf{x}_0|$. In the present case $\mathbf{v} = [1, 0, 0]^T$, the normal is given by $\mathbf{n} = [0, 1, 0]^T$ and $d = y_{\text{ref}}$ and solving the equation for the second coordinate yields the reference distance

$$|\mathbf{x}_{\text{ref}}(\mathbf{x}_0) - \mathbf{x}_0| = \frac{y_{\text{ref}}}{\hat{k}_y^P(\mathbf{x}_0)} = \frac{k}{\phi_{zz}''G(\mathbf{x}_{\text{ref}}(\mathbf{x}_0) - \mathbf{x}_0)}. \quad (3.20)$$

Hence the general 2.5D WFS driving function, ensuring amplitude correct synthesis on a reference line reads as

$$D(\mathbf{x}_0, \omega) = -\sqrt{\frac{8\pi}{jk}} \sqrt{\frac{k}{|\phi_{zz}''(\mathbf{x}_0)| + \frac{k_y^P(\mathbf{x}_0)}{y_{\text{ref}}}}} j k_y^P(\mathbf{x}_0) P(\mathbf{x}_0, \omega). \quad (3.21)$$

For the special case of a virtual point source $|\phi_{zz}''(\mathbf{x}_0)| = \frac{k}{|\mathbf{x}_0 - \mathbf{x}_s|}$ and $k_y^P(\mathbf{x}_0) = k \frac{y_0 - y_s}{|\mathbf{x}_0 - \mathbf{x}_s|}$ holds and the driving function simplifies to

$$D(\mathbf{x}_0, \omega) = \frac{1}{4\pi} \sqrt{\frac{8\pi}{jk}} \sqrt{\frac{y_{\text{ref}}}{y_{\text{ref}} - y_s}} j k y_s \frac{e^{-jk|\mathbf{x}_0 - \mathbf{x}_s|}}{|\mathbf{x}_0 - \mathbf{x}_s|^{\frac{3}{2}}}. \quad (3.22)$$

This result is precisely equivalent with the traditional WFS driving function [Ver97, (2.27)], [Sta97, (3.16)&(3.17)] of a point source, and furthermore identical to the farfield/high-frequency approximated explicit solution presented in the next section [SA10, (25)], [Sch16, Ch. 2.3].

The result of synthesis is depicted in Figure 3.6 confirming, that by applying the derived driving functions amplitude correct synthesis is ensured along the reference line.

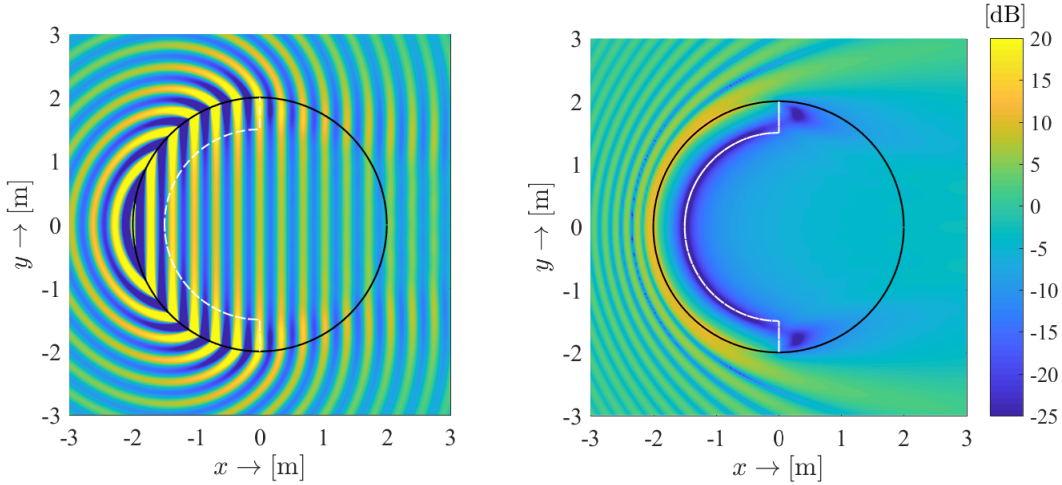


Figure 3.7. 2.5D synthesis of a 2D plane wave with the angular frequency $\omega_0 = 2\pi \cdot 1\text{krad/s}$ propagating into the direction $\mathbf{k}^{\text{PW}} = [k_x^{\text{PW}}, 0, 0]^T$. The SSD is a circular one, with the radius $R_{\text{SSD}} = 2\text{ m}$. The reference curve is a circle with the radius $R_{\text{ref}} = 1.5\text{ m}$. Figure (a) depicts the real part of the synthesized field, (b) shows the error of synthesis.

Application example: Synthesis of a plane wave applying a circular SSD

As a second example the synthesis of a plane wave applying a circular SSD with the radius of R_{SSD} is presented. The synthesis is referenced to a concentric circle inside the SSD with the radius R_{ref} . For this geometry the explicit driving functions are also known, which are however not discussed in details in the present thesis.

Again, the system of equations describing the reference distance for each SSD element is given by

$$\mathbf{x}_{\text{ref}}(\mathbf{x}_0) = \mathbf{x}_0 + \hat{\mathbf{k}}^P(\mathbf{x}_0)|\mathbf{x}_{\text{ref}}(\mathbf{x}_0) - \mathbf{x}_0| \quad (3.23)$$

$$|\mathbf{x}_{\text{ref}}(\mathbf{x}_0)| = R_{\text{ref}}. \quad (3.24)$$

Expressing the reference distance leads to a second order equation. By exploiting that $|\mathbf{x}_0| = R_{\text{SSD}}$, $|\hat{\mathbf{k}}^P(\mathbf{x}_0)| = 1$ and taking only the smaller root into consideration—corresponding to the closer arc of the reference circle to the actual SSD position—yields the reference distance

$$|\mathbf{x}_{\text{ref}}(\mathbf{x}_0) - \mathbf{x}_0| = -R_{\text{SSD}} \left(\hat{k}_r^P(\mathbf{x}_0) + \sqrt{\hat{k}_r^P(\mathbf{x}_0)^2 + \left(\frac{R_{\text{ref}}}{R_{\text{SSD}}} \right)^2 - 1} \right), \quad (3.25)$$

with $\hat{k}_r^P(\mathbf{x}_0)$ denoting the radial component of the normalized wavenumber vector. Applying the reference distance to the general 2.5D WFS driving functions (3.12) allows the synthesis of an arbitrary sound field referenced on a reference circle inside the SSD.

Assume the special case of a virtual 2D plane wave, propagating parallel to the synthesis plane described by the wavenumber vector $\mathbf{k}^{\text{PW}} = [k_x^{\text{PW}}, k_y^{\text{PW}}, 0]^T$. For a

2D sound field $\phi_{zz}''^P(\mathbf{x}_0) = 0$ holds and the reference function is given by the reference distance itself. In this case the actual form of the driving function reads

$$D(\mathbf{x}_0, \omega) = -w(\mathbf{x}_0) \sqrt{\frac{8\pi}{jk}} \sqrt{|\mathbf{x}_{\text{ref}}(\mathbf{x}_0) - \mathbf{x}_0|} j k_r^{\text{PW}}(\mathbf{x}_0) e^{-j \langle \mathbf{k}^{\text{PW}}, \mathbf{x}_0 \rangle}, \quad (3.26)$$

with the reference distance given by (3.25).

The result of synthesis, along with the error of synthesis is depicted in Figure 3.7.

3.2 Explicit solution: Spectral Division Method

The explicit solution for the general SFS problem utilizes compact operator theory by exploiting that integral (3.1) constitutes a compact Fredholm operator with the kernel being the Green's function [Ahr12; MF53]. Such an operator and the involved acoustic fields can be expanded into the series of orthogonal eigenfunctions of the wave equation on a control surface, that form a complete basis of the solution. The inverse problem can be straightforwardly solved for the driving function expansion coefficients by a comparison of the corresponding eigenvalues, as long as none of the expansion coefficients of the operator kernel is zero. Otherwise the problem is termed *ill-conditioned*. Finally the explicit analytical solution is found for the driving function as an infinite sum of the weighted basis functions. The method is often referred to as *mode-matching* solutions, since the eigenfunctions of the given geometry are termed the *modes*.

This solution utilizing the single layer potential is unique for general enclosures and also for the—strictly speaking—non-enclosing planar case as shown in [ZS13] and [Faz10] respectively. In contrary sound field control utilizing the Kirchhoff-Helmholtz formulation would be non-unique on the eigenfrequencies of the enclosure due to resonance phenomena.

The determination of the appropriate eigenfunctions for a general geometry is a tough challenge. For spherical and circular geometries spherical and circular harmonics form the demanded basis functions. For a rigorous treatment for mode-matching SFS using spherical and circular SSDs see [Ahr10; Zot09; Ahr12; AS09b; AS09a; AS08; SS14] and [Koy+14] for the cylindrical solution. In the present thesis only the planar and linear geometries are investigated in details.

3.2.1 3D Spectral Division Method

Assume an infinite planar SSD along the $y = 0$ plane. The synthesized field in this geometry is given by a Fredholm-integral of the first kind

$$P(\mathbf{x}, \omega) = \iint_{-\infty}^{\infty} D(x_0, z_0, \omega) G(x - x_0, y, z - z_0) dx_0 dz_0 = D(x, z, \omega) *_{x,z} G(x, y, z, \omega), \quad (3.27)$$

describing a continuous convolution along the SSD plane. Here $G(x, y, z, \omega)$ denotes the sound field of a secondary source element placed at the origin.

For this geometry the orthogonal basis is given by the continuous set of exponentials, therefore the decomposition of the involved quantities is given by a double Fourier-transform [Ahr12; AW05; SS14], with the physical interpretation of a plane wave decomposition. Applying the convolution theorem to the angular spectrum representation the convolution may be transformed into a multiplication [Gir+01]:

$$\tilde{P}(k_x, y, k_z, \omega) = \tilde{D}(k_x, k_z, \omega) \tilde{G}(k_x, y, k_z, \omega). \quad (3.28)$$

The expansion coefficient are therefore obtained by a comparison of spectral coefficients and the driving function takes the form:

$$\tilde{D}(k_x, k_z, \omega) = \frac{\tilde{P}(k_x, y, k_z, \omega)}{\tilde{G}(k_x, y, k_z, \omega)} = \frac{\mathcal{F}\{P(\mathbf{x}, \omega)\}}{\mathcal{F}\{G(\mathbf{x}, \omega)\}}, \quad (3.29)$$

$$D(x_0, z_0, \omega) = \frac{1}{4\pi^2} \iint_{-\infty}^{\infty} \tilde{D}(k_x, k_z, \omega) e^{-j(k_x x_0 + k_z z_0)} dk_x dk_z. \quad (3.30)$$

Since the driving function spectrum is yielded by a division in the spectral domain the approach is termed the *Spectral Division Method* [AS10a; AS12; AS11; AS10b].

The method does not pose any constraint on the integral kernel. Theoretically an arbitrary transfer function may be assigned for the SSD elements: as long the problem is well-conditioned—i.e. the spectrum of the transfer function does not exhibit zeros—unique driving functions may be derived applying the above.

Substituting the $k_x - k_z$ representation of the 3D Green's function extracted from the *Weyl's integral representation* [Wil99; Lal68] presented in table 1.1 the driving function (3.30) reads as

$$D(x_0, z_0, \omega) = \frac{1}{4\pi^2} \iint_{-\infty}^{\infty} 2jk_y \frac{\tilde{P}(k_x, y, k_z, \omega)}{e^{-jk_y|y|}} e^{-j(k_x x_0 + k_z z_0)} dk_x dk_z. \quad (3.31)$$

with k_y defined as (1.27) being $k_y = \sqrt{(\frac{\omega}{c})^2 - k_x^2 - k_z^2}$ in the propagation region. Express the target field by it's spectrum measured along $y = 0$ by extrapolating according to (1.29)—i.e. as $\tilde{P}(k_x, y, k_z, \omega) = \tilde{P}(k_x, 0, k_z, \omega) e^{-jk_y y}$ the spectral division can be carried out, with the exponential pressure propagators canceling out, and the driving function becomes independent from the y -coordinate. The driving function in the wavenumber domain therefore reads as

$$\tilde{D}(k_x, k_z, \omega) = 2jk_y \tilde{P}(k_x, 0, k_z, \omega). \quad (3.32)$$

Comparison with (1.31) reveals, that multiplication by k_y represents differentiation along the y -dimension, i.e.

$$\tilde{D}(k_x, k_z, \omega) = -2 \left. \frac{\partial}{\partial y} \tilde{P}(k_x, y, k_z, \omega) \right|_{y=0}. \quad (3.33)$$

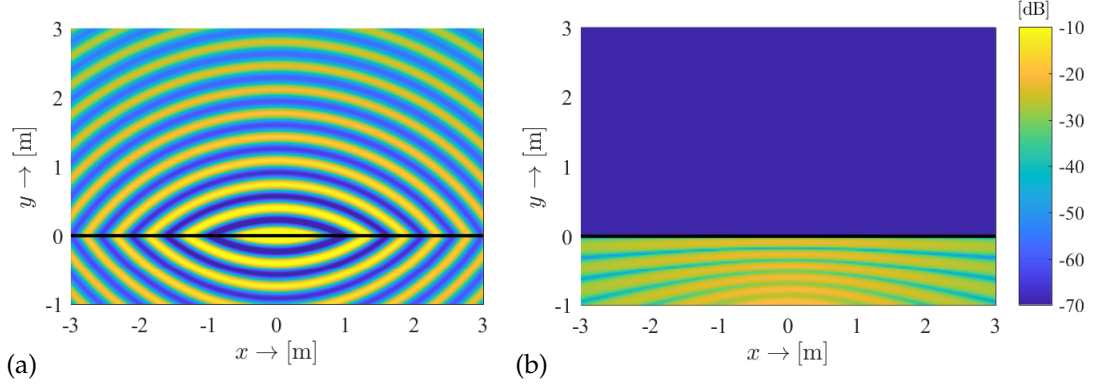


Figure 3.8. Synthesis of a virtual point source using a planar SSD based on SDM driving functions. The SSD is located at $\mathbf{x}_0 = [x_0, 0, z_0]^T$, denoted by a solid black line. The virtual source is located at $\mathbf{x}_s = [0, -2, 0]^T$ oscillating at $\omega_0 = 2\pi \cdot 1$ krad/sec. The figures depict the real part of the synthesized field (a) and the deviation from the target sound field (b) measured at $z = 0$.

Straightforwardly, the explicit expression of the driving function in the spatial domain is obtained by the corresponding inverse Fourier-transform according to (3.30):

$$D(x_0, z_0, \omega) = -2 \frac{\partial}{\partial y} P(\mathbf{x}, \omega) \Big|_{y=0}. \quad (3.34)$$

The planar SDM driving function are therefore completely equivalent to that of the implicit solution, in a planar geometry provided by the Rayleigh integral. The coincidence of the explicit and implicit driving functions is a consequence of the uniqueness of the problem in the present geometry. It is also indirectly proven above, that the wavefield extrapolation equations are the spectral domain representations of the Rayleigh integrals.

Application example: Synthesis of a 3D point source using a planar SSD

Assume a 3D virtual point source located at $\mathbf{x}_s = [x_s, y_s, z_s]^T$, with $y_s < 0$, i.e. behind the SSD plane, which is located at $\mathbf{x}_0 = [x_0, 0, z_0]^T$. The wavenumber domain representation of the driving function is obtained by substituting the angular spectrum of the virtual point source—applying the Fourier-shift theorem—into either (3.29) or directly into (3.32):

$$\tilde{D}(k_x, k_z, \omega) = \frac{-\frac{j}{2} e^{-jk_y|y-y_s|}}{k_y} e^{j(k_x x_s + k_z z_s)} = e^{-jk_y|y_s|} e^{j(k_x x_s + k_z z_s)}. \quad (3.35)$$

The double inverse Fourier-transform may be carried out analytically, by taking the y -derivative of the Weyl's integral representation of a 3D point source (See [Wil99, (2.65)]):

$$\frac{\partial}{\partial y} G(\mathbf{x}_0 - \mathbf{x}_s, \omega) = \frac{1}{4\pi^2} \iint_{-\infty}^{\infty} -\frac{1}{2} e^{-jk_y|y-y_s|} e^{j(k_x x_s + k_z z_s)} e^{-j(k_x x_0 + k_z z_0)} dk_x dk_z, \quad (3.36)$$

Comparing (3.35) and (3.36) it is revealed, that the driving function in the spatial domain is given by

$$D(x_0, z_0, \omega) = -2 \frac{\partial}{\partial y} G(\mathbf{x}_0 - \mathbf{x}_s, \omega)|_{y=0} = -\frac{y_s}{2\pi} \left(\frac{1}{|\mathbf{x}_0 - \mathbf{x}_s|} + jk \right) \frac{e^{-jk|\mathbf{x}_0 - \mathbf{x}_s|}}{|\mathbf{x}_0 - \mathbf{x}_s|^2}, \quad (3.37)$$

which is in agreement with equation (3.34).

The result of synthesizing a steady-state point source is illustrated in Figure 3.8. In the target sound field perfect synthesis is achieved, as it is indicated in Figure 3.8 (b) depicting the difference between the synthesized and the target sound field. Obviously, the figure also presents the result of 3D WFS of a spherical wave without applying the high-frequency gradient approximation.

3.2.2 2.5D Spectral Division Method

Assume an infinite linear set of point sources, located at $\mathbf{x}_0 = [x_0, 0, 0]^T$. The synthesized field in this arrangement reads as

$$P(x, y, z, \omega) = \int_{-\infty}^{\infty} D(x_0, \omega) G(x - x_0, y, z, \omega) dx_0. \quad (3.38)$$

Similarly to the planar case the basis functions for a linear SSD are given by exponentials: by realizing that the above equation is a convolution along the x -axis, the convolution is transformed into a multiplication by means of a forward Fourier-transform

$$\tilde{P}(k_x, y, z, \omega) = \tilde{D}(k_x, \omega) \tilde{G}(k_x, y, z, \omega). \quad (3.39)$$

The driving function spectra is then obtained as a spectral ratio

$$\tilde{D}(k_x, \omega) = \frac{\tilde{P}(k_x, y, z, \omega)}{\tilde{G}(k_x, y, z, \omega)} = \frac{\mathcal{F}_x \{ P(\mathbf{x}, \omega) \}}{\mathcal{F}_x \{ G(\mathbf{x}, \omega) \}}, \quad (3.40)$$

and the frequency domain driving function therefore reads as

$$D(x_0, \omega) = \frac{1}{2\pi} \int_{-\infty}^{\infty} \frac{\tilde{P}(k_x, y, z, \omega)}{\tilde{G}(k_x, y, z, \omega)} e^{-j k_x x_0} dk_x. \quad (3.41)$$

Again, theoretically the transfer function may describe the field of an arbitrary sound source, as long as it does not exhibit zeros in order to keep the problem well-conditioned.

Unlike the planar case the present driving function contains both y and z positions, thus the driving function depends on the listener position: Equation (3.41) may be solved only for positions on the surface of a cylinder with fixed radius $d = \sqrt{y^2 + z^2}$ [Ahr10, p. 60.]. This is a direct consequence of the fact, that the pressure of an arbitrary 3D sound field measured on the SSD does not determine completely the pressure on the reference line—and vice versa. Furthermore an infinite line source—i.e. the SSD—can only radiate wavefronts with cylindrical symmetry as it was discussed in details in ??, therefore phase correct synthesis may be assured only in a plane

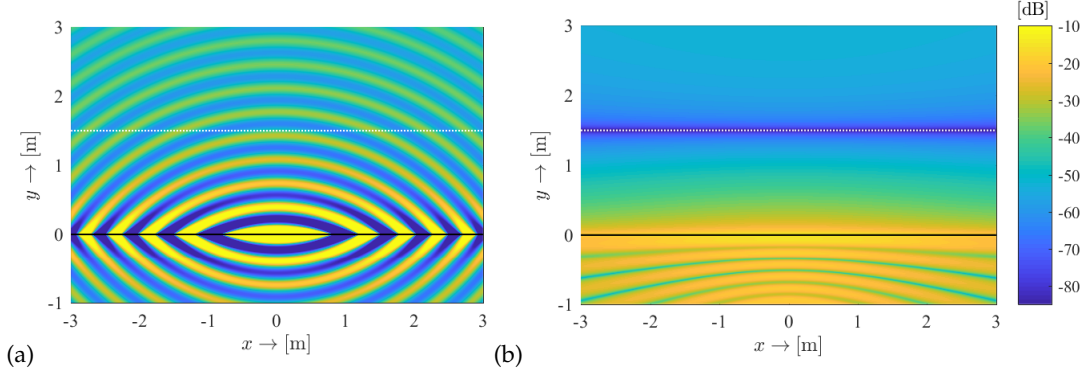


Figure 3.9. Synthesis of a virtual point source using a linear SSD applying the SDM driving functions. The SSD is located at $\mathbf{x}_0 = [x_0, 0, 0]^T$, denoted by a solid black line. The virtual source is located at $\mathbf{x}_s = [0, -2, 0]^T$ oscillating at $\omega_0 = 2\pi \cdot 1000$ rad/sec. The reference line was set to $y_{\text{ref}} = 1.5$ m. The figure depicts the synthesized field at the synthesis plane ($z = 0$) with (a) depicting the real part of the synthesized field, (b) depicting the error of synthesis.

containing the SSD in which the radial wavenumber of the synthesized field and the target field coincide. Amplitude correct synthesis is assured in this plane at a distance $d_{\text{ref}} = \sqrt{y^2 + z^2}$ for which driving functions are calculated.

For practical applications we choose the horizontal plane $z = 0$ for the plane of synthesis, reference the driving functions to the *reference line*, by setting $y = y_{\text{ref}}$ and require that for the virtual field $k_z(x, y, 0) = 0$ holds. The driving function thus reads as

$$D(x_0, \omega) = \frac{1}{2\pi} \int_{-\infty}^{\infty} \frac{\tilde{P}(k_x, y_{\text{ref}}, 0, \omega)}{\tilde{G}(k_x, y_{\text{ref}}, 0, \omega)} e^{-jk_x x_0} dk_x. \quad (3.42)$$

In this geometry amplitude correct synthesis is restricted to the reference line.

It is worth noting that the analytic Fourier-transform coefficients of the target sound field are available only for limited simple virtual source models. Even in these cases the inverse transform of the driving functions rarely can be evaluated analytically, therefore numerical transforms are needed. For a practical and optimized implementation of the SDM for an arbitrary target sound field refer to [Ahr+13].

Application example: Synthesis of a 3D point source using a linear SSD

As an example for the 2.5D explicit driving functions the synthesis of a 3D point source, positioned at $\mathbf{x}_s = [x_s, y_s, 0]^T$, with $y_s < 0$ is presented. The SSD is a linear one, located at $\mathbf{x}_0 = [x_0, 0, 0]^T$. The explicit driving function for a linear SSD is given by (3.42). Substituting the spectra of the virtual and the secondary point sources as given in table 1.1, with applying the Fourier-shift theorem the driving function is given as

$$\hat{D}(k_x, \omega) = \frac{-\frac{j}{4} H_0^{(2)} \left(\sqrt{\left(\frac{\omega}{c}\right)^2 - k_x^2} |y_{\text{ref}} - y_s| \right) e^{jk_x x_s}}{-\frac{j}{4} H_0^{(2)} \left(\sqrt{\left(\frac{\omega}{c}\right)^2 - k_x^2} |y_{\text{ref}}| \right)}, \quad (3.43)$$

and in the spatial domain as

$$D(x_0, \omega) = \frac{1}{2\pi} \int_{-\infty}^{\infty} \frac{H_0^{(2)} \left(\sqrt{\left(\frac{\omega}{c}\right)^2 - k_x^2} |y_{\text{ref}} - y_s| \right)}{H_0^{(2)} \left(\sqrt{\left(\frac{\omega}{c}\right)^2 - k_x^2} |y_{\text{ref}}| \right)} e^{-jk_x(x_0 - x_s)} dk_x. \quad (3.44)$$

The synthesized field using this driving function is depicted in 3.9 (a). As it can be seen from Figure (b) displaying the deviation of the synthesized field from the target field, application of the explicit driving function ensures perfect synthesis on the reference line. In other parts of the space amplitude errors are present.

As discussed in [SA10] the derived driving function spectrum can be simplified by applying the large-argument/asymptotic approximation of the Hankel function, given by (2.51). The asymptotic form gives a fair approximation for (3.44) if $k_y|y_{\text{ref}}| \gg 1$ holds (since $y_{\text{ref}} - y_s > y_{\text{ref}}$), which is valid in the far field of the SSD in front of the virtual source, where $k_y \gg k_x$ dominates the inverse transform. Applying the Hankel's function approximation the inverse transform can be carried out analytically, resulting in

$$D(x_0, \omega) \approx \frac{1}{2} \sqrt{\frac{y_{\text{ref}}}{y_{\text{ref}} - y_0}} j \frac{\omega}{c} \frac{y_0}{|\mathbf{x}_0 - \mathbf{x}_s|} H_1^{(2)} \left(\frac{\omega}{c} |\mathbf{x}_0 - \mathbf{x}_s| \right) \quad (3.45)$$

as given by [SA10, (24)]. By a further large-argument approximation of the Hankel function returns the 2.5D WFS driving function for a 3D point source referencing the synthesis on a reference line, given by (3.22). The equivalence of the SDM and 2.5D WFS referencing the synthesis of a virtual plane wave on a reference line was further discussed in [Fir+17; SS16; Sch16]. The general relation of the explicit solution and 2.5D WFS is discussed in the following section.

3.2.3 Approximate explicit solution in the spatial domain

As discussed in 2.3.3 the stationary phase approximation allows the evaluation of forward and inverse Fourier integrals around stationary positions in the spatial and spectral domain. In the followings the SPA is employed in order to give an approximate formulation for the 2.5D explicit driving functions purely in the spatial domain. The derivation consists of two main steps

- First the spectral driving functions are expressed in an asymptotic form. The calculus can be done by assuming, that the involved spectra are obtained via the SPA of the corresponding forward Fourier-transforms. This step links the spectral coefficients to stationary positions in the spatial domain.
- It is followed by the inverse Fourier transform of the asymptotic spectral driving functions. The evaluation of the inverse transform with the SPA relates the forward transform stationary positions to positions along the SSD.

Asymptotic approximation of the explicit driving functions

The derivation starts from the 2.5D explicit driving functions in the wavenumber domain given by (3.40)

$$\tilde{D}(k_x, \omega) = \frac{\tilde{P}(k_x, y, 0, \omega)}{\tilde{G}(k_x, y, 0, \omega)}, \quad (3.46)$$

ensuring perfect synthesis along a line with fixed y -coordinate. In the following for the sake of brevity and transparency ω and z dependency is suppressed, the latter since the driving functions are defined at $z = 0$. By definition the wavenumber content of the involved quantities is obtained via a forward Fourier transform, with the involved sound fields expressed by their polar form

$$\hat{P}(k_x, y) = \int_{-\infty}^{\infty} A^P(x, y) e^{j\phi^P(x, y)} e^{jk_x x} dx, \quad (3.47)$$

$$\hat{G}(k_x, y) = \int_{-\infty}^{\infty} A^G(x, y) e^{j\phi^G(x, y)} e^{jk_x x} dx. \quad (3.48)$$

It is assumed, that the involved spectra are obtained by using the SPA: under high-frequency assumptions the Fourier integrals may be approximated by evaluation around their stationary point $x_P^*(k_x)$ and $x_G^*(k_x)$, where their phase derivative vanishes, i.e. the stationary positions are defined as

$$\begin{aligned} \frac{\partial}{\partial x} (\phi^P(x, y) + k_x x) \Big|_{x=x_P^*(k_x)} &= 0 \quad \rightarrow \quad k_x^P(x_P^*(k_x), y) = k_x \\ \frac{\partial}{\partial x} (\phi^G(x, y) + k_x x) \Big|_{x=x_G^*(k_x)} &= 0 \quad \rightarrow \quad k_x^G(x_G^*(k_x), y) = k_x. \end{aligned} \quad (3.49)$$

Again, since it is assumed, that $k_z^P(x, y) = k_z^G(x, y) = k_z = 0$ holds in the plane of investigation, therefore the stationary positions are found along a given y , where the local propagation direction of the virtual field and the Green's function matches to that of the spectral plane wave, defined by k_x . The properties of the involved wave fields at these positions will dominate the corresponding Fourier integrals. Hence, the forward transform defines two particular positions in the space, linked together via the actual spectral wavenumber. Note, that it is assumed, that in the virtual sound field each local propagation direction is unique, i.e. a unique stationary position can be found. This statement trivially does not hold even in the simplest case of a virtual plane wave. The final result of the derivation however may be applied for such virtual fields without any modification.

Having defined the stationary positions, the forward Fourier transforms can be evaluated by the SPA. With accounting for the negative second phase-derivatives—

since both the virtual sound field and the Green's function are diverging—their spectra can be approximated as [Tra+14, Ch. 5]

$$\hat{P}(k_x, y) \approx \sqrt{\frac{2\pi}{j |\phi_{xx}^{P''}(x_P^*(k_x), y)|}} A^P(x_P^*(k_x), y) e^{jk_x \cdot x_P^*(k_x)}, \quad (3.50)$$

$$\hat{G}(k_x, y) \approx \sqrt{\frac{2\pi}{j |\phi_{xx}^{G''}(x_G^*(k_x), y)|}} A^G(x_G^*(k_x), y) e^{jk_x \cdot x_G^*(k_x)}. \quad (3.51)$$

The asymptotic approximation of the SDM driving functions on a given spectral component therefore reads

$$\hat{D}(k_x, y) \approx \sqrt{\frac{|\phi_{G,xx}''(x_G^*(k_x), y)|}{|\phi_{P,xx}''(x_P^*(k_x), y)|}} \frac{P(x_P^*(k_x), y)}{G(x_G^*(k_x), y)} e^{jk_x \cdot (x_P^*(k_x) - x_G^*(k_x))}. \quad (3.52)$$

Explicit driving functions in the spatial domain

Using the asymptotic approximation of the SDM spectrum the spatial driving functions are obtained via an inverse spatial Fourier transform:

$$D(x_0, y) = \frac{1}{2\pi} \int_{-\infty}^{\infty} \sqrt{\frac{|\phi_{G,xx}''(x_G^*(k_x), y)|}{|\phi_{P,xx}''(x_P^*(k_x), y)|}} \frac{P(x_P^*(k_x), y)}{G(x_G^*(k_x), y)} e^{jk_x \cdot (x_P^*(k_x) - x_G^*(k_x))} e^{-jk_x x_0} dk_x. \quad (3.53)$$

Again, the integral is approximated using the SPA, with the phase function under investigation given by

$$\Phi(k_x) = \phi^P[x_P^*(k_x), y] - \phi^G[x_G^*(k_x), y] + k_x x_P^*(k_x) - k_x x_G^*(k_x) - k_x x_0. \quad (3.54)$$

As it was discussed in 2.3.3, generally speaking in the inverse transform of an arbitrary wave field P each wavenumber component k_x will dominate one spatial position x_0 , where the actual wavenumber component $k_x(x_0)$ coincides with the local wavenumber of the sound field $k_x^P(x_0)$. For the present case this wavenumber is found as the stationary phase wavenumber $k_x^*(x_0)$ of integral (3.53) [Tra+14].

The derivative of the spectral phase function (3.54) can be evaluated by applying the chain rule, resulting in

$$\begin{aligned} \frac{\partial}{\partial k_x} \Phi(k_x) = & \\ x_{P,k_x}^{*'}(k_x) \underbrace{\left(\phi_x^P[x_P^*(k_x), y] + k_x \right)}_{=0} - x_{G,k_x}^{*'}(k_x) \underbrace{\left(\phi_x^G[x_G^*(k_x), y] + k_x \right)}_{=0} + x_P^*(k_x) - x_G^*(k_x) - x_0, \end{aligned} \quad (3.55)$$

where $x_{k_x}^{*'}(k_x)$ is the rate of change of the forward transform stationary positions with respect to the change of the spectral wavenumber, and the bracketed terms cancel out

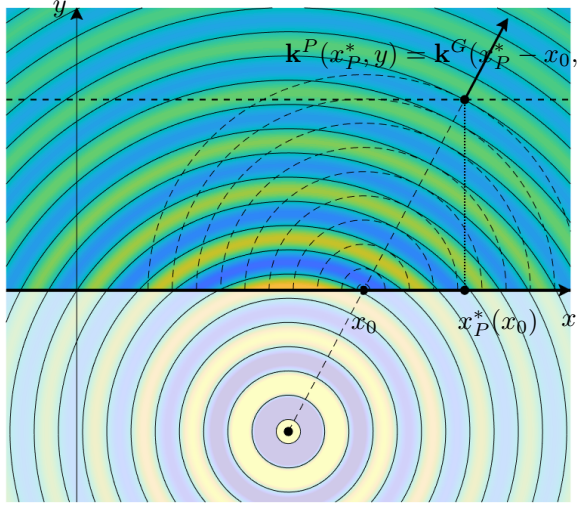


Figure 3.10. Illustration of the evaluation position $x_P^*(x_0)$ (and $x_G^*(x_0)$) as the function of x_0 . For a given SSD position x_0 the stationary positions is found on a given reference line $y = \text{const}$, where the virtual field propagation direction coincides with that of the Green's function translated into x_0 . At $x_P^*(x_0)$ the local curvature of the translated Green's function is always greater, than that of the virtual field.

according to the definition of the stationary points (3.49). The stationary wavenumber $k_x^*(x_0)$ is then found where

$$\frac{\partial}{\partial k_x} \Phi(k_x) \Big|_{k_x=k_x^*(x_0)} = x_P^*(k_x^*(x_0)) - x_G^*(k_x^*(x_0)) - x_0 = 0 \quad (3.56)$$

holds. This definition relates the evaluation points x_P^* and x_G^* directly to the actual SSD coordinate x_0 , therefore the intermediate stationary wavenumber (k_x^*) dependency may be omitted i.e. $x_P^*(k_x^*(x_0)) \rightarrow x_P^*(x_0)$ and $x_G^*(k_x^*(x_0)) \rightarrow x_G^*(x_0)$ may be written.

The definitions for the forward and inverse transform stationary points (3.49) and (3.49) completely define the evaluation points x_P^*, x_G^* for a given SSD position x_0 independently of the spectral wavenumber: by expressing (3.49) with (3.56) for an arbitrary x_0 position the evaluation points along a fixed y is found, where

$$k_x^P(x_P^*(x_0), y) = k_x^G(x_P^*(x_0) - x_0, y), \quad (3.57)$$

is satisfied. This results states, that *for a given SSD coordinate x_0 the evaluation point x_P^* is found on the reference line, where the local propagation direction of the target field P coincides with that of a point source positioned at $[x_0, 0, 0]^T$ measured on the reference line*. For an illustration refer to Figure 3.10.

Having found the stationary position for (3.53) in order to apply the SPA one still needs the phase function's second derivative around the stationary position and its sign. The second derivative is obtained by a further differentiation of (3.55) with respect to k_x leads to

$$\begin{aligned} \frac{\partial^2}{\partial k_x^2} \Phi(k_x) &= x_{P,k_x k_x}^{'''}(k_x) \underbrace{\left(\phi_x^{P'}[x_P^*(k_x), y] + k_x \right)}_{=0} + x_{P,k_x}^{'''}(k_x) \left(x_{P,k_x}^{'''}(k_x) \phi_{xx}^{P''}[x_P^*(k_x), y] + 2 \right) - \\ &- x_{G,k_x k_x}^{'''}(k_x) \underbrace{\left(\phi_x^{G'}[x_G^*(k_x), y] + k_x \right)}_{=0} - x_{G,k_x}^{'''}(k_x) \left(x_{G,k_x}^{'''}(k_x) \phi_{xx}^{G''}[x_G^*(k_x), y] + 2 \right). \end{aligned} \quad (3.58)$$

The required rate of change of the stationary positions ($x_P^{*'}(k_x)$ and $x_G^{*'}(k_x)$) the second derivative can be obtained by differentiating equations (3.55) with respect to k_x , resulting in

$$x_{P,k_x}^{*'}(k_x) = -\frac{1}{\phi_{xx}^{P''}[x_P^*(k_x), y]}, \quad x_{G,k_x}^{*'}(k_x) = -\frac{1}{\phi_{xx}^{G''}[x_G^*(k_x), y]}. \quad (3.59)$$

Thus the second derivative is given by

$$\frac{\partial^2}{\partial k_x^2} \Phi(k_x) = \frac{\phi_{xx}^{P''}[x_P^*(k_x), y] - \phi_{xx}^{G''}[x_G^*(k_x), y]}{\phi_{xx}^{P''}[x_P^*(k_x), y] \phi_{xx}^{G''}[x_G^*(k_x), y]}. \quad (3.60)$$

The second derivatives describe the curvature of the wavefront along the x -direction, as given by (B.5), being maximal in absolute value for a point source. Obviously, for any source distribution behind the SSD the wavefront curvature is smaller at $y > 0$ than the curvature of the stationary SSD element's wavefront, i.e.

$$\phi_{xx}^{P''}(x_P^*(k_x), y) > \phi_{xx}^{G''}(x_G^*(k_x), y) \quad (3.61)$$

holds and the sign of (3.60) is positive.

These results now may be substituted back into the SPA (2.25) of the inverse transform (3.53). For the sake of brevity in the followings the evaluation point is denoted by $x_P^* \rightarrow x^*$. Denoting the stationary position by $\mathbf{x}_{\text{ref}}(\mathbf{x}_0) = [x^*(x_0), y, 0]^T$ the resulting driving function is formulated as

$$D(x_0) = \sqrt{\frac{|\phi_{xx}^{G''}(\mathbf{x}_{\text{ref}}(\mathbf{x}_0) - \mathbf{x}_0)|^2}{|\phi_{xx}^{P''}(\mathbf{x}_{\text{ref}}(\mathbf{x}_0)) - \phi_{xx}^{G''}(\mathbf{x}_{\text{ref}}(\mathbf{x}_0) - \mathbf{x}_0)|}} \sqrt{\frac{j}{2\pi}} \frac{P(\mathbf{x}_{\text{ref}}(\mathbf{x}_0))}{G(\mathbf{x}_{\text{ref}}(\mathbf{x}_0) - \mathbf{x}_0)}, \quad (3.62)$$

where $k_x^P(\mathbf{x}_{\text{ref}}(\mathbf{x}_0)) = k_x^G(\mathbf{x}_{\text{ref}}(\mathbf{x}_0) - \mathbf{x}_0)$ holds. This result states, that an arbitrary sound field may be synthesized by finding the positions along the reference line, where the propagation direction/wavefront of the target field matches the field of the actual SSD elements. In this stationary position the driving functions are obtained by the ratio of the target field and the actual SSD element, corrected by the factor, containing the wavefront curvatures at the same position. Therefore the explicit, global solution can be approximated by simple local wavefront matching.

Expressing the second derivatives in terms of the principal radii according to (B.5) and exploiting, that by definition $\hat{k}_y^G(\mathbf{x}_{\text{ref}}(\mathbf{x}_0) - \mathbf{x}_0) = \hat{k}_y^P(\mathbf{x}_{\text{ref}}(\mathbf{x}_0))$ holds the driving function can be cast into the form

$$D(x_0) = \underbrace{\sqrt{\frac{\rho^P(\mathbf{x}_{\text{ref}}(\mathbf{x}_0))}{\rho^P(\mathbf{x}_{\text{ref}}(\mathbf{x}_0)) - \rho^G(\mathbf{x}_{\text{ref}}(\mathbf{x}_0) - \mathbf{x}_0)}}}_{\text{virtual source compensation}} \underbrace{\sqrt{\frac{jk}{2\pi\rho^G(\mathbf{x}_{\text{ref}}(\mathbf{x}_0) - \mathbf{x}_0)}}}_{\text{SSD compensation}} \underbrace{\frac{\hat{k}_y^P(\mathbf{x}_{\text{ref}}(\mathbf{x}_0))P(\mathbf{x}_{\text{ref}}(\mathbf{x}_0))}{G(\mathbf{x}_{\text{ref}}(\mathbf{x}_0) - \mathbf{x}_0)}}}_{\text{2D explicit driving function}} \quad (3.63)$$

with ρ^P and ρ^G being the principal radii of the target field and the Green's function along the horizontal direction normalized by k . The formulation implies the fact, that similarly to the implicit solution, the explicit driving functions also applies the derivative of the target field, measured on the reference position. Furthermore, the driving

function explicitly contains the SSD compensation factor presented in (3.16), correcting the applied 3D SSD elements to 2D ones. The virtual source compensation factor is the reciprocal of that, presented for the implicit solution, given by $\sqrt{\rho^P(\mathbf{x}_{\text{ref}})/\rho^P(\mathbf{x}_0)}$.

One important fact is pointed out here: although having derived the above driving functions in terms of a forward and inverse spatial Fourier transform along a straight line, there is no restriction on the y -coordinate of the stationary point in (3.62) due to the local approximations involved: the y -coordinate might be x_0 -dependent. This means, that an arbitrary referencing curve may be defined as $\mathbf{x}_{\text{ref}}(x_0)$, and the driving functions can be calculated by finding the stationary positions satisfying $k_x^P(\mathbf{x}_{\text{ref}}(x_0)) = k_x^G(\mathbf{x}_{\text{ref}}(x_0) - \mathbf{x}_0)$ along this curve. Evaluating the driving functions in the stationary positions will result in amplitude correct synthesis along the reference curve. This means, that the presented driving functions are equivalent to the 2.5D WFS driving functions with the important difference that here the target field needs to be evaluated on the reference curve. Furthermore, within the validity of the Kirchhoff-approximation also the SSD has to be not necessarily linear: the spatial explicit driving functions can be applied using an arbitrary shaped SSD contour. Obviously in that case (3.63) has to be evaluated with $\hat{k}_y^P(\mathbf{x}_{\text{ref}}(x_0)) \rightarrow \hat{k}_n^P(\mathbf{x}_{\text{ref}}(x_0))$, i.e. with the wavenumber component along the normal of the actual SSD element. Similarly the second derivatives in (3.62) have to be evaluated along the direction, defined by the actual SSD element.

In the followings first a simple example is presented in order to demonstrate the validity of the spatial SDM driving functions.

Application example: Synthesis of a 3D point source using a linear SSD

Consider the synthesis of a 3D point source at $\mathbf{x}_s = [x_s, y_s, 0]^T$ with $y_s < 0$, referencing the synthesis to a circle around the virtual point source with the radius of R_{ref} . The linear SSD is located at $\mathbf{x}_0 = [x_0, 0, 0]^T$. Along with the equation describing the reference curve $\mathbf{x}_{\text{ref}}(x_0) = [x^*(x_0), y^*(x_0), 0]^T$ the stationary points satisfy the following equations

$$\mathbf{k}^G(\mathbf{x}_{\text{ref}}(\mathbf{x}_0) - \mathbf{x}_s) = \mathbf{k}^G(\mathbf{x}_{\text{ref}}(\mathbf{x}_0) - \mathbf{x}_0), \quad (3.64)$$

$$|\mathbf{x}_{\text{ref}} - \mathbf{x}_s| = R_{\text{ref}}. \quad (3.65)$$

The solution for the equations is given by

$$\mathbf{x}_{\text{ref}}(\mathbf{x}_0) = \mathbf{x}_s + R_{\text{ref}} \frac{\mathbf{x}_0 - \mathbf{x}_s}{|\mathbf{x}_0 - \mathbf{x}_s|}. \quad (3.66)$$

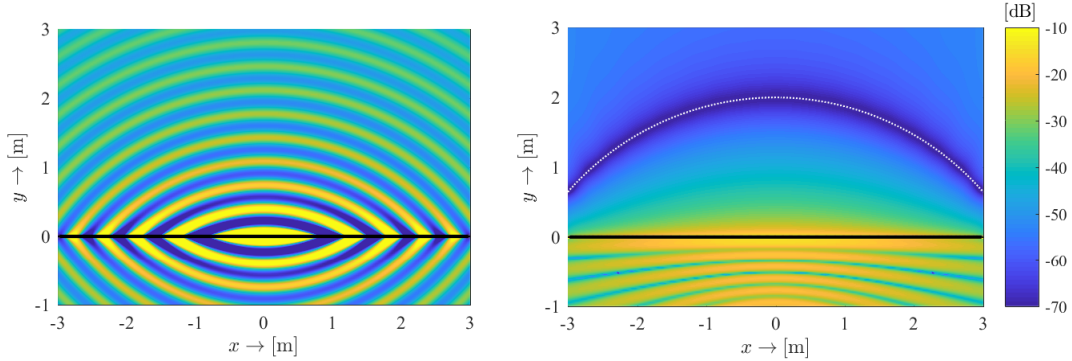


Figure 3.11. 2.5D synthesis of a 3D point source located at $\mathbf{x}_s = [0, -2, 0]^T$, radiating at $\omega_0 = 2\pi \cdot 1\text{krad/s}$. The synthesis is referenced on a circle around the virtual source, with a radius of $R_{\text{ref}} = 4\text{ m}$. Figure (a) depicts the real part of the synthesized field, (b) shows the error of synthesis.

Substituting the spherical virtual field into (3.63)—with the principal radii given by simple distances from the point sources—yields the explicit driving function in the spatial domain for a virtual point source.

$$D(x_0) = \sqrt{\frac{|\mathbf{x}_{\text{ref}} - \mathbf{x}_s|}{|\mathbf{x}_{\text{ref}} - \mathbf{x}_s| - |\mathbf{x}_{\text{ref}} - \mathbf{x}_0|}} \sqrt{\frac{jk}{2\pi|\mathbf{x}_{\text{ref}} - \mathbf{x}_0|}} \hat{k}_y^G(\mathbf{x}_{\text{ref}}(\mathbf{x}_0) - \mathbf{x}_s) \frac{G(\mathbf{x}_{\text{ref}}(\mathbf{x}_0) - \mathbf{x}_s)}{G(\mathbf{x}_{\text{ref}}(\mathbf{x}_0) - \mathbf{x}_0)} \quad (3.67)$$

Substituting the reference position coordinates along the reference circle (3.66) specifies the driving functions optimizing the synthesis on the reference circle

$$D(x_0) = -y_s \sqrt{\frac{R_{\text{ref}} - |\mathbf{x}_0 - \mathbf{x}_s|}{R_{\text{ref}}}} \sqrt{\frac{jk}{2\pi}} \frac{e^{-jk|\mathbf{x}_0 - \mathbf{x}_s|}}{|\mathbf{x}_0 - \mathbf{x}_s|^{\frac{3}{2}}} \quad (3.68)$$

Investigating Figure 3.11 verifies, that the synthesis is optimized on the prescribed reference curve.

3.3 Relation of implicit and explicit solutions

Finally, utilizing the high-frequency spatial explicit driving functions (3.62) the general relationship between the explicit and implicit solutions is highlighted. This is done by expressing the target field at the reference point by a 3D Neumann Rayleigh integral, approximated by the SPA along all dimensions.

$$P(\mathbf{x}, \omega) = 2 \iint_{-\infty}^{\infty} jk_y^P(\mathbf{x}_0) P(\mathbf{x}_0, \omega) G(\mathbf{x} - \mathbf{x}_0) d\mathbf{x}_0. \quad (3.69)$$

As discussed in 3.1.1, the stationary position on the Rayleigh plane $\mathbf{x}_0^*(\mathbf{x})$ is found, where

$$k_x^P(\mathbf{x}_0^*(\mathbf{x})) = k_x^G(\mathbf{x} - \mathbf{x}_0^*(\mathbf{x})) \quad (3.70)$$

holds, with $\mathbf{x} = [x, y, 0]^T$ and $\mathbf{x}_0^*(\mathbf{x}) = [x_0^*(x), 0, 0]^T$, since the vertical stationary point trivially remains at $z = 0$. Accounting for the negative second derivatives for a

diverging field, around the stationary point the the asymptotic approximation of the 3D Rayleigh integral reads

$$P(\mathbf{x}) \approx -2 \frac{2\pi}{j} \frac{1}{\sqrt{|\phi_{zz}^{P''}(\mathbf{x}_0^*(\mathbf{x})) + \phi_{zz}^{G''}(\mathbf{x} - \mathbf{x}_0^*(\mathbf{x}))|}} \frac{1}{\sqrt{|\phi_{xx}^{P''}(\mathbf{x}_0^*(\mathbf{x})) + \phi_{xx}^{G''}(\mathbf{x} - \mathbf{x}_0^*(\mathbf{x}))|}} \times \frac{\partial P(\mathbf{x})}{\partial y} \Big|_{\mathbf{x}=\mathbf{x}_0^*(\mathbf{x})} G(\mathbf{x} - \mathbf{x}_0^*(\mathbf{x})), \quad (3.71)$$

or written in terms of the principal radii (and applying the high-frequency gradient approximation, in order to simplify by $k_y^P(\mathbf{x}^*(\mathbf{x}_0))$)

$$P(\mathbf{x}) \approx 4\pi \sqrt{\frac{\rho_1^P(\mathbf{x}_0^*) \rho_1^G(\mathbf{x} - \mathbf{x}_0^*)}{\rho_1^P(\mathbf{x}_0^*) + \rho_1^G(\mathbf{x} - \mathbf{x}_0^*)}} \sqrt{\frac{\rho_2^P(\mathbf{x}_0^*) \rho_2^G(\mathbf{x} - \mathbf{x}_0^*)}{\rho_2^P(\mathbf{x}_0^*) + \rho_2^G(\mathbf{x} - \mathbf{x}_0^*)}} P(\mathbf{x}_0^*(\mathbf{x})) G(\mathbf{x} - \mathbf{x}_0^*(\mathbf{x})), \quad (3.72)$$

In order to express (3.62) in terms of the involved quantities measured along the SSD, one still needs to express the second derivative of the target field's phase $\phi_{xx}^{P''}(\mathbf{x})$ at an arbitrary receiver position \mathbf{x} in terms of the second derivative taken on the SSD at the stationary point $\phi_{xx}^{P''}(\mathbf{x}_0^*(\mathbf{x}))$. This is possible by expressing the second derivative of the asymptotic Rayleigh integral's phase function (3.71), i.e. from

$$\begin{aligned} \phi_{xx}^{P''}(\mathbf{x}) &= \frac{\partial^2}{\partial x^2} (\phi^P(\mathbf{x}_0^*(\mathbf{x})) + \phi^G(\mathbf{x} - \mathbf{x}_0^*(\mathbf{x}))) = \mathbf{x}_{0,xx}^{'''}(\mathbf{x}) \underbrace{(\phi_x^{P'}(\mathbf{x}_0^*(\mathbf{x})) - \phi_x^{G'}(\mathbf{x} - \mathbf{x}_0^*(\mathbf{x})))}_{=0} + \\ &+ \mathbf{x}_{0,x}^{*''}(\mathbf{x})^2 \phi_{xx}^{P''}(\mathbf{x}_0^*(\mathbf{x})) + (1 - \mathbf{x}_{0,x}^{*''}(\mathbf{x}))^2 \phi_{xx}^{G''}(\mathbf{x} - \mathbf{x}_0^*(\mathbf{x})). \end{aligned} \quad (3.73)$$

Again, the rate of change of the stationary position due to change in the evaluation position $\mathbf{x}_{0,x}^{*''}(\mathbf{x})$ has to be expressed, found by the differentiating the implicit definition of the stationary position (3.70):

$$\mathbf{x}_{0,x}^{*''}(\mathbf{x}) = \frac{\phi_{xx}^{G''}(\mathbf{x} - \mathbf{x}_0^*(\mathbf{x}))}{\phi_{xx}^{G''}(\mathbf{x} - \mathbf{x}_0^*(\mathbf{x})) - \phi_{xx}^{P''}(\mathbf{x}_0^*(\mathbf{x}))}. \quad (3.74)$$

Finally the required second derivative reads as

$$\phi_{xx}^{P''}(\mathbf{x}) = \frac{\phi_{xx}^{P''}(\mathbf{x}_0^*(\mathbf{x})) \phi_{xx}^{G''}(\mathbf{x} - \mathbf{x}_0^*(\mathbf{x}))}{\phi_{xx}^{P''}(\mathbf{x}_0^*(\mathbf{x})) + \phi_{xx}^{G''}(\mathbf{x} - \mathbf{x}_0^*(\mathbf{x}))} \quad (3.75)$$

valid assuming high frequency conditions. In terms of the principal radii the equation states, that

$$\rho^P(\mathbf{x}) = \rho^P(\mathbf{x}_0^*(\mathbf{x})) + \rho^G(\mathbf{x} - \mathbf{x}_0^*(\mathbf{x})) \quad (3.76)$$

reflecting the simple fact, the principal radii of an arbitrary field grows simply linearly with further propagation from \mathbf{x}_0 to \mathbf{x} , while obviously the curvature, and thus the second phase derivatives are added reciprocally. This finding may be employed in order to simplify (3.72). For the special case of the 3D Green's function $\rho_1^G(\mathbf{x} - \mathbf{x}_0^*) =$

$\rho_2^G(\mathbf{x} - \mathbf{x}_0^*) = |\mathbf{x} - \mathbf{x}_0^*|$ holds and by substituting the explicit expression for the Green's function the equation simplifies to

$$P(\mathbf{x}) \approx P(\mathbf{x}_0^*(\mathbf{x})) \sqrt{\frac{\rho_1^P(\mathbf{x}_0^*) \rho_2^P(\mathbf{x}_0^*)}{\rho_1^P(\mathbf{x}) \rho_2^P(\mathbf{x})}} e^{-jk|\mathbf{x} - \mathbf{x}_0^*(\mathbf{x})|}, \quad (3.77)$$

where $\rho_1^P(\mathbf{x}) \cdot \rho_2^P(\mathbf{x})$ is the reciprocal of the Gaussian curvature of the wavefront. Thus, in a ray-tracing manner the wave field is approximated locally by its value at the stationary position: the numerator of the amplitude factor approximates the field in the source position, attenuated by the denominator, given by (3.76), while a simple phase shift term corresponds to the propagation time delay. Also, the equation reflects the fact, that the intensity of the wave field is proportional to the Gaussian curvature of the wavefront, being a well-known fact in the field of optics [BW70, Sec. 3.1], [Bou+97, Sec. 1.3].

Comparing the definition of the stationary points for the Rayleigh integral (3.70) and the stationary SDM evaluation points (3.57), it is revealed, that they describe stationary point pairs. Therefore in the spatial SDM driving function (3.62) both the target field and the second phase derivative at the evaluation point $x^*(x_0)$ can be expressed by the corresponding quantities taken at x_0 , by using (3.71) and (3.75), respectively, with a substitution of $\mathbf{x}_0^*(\mathbf{x}) \rightarrow [x_0, 0, 0]^T$ and $\mathbf{x} \rightarrow [x^*(x_0), y, 0]^T$.

Substituting (3.75) into (3.62) yields the spatial SDM driving functions in terms of the curvatures measured on the SSD

$$D(x_0) \approx \sqrt{|\phi_{xx}^{P''}(x_0, 0) + \phi_{xx}^{G''}(x^*(x_0) - x_0, y)|} \sqrt{\frac{j}{2\pi}} \frac{P(x^*(x_0), y)}{G(x^*(x_0) - x_0, y)}. \quad (3.78)$$

Finally, by expressing the target field by (3.71), the Green's function vanishes and one obtains the asymptotic form of the spatial SDM driving functions written in terms of the target field taken on the SSD

$$D(x_0) \approx \sqrt{\frac{8\pi}{j}} \frac{1}{\sqrt{|\phi_{zz}^{P''}(x_0, 0) + \phi_{zz}^{G''}(x^*(x_0) - x_0, y)|}} j k_y^P(\mathbf{x}_0) P(\mathbf{x}_0). \quad (3.79)$$

Comparing with (3.12) reveals, that the asymptotic SDM driving functions exactly coincide the 2.5D WFS driving function. It is important to note, that the WFS driving functions were obtained from the 2.5D Neumann Rayleigh integral in an intuitive manner, by introducing the reference curve concept with interchanging the role of the receiver position and its stationary SSD position. On the other hand the driving function (3.79) inherently contains the horizontal SPA and the reference curve concept. It is therefore verified that under high-frequency assumptions WFS is the asymptotic or local approximation of the global explicit solution.

3.4 Summary

TODO:

- Write matlab code to regenerate figs 1.6 and 2.6
- Check the stat.position def. for the Rayleigh and KHI!
- Check curvature / radii definitions, normalized or not!
- Check 3.2/3.3. what goes to appendix
- Maybe the beginning of 3.3 may go to the 2.3.2 (or to appendix)
- Check a (-1) multipl. in 3.15

Appendices

A

Appendix A

A.1 Derivation of Green's theorem

The Gauss, or divergence theorem states, that if a vector space, described by vector-vector function $\mathbf{u}(\mathbf{x})$ is non-singular and differentiable over a bounded region Ω , with a boundary denoted by $\partial\Omega$, then the integral of the divergence of the vector-space over the whole region equals to the total flux, measured on the boundary surface (refer to figure 1.1 for the problem geometry):

$$\int_{\Omega} \nabla \cdot \mathbf{u}(\mathbf{x}) d\Omega = \int_{\partial\Omega} \langle \mathbf{u}(\mathbf{x}), \mathbf{n}_o \rangle d\partial\Omega, \quad (\text{A.1})$$

where \mathbf{n}_o is the outward-pointing unit normal vector on the boundary.

Let's express the arbitrary vector-vector function $\mathbf{u}(\mathbf{x})$ as the combination of two twice continuously differentiable vector-scalar functions:

$$\mathbf{u}(\mathbf{x}) = \Phi(\mathbf{x}) \nabla \Psi(\mathbf{x}) - \nabla \Phi(\mathbf{x}) \Psi(\mathbf{x}). \quad (\text{A.2})$$

Using the chain rule the divergence of these terms are obtained as

$$\nabla \cdot (\Phi(\mathbf{x}) \nabla \Psi(\mathbf{x})) = \nabla \Phi(\mathbf{x}) \cdot \nabla \Psi(\mathbf{x}) + \Phi(\mathbf{x}) \nabla^2 \Psi(\mathbf{x}) \quad (\text{A.3})$$

$$\nabla \cdot (\nabla \Phi(\mathbf{x}) \Psi(\mathbf{x})) = \nabla \Phi(\mathbf{x}) \cdot \nabla \Psi(\mathbf{x}) + \nabla^2 \Phi(\mathbf{x}) \Psi(\mathbf{x}), \quad (\text{A.4})$$

thus

$$\int_{\Omega} \left\{ \Phi(\mathbf{x}) \nabla^2 \Psi(\mathbf{x}) - \nabla^2 \Phi(\mathbf{x}) \Psi(\mathbf{x}) \right\} d\Omega = \int_{\partial\Omega} \langle \Phi(\mathbf{x}) \nabla \Psi(\mathbf{x}) - \nabla \Phi(\mathbf{x}) \Psi(\mathbf{x}), \mathbf{n}_o \rangle d\partial\Omega. \quad (\text{A.5})$$

By replacing the outward-pointing normal vector with the inward normal: $\mathbf{n}_i = -\mathbf{n}_o$, and denoting the normal derivative on the surface by $\frac{\partial}{\partial n}$ we obtain the *Green's theorem*:

$$\int_{\Omega} \left\{ \Phi(\mathbf{x}) \nabla^2 \Psi(\mathbf{x}) - \nabla^2 \Phi(\mathbf{x}) \Psi(\mathbf{x}) \right\} d\Omega = \int_{\partial\Omega} \frac{\partial \Phi(\mathbf{x})}{\partial n} \Psi(\mathbf{x}) - \Phi(\mathbf{x}) \frac{\partial \Psi(\mathbf{x})}{\partial n} d\partial\Omega. \quad (\text{A.6})$$

B

Appendix B

B.1 Notes on the Hessian of the phase function

B.1.1 Definition of the principal curvatures and principal directions

Assume a wave field, described by the general polar form $P(\mathbf{x}, \omega) = A^P(\mathbf{x}, \omega)e^{j\phi^P(\mathbf{x}, \omega)}$. Supposing, that the amplitude changes slowly, compared to the phase function the local dispersion relation $|\nabla\phi(\mathbf{x}, \omega)| = \frac{\omega}{c} = k$ holds and the equation describing an arbitrary wavefront i.e. $\phi^P(\mathbf{x}, \omega) - C = 0$ is the *normalform* of the given surface [Har99; Har01]. The Hessian matrix of the function is given by the symmetric matrix

$$H^P = \frac{\partial^2}{\partial x_i \partial x_j} \phi^P(\mathbf{x}, \omega) = \begin{bmatrix} \phi_{xx}^{P''}(\mathbf{x}, \omega) & \phi_{xy}^{P''}(\mathbf{x}, \omega) & \phi_{xz}^{P''}(\mathbf{x}, \omega) \\ \phi_{xy}^{P''}(\mathbf{x}, \omega) & \phi_{yy}^{P''}(\mathbf{x}, \omega) & \phi_{yz}^{P''}(\mathbf{x}, \omega) \\ \phi_{xz}^{P''}(\mathbf{x}, \omega) & \phi_{yz}^{P''}(\mathbf{x}, \omega) & \phi_{zz}^{P''}(\mathbf{x}, \omega) \end{bmatrix}, \quad i, j = 1, 2, 3. \quad (\text{B.1})$$

with the eigenvalues $\lambda_1, \lambda_2, \lambda_3$ and the corresponding eigenvectors $\mathbf{v}_1, \mathbf{v}_2, \mathbf{v}_3$. Since the function under consideration is a normalform, therefore the following properties hold

- $\lambda_3 = 0$ with the eigenvector $\mathbf{v}_3 = -\nabla\phi^P(\mathbf{x}, \omega)/k = \hat{\mathbf{k}}^P(\mathbf{x})$, i.e. being the normal of the wavefront
- $\lambda_1 = -k \cdot \kappa_1^P(\mathbf{x}), \lambda_2 = -k \cdot \kappa_2^P(\mathbf{x})$ being proportional to the *main or principal curvatures* of the wavefront and $\rho_1^P(\mathbf{x}) = 1/\kappa_1^P(\mathbf{x}), \rho_2^P(\mathbf{x}) = 1/\kappa_2^P(\mathbf{x})$ being the *principal radii*. The principal curvatures and radii are defined as the following: Consider all the planes containing the normal of the surface at the point of investigation, defined by the surface normal and vector \mathbf{v} , being the tangent of the surface. The curvature is defined as the quadratic form

$$\kappa = \mathbf{v} H^P \mathbf{v}^T. \quad (\text{B.2})$$

The main curvatures are then defined as the minimum and maximum values of curvature, i.e. the reciprocal of the osculating circles' radii (the principal radii). The corresponding eigenvectors \mathbf{v}_1 and \mathbf{v}_2 are the tangential, orthogonal unit vectors pointing into the direction of the maximal and minimal curvatures.

Finally, as the general case the Hessian matrix of an arbitrary wavefront can be written in terms of the principal curvatures and the corresponding eigenvectors as

$$H^P = -k \left(\kappa_1 \mathbf{v}_1 \mathbf{v}_1^T + \kappa_2 \mathbf{v}_2 \mathbf{v}_2^T \right) = -k \mathbf{V} \mathbf{K} \mathbf{V}^T, \quad (\text{B.3})$$

where $\mathbf{V} = [\mathbf{v}_1 \ \mathbf{v}_2]$ and $\mathbf{K} = \begin{bmatrix} \kappa_1 & 0 \\ 0 & \kappa_2 \end{bmatrix}$ are the matrices of the eigenvectors and the curvatures.

For the special case of the three-dimensional Green's function positioned at \mathbf{x}_0 , only eigenvector corresponding for λ_3 is well-defined over the spherical /umbilical wavefront, being a radial directed normal vector. λ_2 and λ_3 may be arbitrary orthogonal vectors in the plane, tangent to the surface in the point of investigation \mathbf{x} , with the corresponding principal curvatures being $\kappa_1^G(\mathbf{x}) = \kappa_2^G(\mathbf{x}) = 1/|\mathbf{x} - \mathbf{x}_0|$.

In the present treatise when dealing with 2.5D problems it is a standard prerequisite, that in the plane of investigation ($z = 0$) all the involved wave fields propagate along the horizontal direction ($k_z(x, y, 0) \equiv 0$), thus the Hessian of the phase function becomes

$$H^P = \begin{bmatrix} \phi_{xx}^{P''}(\mathbf{x}, \omega) & \phi_{xy}^{P''}(\mathbf{x}, \omega) & 0 \\ \phi_{xy}^{P''}(\mathbf{x}, \omega) & \phi_{yy}^{P''}(\mathbf{x}, \omega) & 0 \\ 0 & 0 & \phi_{zz}^{P''}(\mathbf{x}, \omega) \end{bmatrix}, \quad (\text{B.4})$$

with the trivial eigenvector/principal direction $\mathbf{v}_2 = [0, 0, 1]^T$ and the corresponding principal curvature $\kappa_2^P(\mathbf{x}) = -\frac{1}{k} \phi_{zz}^{P''}(\mathbf{x}, \omega)$. Furthermore, considering, that the eigenvector with a zero eigenvalue is given by $\mathbf{v}_3 = \hat{\mathbf{k}}^P(\mathbf{x}) = [\hat{k}_x^P(\mathbf{x}), \hat{k}_y^P(\mathbf{x}), 0]^T$ and \mathbf{v}_1 is orthogonal to \mathbf{v}_2 and \mathbf{v}_3 , therefore $\mathbf{v}_1 = [\hat{k}_y^P(\mathbf{x}), \hat{k}_x^P(\mathbf{x}), 0]^T$ holds. From simple geometrical considerations and applying (B.2) the elements of the Hessian matrix can be expressed as

$$H^P = -k \begin{bmatrix} \hat{k}_y^P(\mathbf{x})^2 \kappa_1^P(\mathbf{x}) & \hat{k}_x^P(\mathbf{x}) \hat{k}_y^P(\mathbf{x}) \kappa_1^P(\mathbf{x}) & 0 \\ \hat{k}_x^P(\mathbf{x}) \hat{k}_y^P(\mathbf{x}) \kappa_1^P(\mathbf{x}) & \hat{k}_x^P(\mathbf{x})^2 \kappa_1^P(\mathbf{x}) & 0 \\ 0 & 0 & \kappa_2^P(\mathbf{x}) \end{bmatrix}. \quad (\text{B.5})$$

In the aspect of the present treatise the signature and the determinant of the Hessian in the stationary position is of importance. In the followings these properties will be discussed when the SPA is applied for the Rayleigh integral.

B.1.2 Hessian for the SPA applied for the Rayleigh-integral

Assume the Rayleigh-integral, written onto the plane $y = 0$, with the high-frequency gradient approximation applied:

$$P(\mathbf{x}, \omega) = 2 \int_{-\infty}^{\infty} j k_y^P(\mathbf{x}_0) P(\mathbf{x}_0, \omega) G(\mathbf{x} - \mathbf{x}_0, \omega) dx_0 dz_0. \quad (\text{B.6})$$

By definition the stationary position for the integral is found where

$$\nabla_{\mathbf{x}_0} \phi^P(\mathbf{x}_0, \omega) = -\nabla_{\mathbf{x}_0} \phi^G(\mathbf{x} - \mathbf{x}_0, \omega) \quad (\text{B.7})$$

Geometrically the stationary position $\mathbf{x}_0^*(\mathbf{x})$ is found where the normals of the involved wavefronts coincide on the Rayleigh plane, i.e. where the wavefront of P is tangential with the spherical wavefront of the Green's function. Around the stationary point the phase function (B.7) gives the phase of sound field P measured at \mathbf{x} .

$$\phi^P(\mathbf{x}, \omega) = \phi^P(\mathbf{x}_0^*(\mathbf{x}), \omega) + \phi^G(\mathbf{x} - \mathbf{x}_0^*(\mathbf{x}), \omega) \quad (\text{B.8})$$

The 3x3 Hessian of the integrand's phase function is defined as

$$H_{kl} = H_{kl}^P + H_{kl}^G = \frac{\partial^2}{\partial x_{0k} \partial x_{0l}} (\phi^P(\mathbf{x}_0, \omega) + \phi^G(\mathbf{x} - \mathbf{x}_0, \omega)), \quad k, l = 1, 2, 3. \quad (\text{B.9})$$

Obviously, the eigenfunctions of H_{kl}^P and H_{kl}^G are the principal curvatures of the target field and the Green's function measured at the stationary position $\mathbf{x}_0^*(\mathbf{x})$. Since the principal directions for the Green's function's wavefront are not well-defined, they can be chosen to coincide with the principal directions of H^P . Therefore at the stationary point the eigenvectors of H^P and H^G coincide and their eigenvalues are additive. The eigenvalues of the resultant matrix are therefore simply given as

$$\lambda_1(\mathbf{x}) = \lambda_1^P(\mathbf{x}_0^*(\mathbf{x})) + \lambda_1^G(\mathbf{x} - \mathbf{x}_0^*(\mathbf{x})) = -k (\kappa_1^P(\mathbf{x}_0^*(\mathbf{x})) + \kappa_1^G(\mathbf{x} - \mathbf{x}_0^*(\mathbf{x}))), \quad (\text{B.10})$$

$$\lambda_2(\mathbf{x}) = \lambda_2^P(\mathbf{x}_0^*(\mathbf{x})) + \lambda_2^G(\mathbf{x} - \mathbf{x}_0^*(\mathbf{x})) = -k (\kappa_2^P(\mathbf{x}_0^*(\mathbf{x})) + \kappa_2^G(\mathbf{x} - \mathbf{x}_0^*(\mathbf{x}))), \quad (\text{B.11})$$

$$\lambda_3(\mathbf{x}) = \lambda_3^P(\mathbf{x}_0^*(\mathbf{x})) + \lambda_3^G(\mathbf{x} - \mathbf{x}_0^*(\mathbf{x})) = 0. \quad (\text{B.12})$$

In the aspect of the followings it's important to investigate the local principal curvatures and the principal radii of the described wavefront of P at the evaluation point \mathbf{x} . The curvatures are defined as the eigenvalues (normalized by $-k$) of the Hessian

$$H_{ij}^P = \frac{\partial^2}{\partial x_i \partial x_j} \phi^P(\mathbf{x}, \omega) = \frac{\partial^2}{\partial x_i \partial x_j} (\phi^P(\mathbf{x}_0^*(\mathbf{x}), \omega) + \phi^G(\mathbf{x} - \mathbf{x}_0^*(\mathbf{x}), \omega)) \quad (\text{B.13})$$

measured at \mathbf{x} . By applying the chain rule the derivative is expressed as

$$\begin{aligned} H_{ij}^P &= \frac{\partial}{\partial x_j} \left(\frac{\partial x_{0k}}{\partial x_i} \frac{\partial \phi^P(x_{0k}, \omega)}{\partial x_{0k}} + \frac{\partial(x_k - x_{0k})}{\partial x_i} \frac{\partial \phi^G(x_k - x_{0k}, \omega)}{\partial(x_k - x_{0k})} \right) = \\ &\quad \underbrace{\frac{\partial^2 x_{0k}}{\partial x_i \partial x_j} \left(\frac{\partial \phi^P(x_{0k}, \omega)}{\partial x_{0k}} + \frac{\partial \phi^G(x_k - x_{0k}, \omega)}{\partial(x_k - x_{0k})} \right)}_{=0} \\ &\quad + \frac{\partial x_{0k}}{\partial x_i} \frac{\partial x_{0l}}{\partial x_j} \underbrace{\frac{\partial^2 \phi^P(x_{0k}, \omega)}{\partial x_{0k} \partial x_{0l}}}_{H_{kl}^P} + \frac{\partial(x_k - x_{0k})}{\partial x_i} \frac{\partial(x_l - x_{0l})}{\partial x_j} \underbrace{\frac{\partial^2 \phi^G(x_k - x_{0k}, \omega)}{\partial(x_k - x_{0k}) \partial(x_l - x_{0l})}}_{H_{kl}^G} \quad (\text{B.14}) \end{aligned}$$

where the underbraced part of equation equals to zero by the definition of the stationary position. By introducing the matrix $\nabla_{\mathbf{x}} \mathbf{x}_0$ for the rate of change of the stationary position with respect to the change in any coordinate of the evaluation point, defined as

$$[\nabla_{\mathbf{x}} \mathbf{x}_0]_{lj} = \frac{\partial x_{0l}}{\partial x_j} = \left[\begin{array}{c|c|c} \frac{\partial \mathbf{x}_0^*(\mathbf{x})}{\partial x} & \frac{\partial \mathbf{x}_0^*(\mathbf{x})}{\partial y} & \frac{\partial \mathbf{x}_0^*(\mathbf{x})}{\partial z} \end{array} \right] \quad (\text{B.15})$$

the Hessian under consideration can be written in a matrix form as

$$H_{ij}^P = (\nabla_{\mathbf{x}} \mathbf{x}_0)^T H_{kl}^P (\nabla_{\mathbf{x}} \mathbf{x}_0) + (\mathbf{I} - \nabla_{\mathbf{x}} \mathbf{x}_0)^T H_{kl}^G (\mathbf{I} - \nabla_{\mathbf{x}} \mathbf{x}_0) \quad (\text{B.16})$$

In order to express this gradient of the stationary position its definition (B.7) is reconsidered, rewritten in terms of an arbitrary component of the gradient, taken at the stationary position as

$$\frac{\partial}{\partial x_{0k}} \phi^P(\mathbf{x}_0^*(\mathbf{x}), \omega) - \frac{\partial}{\partial x_{0k}} \phi^G(\mathbf{x} - \mathbf{x}_0^*(\mathbf{x}), \omega) = 0 \quad (\text{B.17})$$

Taking a further derivative with respect to x_j results in

$$\frac{\partial^2}{\partial x_{0l} \partial x_{0k}} \phi^P(\mathbf{x}_0^*(\mathbf{x}), \omega) \frac{\partial x_{0l}}{\partial x_j} - \frac{\partial^2}{\partial x_{0l} \partial x_{0k}} \phi^G(\mathbf{x} - \mathbf{x}_0^*(\mathbf{x}), \omega) \frac{\partial}{\partial x_j} (x_l - x_{0l}) = 0, \quad (\text{B.18})$$

or written in a matrix form

$$H_{kl}^P \nabla_{\mathbf{x}} \mathbf{x}_0 - H_{kl}^G (\mathbf{I} - \nabla_{\mathbf{x}} \mathbf{x}_0) = 0 \rightarrow (H_{kl}^P + H_{kl}^G) \nabla_{\mathbf{x}} \mathbf{x}_0 = H_{kl}^G. \quad (\text{B.19})$$

In order to invert the matrix $H_{kl}^P + H_{kl}^G$ the involved matrices are expressed in the form, given in (B.3), i.e. by transforming it into its eigenspace:

$$\mathbf{V} (\mathbf{K}^P + \mathbf{K}^G) \mathbf{V}^T \cdot \nabla_{\mathbf{x}} \mathbf{x}_0 = \mathbf{V} \mathbf{K}^G \mathbf{V}^T, \quad (\text{B.20})$$

where \mathbf{K}^P and \mathbf{K}^G are 2x2 diagonal matrices of the curvatures of P and G at the stationary point, and \mathbf{V} is a 3x2 matrix consisting of the two corresponding eigenvectors. Since the two columns of \mathbf{V} are orthonormal, and the inverse of a 2x2 diagonal matrix can be calculated easily, therefore the gradient of the stationary position reads as

$$\nabla_{\mathbf{x}} \mathbf{x}_0 = \mathbf{V} \frac{\mathbf{K}^G}{\mathbf{K}^P + \mathbf{K}^G} \mathbf{V}^T = \mathbf{V} \begin{bmatrix} \frac{\kappa_1^G}{\kappa_1^P + \kappa_1^G} & 0 \\ 0 & \frac{\kappa_2^G}{\kappa_2^P + \kappa_2^G} \end{bmatrix} \mathbf{V}^T, \quad (\text{B.21})$$

and obviously

$$\mathbf{I} - \nabla_{\mathbf{x}} \mathbf{x}_0 = \mathbf{V} \frac{\mathbf{K}^P}{\mathbf{K}^P + \mathbf{K}^G} \mathbf{V}^T \quad (\text{B.22})$$

holds.

Finally, the Hessian at the evaluation point, given by (B.16) is expressed in the same eigenspace with $H_{kl}^P = -k\mathbf{V}\mathbf{K}^P\mathbf{V}^T$ and $H_{kl}^G = -k\mathbf{V}\mathbf{K}^G\mathbf{V}^T$. Exploiting that $\mathbf{V}^T\mathbf{V} = \mathbf{I}$ leads to

$$H_{ij}^P = -k\mathbf{V} \frac{\mathbf{K}^P \mathbf{K}^G}{\mathbf{K}^P + \mathbf{K}^G} \mathbf{V}^T = -k\mathbf{V} \begin{bmatrix} \frac{\kappa_1^P \kappa_1^G}{\kappa_1^P + \kappa_1^G} & 0 \\ 0 & \frac{\kappa_2^P \kappa_2^G}{\kappa_2^P + \kappa_2^G} \end{bmatrix} \mathbf{V}^T = -k\mathbf{V} \begin{bmatrix} \frac{1}{\rho_1^P + \rho_1^G} & 0 \\ 0 & \frac{1}{\rho_2^P + \rho_2^G} \end{bmatrix} \mathbf{V}^T \quad (\text{B.23})$$

This result states, that if the Rayleigh integral describes a sound field at \mathbf{x} , then the principal curvatures and radii of the field can be written in terms of that, measured on the Rayleigh boundary, as

$$\kappa^P(\mathbf{x}) = \frac{\kappa^P(\mathbf{x}_0^*(\mathbf{x})) \kappa^G(\mathbf{x} - \mathbf{x}_0^*(\mathbf{x}))}{\kappa^P(\mathbf{x}_0^*(\mathbf{x})) + \kappa^G(\mathbf{x} - \mathbf{x}_0^*(\mathbf{x}))}, \quad (\text{B.24})$$

$$\rho^P(\mathbf{x}) = \rho^P(\mathbf{x}_0^*(\mathbf{x})) + \rho^G(\mathbf{x} - \mathbf{x}_0^*(\mathbf{x})). \quad (\text{B.25})$$

Furthermore, the corresponding eigenvectors, i.e the direction of the largest and smallest curvature on the wavefront does not change along the direction of propagation.

Evaluation of the Rayleigh integral along xz -dimensions: In the case of approximating the integral with respect to both x and z direction the Hessian of the SPA may be formed from the 3x3 Hessian of the phase function by removing the rows and columns containing the y derivatives, hence by forming its 2x2 principal submatrix. Based on (B.3) the Hessian for the SPA can be expressed in terms of the principal curvatures and the corresponding eigenvectors. With also exploiting, that in the stationary point (B.10) holds the Hessian for the 2D SPA reads as

$$H = -k \begin{bmatrix} v_{1x}^2 (\kappa_1^P + \kappa_1^G) + v_{2x}^2 (\kappa_2^P + \kappa_2^G) & v_{1x} v_{1z} (\kappa_1^P + \kappa_1^G) + v_{2x} v_{2z} (\kappa_2^P + \kappa_2^G) \\ v_{1x} v_{1z} (\kappa_1^P + \kappa_1^G) + v_{2x} v_{2z} (\kappa_2^P + \kappa_2^G) & v_{1z}^2 (\kappa_1^P + \kappa_1^G) + v_{2z}^2 (\kappa_2^P + \kappa_2^G) \end{bmatrix}, \quad (\text{B.26})$$

with $\mathbf{v}_1 = [v_{1x}, v_{1y}, v_{1z}]^T$, $\mathbf{v}_2 = [v_{2x}, v_{2y}, v_{2z}]^T$ and $\kappa^P = \kappa^P(\mathbf{x}_0^*(\mathbf{x}))$, $\kappa^G = \kappa^G(\mathbf{x} - \mathbf{x}_0^*(\mathbf{x}))$.

The eigenvalues of this submatrix cannot be expressed in a general way, however the *interlacing inequalities of principal submatrices* ensures that they have the same sign as λ_2 and λ_3 . The signature of the Hessian is therefore

- assuming a divergent sound field, the eigenvalues of the Hessian are negative (the curvatures are positive) and the signature is given by -2.
- assuming a convergent sound field with both principal curvature being negative *on the Rayleigh plane*, the signature of the Hessian depends on the evaluation position \mathbf{x} . On the parts of the space where the curvature of wavefront P is greater in magnitude than that of the Green's function the eigenvalues of the Hessian positive and it signature is 2. On other parts of the space the signature is -2.

In practice with a simple example it means, that if the Rayleigh integral describes a sound field propagating toward a point, than the signature for an evaluation point

between the Rayleigh plane and the focus point is given by 2, and in other parts of the space, where the waves already diverge after passing the focus point, the signature is -2.

The determinant of the Hessian is given by

$$\det H = -k \left(\kappa_1^P + \kappa_1^G \right) \left(\kappa_2^P + \kappa_2^G \right) (v_{2x}v_{1z} - v_{1x}v_{2z})^2. \quad (\text{B.27})$$

By the definition of cross product of vectors the term $(v_{2x}v_{1z} - v_{1x}v_{2z})$ is the second coordinate of the vector, being perpendicular to \mathbf{v}_1 and \mathbf{v}_2 , i.e. of the normalized local wavenumber vector:

$$\det H = -k \left(\kappa_1^P(\mathbf{x}_0^*(\mathbf{x})) + \kappa_1^G(\mathbf{x} - \mathbf{x}_0^*(\mathbf{x})) \right) \left(\kappa_2^P(\mathbf{x}_0^*(\mathbf{x})) + \kappa_2^G(\mathbf{x} - \mathbf{x}_0^*(\mathbf{x})) \right) \hat{k}_y^P(\mathbf{x}_0^*(\mathbf{x}))^2. \quad (\text{B.28})$$

Note, that the description above is not limited for the Rayleigh integral: if the Kirchhoff-Helmholtz integral is written onto a smooth convex surface with the surface's curvature being significantly smaller than the wavefront curvature, than the surface can be considered locally plane, and the above given description holds with the substitution $\hat{k}_y^P(\mathbf{x}_0^*(\mathbf{x})) \rightarrow \hat{k}_n^P(\mathbf{x}_0^*(\mathbf{x}))$ being the normal component of the local wavenumber vector. This statement is a consequence of the invariance of the determinant with respect to a linear transform.

Obviously, this formulation holds in case a 2D Fourier integral is to be evaluated. In this case the determinant reads as

$$\det H = -\frac{1}{k} \kappa_1^P(\mathbf{x}_0^*(k_x, k_z)) \kappa_2^P(\mathbf{x}_0^*(k_x, k_z)) k_y^2. \quad (\text{B.29})$$

Evaluation of the Rayleigh integral along z -dimension: In the special case of the derivation of the 2.5D Rayleigh integral only the integration along the z -dimension is approximated and the Hessian is simply given by $\phi''_{zz}(\mathbf{x}_0) = \phi''_{zz}(\mathbf{x}_0) + \phi''_{zz}(\mathbf{x} - \mathbf{x}_0)$. Requiring, that in the horizontal plane of investigation $k_z(\mathbf{x}) \equiv 0$ guarantees, that the second derivative is the principal curvature itself (see below), thus around the stationary position reads as

$$\phi''_{zz}(\mathbf{x}_0) = -k \left(\kappa_2^P(\mathbf{x}_0^*(\mathbf{x})) + \kappa_2^G(\mathbf{x} - \mathbf{x}_0^*(\mathbf{x})) \right). \quad (\text{B.30})$$

Obviously for the sign of the second derivative the description given for the 2D SPA case holds.

C

Appendix C

C.1 Wavenumber vector of a point source pair

Given a point source pair positioned symmetrically to the y -axis $\mathbf{x}_1 = [x_1, y_1, 0]^T$, $\mathbf{x}_2 = [-x_1, y_1, 0]^T$ the radiated field reads

$$P(\mathbf{x}, \omega) = \frac{A_1}{4\pi} \frac{e^{-j\frac{\omega}{c}|\mathbf{x}-\mathbf{x}_1|}}{|\mathbf{x}-\mathbf{x}_1|} + \frac{A_2}{4\pi} \frac{e^{-j\frac{\omega}{c}|\mathbf{x}-\mathbf{x}_2|}}{|\mathbf{x}-\mathbf{x}_2|}, \quad (\text{C.1})$$

with the amplitude factors denoted by A_1 and A_2 . Applying the Euler's formula the phase function of the resultant field becomes

$$-\phi^P(\mathbf{x}, \omega) = \arctan \frac{\frac{A_1}{r_1} \sin\left(\frac{\omega}{c}|\mathbf{x}-\mathbf{x}_1|\right) + \frac{A_1}{r_2} \sin\left(\frac{\omega}{c}|\mathbf{x}-\mathbf{x}_2|\right)}{\frac{A_1}{r_1} \cos\left(\frac{\omega}{c}|\mathbf{x}-\mathbf{x}_1|\right) + \frac{A_2}{r_1} \cos\left(\frac{\omega}{c}|\mathbf{x}-\mathbf{x}_2|\right)}. \quad (\text{C.2})$$

The local wavenumber vector, i.e. the gradient of the expression can be calculated by using that

$$\left(\arctan \frac{f}{g} \right)' = \frac{f'g - fg'}{f^2 + g^2}, \quad (\text{C.3})$$

with the derivatives given by

$$f' = A_1 r'_1 \frac{kr_1 \cos(kr_1) - \sin(kr_1)}{r_1^2} + A_2 r'_2 \frac{kr_2 \cos(kr_2) - \sin(kr_2)}{r_2^2} \quad (\text{C.4})$$

$$g' = A_1 r'_1 \frac{-kr_1 \sin(kr_1) - \cos(kr_1)}{r_1^2} + A_2 r'_2 \frac{-kr_2 \sin(kr_2) - \cos(kr_2)}{r_2^2}, \quad (\text{C.5})$$

denoting $r_1 = |\mathbf{x} - \mathbf{x}_1|$ and $r_2 = |\mathbf{x} - \mathbf{x}_2|$ and $k = \frac{\omega}{c}$. By expressing the gradient with several simplification one obtains

$$\phi^{P'} = \frac{k (r'_1 A_1^2 r_2^2 + r'_2 A_2^2 r_1^2 + A_1 A_2 r_1 r_2 (r'_1 + r'_2) \cos(k\Delta r)) - A_1 A_2 (r'_1 r_2 - r'_2 r_1) \sin(k\Delta r)}{r_1^2 r_2^2 A^P(\mathbf{x}, \omega)}, \quad (\text{C.6})$$

with $\Delta r = r_1 - r_2$ and where $A^P(\mathbf{x}, \omega)$ is the amplitude of the resulting field omitting the normalizing factor $1/4\pi$.

$$A^P(\mathbf{x}, \omega) = \sqrt{A_1^2 r_2^2 + A_2^2 r_1^2 + 2 A_1 A_2 r_1 r_2 \cos(k\Delta r)} / r_1 r_2. \quad (\text{C.7})$$

These complex expression along with the amplitude factor describes the interference pattern of the point source pair over the whole listening area: due to destructive interference the amplitude factor vanishes over the zeros of $A^P(\mathbf{x}, \omega)$. At these positions the phase changes rapidly resulting in infinitely large local wavenumber vector lengths.

From the aspect of stereophonic application only the stereo axis is of interest, where $r_1 = r_2$ holds. Due to the symmetry of the geometry along that axis $\frac{\partial}{\partial x}r_1 = -\frac{\partial}{\partial x}r_2$, $\frac{\partial}{\partial y}r_1 = \frac{\partial}{\partial y}r_2$ and $\frac{\partial}{\partial z}r_1 = \frac{\partial}{\partial z}r_2$ holds, and the derivatives of the phase function is given as

$$-\phi_x^{P'} = kr'_x \frac{A_1 - A_2}{A_1 + A_2} \quad (\text{C.8})$$

$$-\phi_y^{P'} = kr'_y. \quad (\text{C.9})$$

and the amplitude factor reads as

$$A^P(0, y, z, \omega) = \frac{A_1 + A_2}{r}. \quad (\text{C.10})$$

D

Appendix D

D.1 2.5D Kirchhoff integral for a 3D point source

Assume a 2D point source, located at $\mathbf{x}_s = [x_s, y_s]^T$. The generated sound field inside the domain, bounded by the contour C can be described by the 2D Kirchhoff approximation in terms of the 2D Green's function. At position $\mathbf{x} \in \mathbb{R}^2$ the field reads

$$P_{2D}(\mathbf{x}, \omega) = 2 \oint_C w(\mathbf{x}_0) j k_n^P(\mathbf{x}_0) P_{2D}(\mathbf{x}_0, \omega) G_{2D}(\mathbf{x} - \mathbf{x}_0, \omega) dC, \quad (\text{D.1})$$

with in the present case $P_{2D}(\mathbf{x}, \omega) = G_{2D}(\mathbf{x} - \mathbf{x}_s, \omega)$. The equality holds within the validity of the stationary phase approximation.

As a first step assume, that in three dimensions, the sound field of a vertical line source is to be described at $z = 0$ in terms of the 3D Green's function. The equation can be rewritten as

$$P_{2D}(\mathbf{x}, \omega) = 2 \oint_C w(\mathbf{x}_0) j k_n^P(\mathbf{x}_0) P_{2D}(\mathbf{x}_0, \omega) \int_{-\infty}^{\infty} G_{3D}(\mathbf{x} - \mathbf{x}_0, \omega) dz_0 dC. \quad (\text{D.2})$$

The inner integral can be approximated by the SPA with the stationary point lying trivially at $z = 0$, resulting in the approximation of the 2D Green's function presented in equation (2.52):

$$P_{2D}(\mathbf{x}, \omega) = 2 \oint_C w(\mathbf{x}_0) j k_n^P(\mathbf{x}_0) P_{2D}(\mathbf{x}_0, \omega) \sqrt{\frac{2\pi|\mathbf{x} - \mathbf{x}_0|}{jk}} G_{3D}(\mathbf{x} - \mathbf{x}_0, \omega) dC. \quad (\text{D.3})$$

Now assume, that instead of a 2D point source, a 3D point source is to be described by (D.3). Since the integral holds only for two dimensional sound fields the 3D field has to be formulated in terms of a 2D sound field with appropriate correction factors. Since P is the sound field of a point source in 2 or 3 dimensions

$$P_{2D}(\mathbf{x}, \omega) = \sqrt{\frac{2\pi|\mathbf{x} - \mathbf{x}_s|}{jk}} P_{3D}(\mathbf{x}, \omega), \quad P_{2D}(\mathbf{x}_0, \omega) = \sqrt{\frac{2\pi|\mathbf{x}_0 - \mathbf{x}_s|}{jk}} P_{3D}(\mathbf{x}, \omega) \quad (\text{D.4})$$

holds. Rewriting (D.3) in terms of the 3D field variables

$$\sqrt{\frac{2\pi|\mathbf{x} - \mathbf{x}_s|}{jk}} P_{3D}(\mathbf{x}, \omega) = 2 \oint_C w(\mathbf{x}_0) j k_n^P(\mathbf{x}_0) \sqrt{\frac{2\pi|\mathbf{x}_0 - \mathbf{x}_s|}{jk}} P_{3D}(\mathbf{x}_0, \omega) \sqrt{\frac{2\pi|\mathbf{x} - \mathbf{x}_0|}{jk}} G_{3D}(\mathbf{x} - \mathbf{x}_0, \omega) dC. \quad (D.5)$$

Finally, simplification and rearrangement leads to the 2.5D formulation of the Kirchhoff integral for the special case of a describing a 3D point source

$$P_{3D}(\mathbf{x}, \omega) = 2 \oint_C w(\mathbf{x}_0) j k_n^P(\mathbf{x}_0) \sqrt{\frac{2\pi|\mathbf{x} - \mathbf{x}_0|}{jk}} \sqrt{\frac{|\mathbf{x}_0 - \mathbf{x}_s|}{|\mathbf{x} - \mathbf{x}_s|}} P_{3D}(\mathbf{x}_0, \omega) G_{3D}(\mathbf{x} - \mathbf{x}_0, \omega) dC. \quad (D.6)$$

The horizontal stationary position for the integral is then found, where $|\mathbf{x} - \mathbf{x}_s| = |\mathbf{x} - \mathbf{x}_0(\mathbf{x})| + |\mathbf{x}_0(\mathbf{x}) - \mathbf{x}_s|$ is satisfied.

Bibliography

- [AB86] J.M. Arnold and B.Eng. "Geometrical theories of wave propagation: a contemporary review". In: *IEE Proceedings J - Optoelectronics* 133.2 (1986), pp. 165–188 (cit. on p. 26).
- [Ahr+13] J. Ahrens, M. Thomas, and I. Tashev. "Efficient Implementation of the Spectral Division Method for Arbitrary Virtual Sound Fields". In: WASPAA. New Paltz, NY, USA, 2013 (cit. on p. 59).
- [Ahr10] J. Ahrens. "The Single-layer Potential Approach Applied to Sound Field Synthesis Including of Non-enclosing Distributions of Secondary Sources". PhD thesis. Technischen Universitat Berlin, 2010 (cit. on pp. 8, 43, 55, 58).
- [Ahr12] J. Ahrens. *Analytic Methods of Sound Field Synthesis*. 1st. Berlin: Springer, 2012 (cit. on pp. 1, 8, 10, 12, 43, 55, 56).
- [Arn95] J.M. Arnold. "Phase-space localization and discrete representations of wave fields". In: *Journal of Optical Society of America* 12.1 (1995), pp. 111–123 (cit. on pp. 37, 38).
- [AS08] J. Ahrens and S. Spors. "An Analytical Approach to Sound Field Reproduction Using Circular and Spherical Loudspeaker Distributions". In: *Acta Acus. Utd. With Acust.* 94 (2008), pp. 988–999 (cit. on p. 55).
- [AS09a] J. Ahrens and S. Spors. "An analytical approach to 2.5D sound field reproduction employing circular distributions of non-omnidirectional loudspeakers". In: *IEEE 17th European Signal Processing Conference*. Glasgow, 2009 (cit. on p. 55).
- [AS09b] J. Ahrens and S. Spors. "On the Secondary Source Type Mismatch in Wave Field Synthesis Employing Circular Distributions of Loudspeakers". In: *Proc. of the 127th Audio Eng. Soc. Convention*. New York, 2009 (cit. on p. 55).
- [AS10a] J. Ahrens and S. Spors. "Sound Field Reproduction Using Planar and Linear Arrays of Loudspeakers". In: *IEEE Trans. Audio, Speech, Lang. Process.* 18.8 (2010), pp. 2038–2050 (cit. on pp. 12, 56).
- [AS10b] J. Ahrens and S. Spors. "Applying the Ambisonics Approach on Planar and Linear Arrays of Loudspeakers". In: *Proc. of the 2nd International Symposium on Ambisonics and Spherical Acoustics*. Paris, France, 2010 (cit. on p. 56).
- [AS11] J. Ahrens and S. Spors. "An analytical approach to local sound field synthesis using linear arrays of loudspeakers". In: *IEEE International Conference on Acoustics, Speech and Signal Processing (ICASSP)*. 2011 (cit. on p. 56).
- [AS12] J. Ahrens and S. Spors. "Applying the Ambisonics Approach to Planar and Linear Distributions of Secondary Sources and Combinations Thereof". In: *Acta Acus. Utd. With Acust.* 98 (2012), pp. 28–36 (cit. on p. 56).

- [AW05] G.B. Arfken and H.J. Weber. *Mathematical Methods for Physicists*. Elsevier, 2005 (cit. on pp. 2, 56).
- [Bai92] Mingsian R. Bai. "Application of BEM (boundary element method)-based acoustic holography to radiation analysis of sound sources with arbitrarily shaped geometries". In: *J. Acoust. Soc. Am.* 92.1 (1992) (cit. on p. 15).
- [Ben+08] Jacob Benesty, M. Mohan Sondhi, and Yiteng Huang, eds. *Springer Handbook of Speech Processing*. Springer, 2008 (cit. on p. 28).
- [Ben+85] J.C. Bennett, K. Barker, and F.O. Edeko. "A New Approach to the Assessment of Stereophonic Sound System Performance". In: *Journal of Audio Engineering Society* 33.5 (1985), pp. 314–321 (cit. on p. 28).
- [Ber+93] A.J. Berkhout, D. de Vries, and P. Vogel. "Acoustic Control by wave field synthesis". In: *J. Acoust. Soc. Am.* 93.5 (1993), pp. 2764–2778 (cit. on p. 51).
- [Ber84] A.J. Berkhout. *Seismic Migration: Imaging of Acoustic Energy by Wavefield Extrapolation*. 2nd edition. Elsevier, 1984 (cit. on p. 20).
- [Ber93] L. L. Beranek. *Acoustics*. Acoustical Society of America, 1993 (cit. on p. 2).
- [BG04] T. D. Carozzi A. M. Buckley and M. P. Gough. "Instantaneous local wave vector estimation from multi-spacecraft measurements using few spatial points". In: *Annales Geophysicae* 22 (2004), pp. 2633–2641 (cit. on p. 23).
- [BH75] N. Bleistein and R. A. Handelsman. *Asymptotic Expansions of Integrals*. 1st. Dover Publications, 1975 (cit. on pp. 31, 32).
- [Bla00] D. T. Blackstock. *Fundamentals of Physical Acoustics*. John Wiley & Sons, 2000 (cit. on pp. 2, 4).
- [Ble+00] N. Bleistein, J.K. Cohen, and J.W. Stockwell Jr. *Mathematics of Multidimensional Seismic Imaging, Migration, and Inversion*. Springer, 2000 (cit. on pp. 30, 33, 39).
- [Ble84] N. Bleistein. *Mathematical Methods for Wave Phenomena*. Academic Press, 1984 (cit. on pp. 26, 30, 32).
- [Bou+97] Daniel Bouche, Frédéric Molinet, and Raj Mittra. *Asymptotic Methods in Electromagnetics*. Springer, 1997 (cit. on pp. 36, 68).
- [BW70] Max Born and Emil Wolf. *Principles of Optics - Electromagnetic Theory of Propagation, Interference and Diffraction of Light*. Fourth Edition. Pergamon Press, 1970 (cit. on pp. 36, 68).
- [CH62] R. Courant and D. Hilbert. *Methods of Mathematical Physics Volume II*. Wiley, 1962 (cit. on p. 18).
- [Cop68] Lawrence G. Copley. "Fundamental Results Concerning Integral Representations in Acoustic Radiation". In: *J. Acoust. Soc. Am.* 44.1 (1968), pp. 28–32 (cit. on p. 17).
- [DeS92] John A. DeSanto. *Scalar Wave Theory: Green's Functions and Applications*. 1st. Berlin: Springer, 1992 (cit. on p. 12).
- [Dev12] A. J. Devaney. *Mathematical Foundations of Imaging, Tomography and Wavefield Inversion*. Cambridge University Press, 2012 (cit. on pp. 6, 12).
- [Duf01] D. G. Duffy. *Green's Functions with Applications*. Chapman and Hall, 2001 (cit. on p. 12).

- [EG04] T.M. Elfouhaily and C.A. Guerin. "A critical survey of approximate scattering wave theories from random rough surfaces". In: *Waves in Random Media* 14.4 (2004) (cit. on p. 30).
- [Faz10] F. M. Fazi. "Sound Field Reproduction". PhD thesis. University of Southampton, 2010 (cit. on pp. 19, 55).
- [Fir+17] G. Firtha, P. Fiala, F. Schultz, and S. Spors. "Improved Referencing Schemes for 2.5D Wave Field Synthesis Driving Functions". In: *IEEE/ACM Trans. Audio, Speech, Lang. Process.* 25.5 (2017), pp. 1117–1127 (cit. on pp. 52, 60).
- [FN13] F.M. Fazi and P.A. Nelson. "Sound field reproduction as an equivalent acoustical scattering problem". In: *J. Acoust. Soc. Am.* 134.5 (2013), pp. 3721–3729 (cit. on p. 19).
- [FR14] P. Fiala and P. Rucz. "NiHu: An open source C++ BEM library". In: *Advances in Engineering Software* 75 (2014), pp. 101–112 (cit. on p. 18).
- [GD04] N. A. Gumerov and R. Duraiswami. *Fast Multipole Methods for the Helmholtz Equation in Three Dimensions*. Elsevier, 2004 (cit. on pp. 1, 11).
- [Gib08] W. C. Gibson. *The Method of Moments in Electromagnetics*. Chapman & Hall, 2008 (cit. on p. 12).
- [Gir+01] B. Girod, R. Rabenstein, and A. Stenger. *Signals and Systems*. Wiley, 2001 (cit. on p. 56).
- [Gol05] Ron Goldman. "Curvature formulas for implicit curves and surfaces". In: *Computer Aided Geometric Design* 22.7 (2005), pp. 632–658 (cit. on p. 26).
- [Har01] Erich Hartmann. "The normalform of a space curve and its application to surface design". In: *The Visual Computer* 17.7 (2001), pp. 445–456 (cit. on pp. 26, 75).
- [Har99] Erich Hartmann. "On the curvature of curves and surfaces defined by normal-forms". In: *Computer Aided Geometric Design* 16.5 (1999), pp. 355–376 (cit. on pp. 26, 75).
- [Hav+08] David Havelock, Sonoko Kuwano, and Michael Vorländer, eds. *Handbook of Signal Processing in Acoustics*. Vol. Volume 1. Springer, 2008 (cit. on p. 27).
- [Her+03] D. W. Herrin, F. Martinus, T. W. Wu, and A. F. Seybert. "A New Look at the High Frequency Boundary Element and Rayleigh Integral Approximations". In: *SAE Technical Paper*. SAE International, May 2003 (cit. on p. 30).
- [How07] M.S. Howe. *Hydrodynamics and Sound*. Cambridge University Press, 2007 (cit. on pp. 4, 14).
- [Jen+07] Finn B. Jensen, William A. Kuperman, Michael B. Porter, and Henrik Schmidt. *Computational Ocean Acoustics*. Ed. by William H. Hartmann. Springer, 2007 (cit. on p. 4).
- [Kel67] Oliver Dimon Kellogg. *Foundations of Potential Theory*. Frederick Ungar Publishing Company, 1967 (cit. on p. 18).
- [Kin+00] L.E. Kinsler, A.R. Frey, and A.B. Coppens. *Fundamentals of Acoustics*. 4th. Wiley and Sons, 2000 (cit. on pp. 4, 25).
- [Kir07] Stephen Kirkup. *The Boundary Element Method in Acoustics*. Journal of Computational Acoustics, 2007 (cit. on p. 15).

- [Koy+14] Shoichi Koyama, Kenichi Furuya, Yusuke Hiwasaki, Yoichi Haneda, and Yoiti Suzuki. "Wave Field Reconstruction Filtering in Cylindrical Harmonic Domain for With-Height Recording and Reproduction". In: *IEEE/ACM TRANSACTIONS ON AUDIO, SPEECH, AND LANGUAGE PROCESSING* 22.10 (Oct. 2014), pp. 1546–1557 (cit. on p. 55).
- [Lal68] É. Lalor. "Inverse Wave Propagator". In: *Journal of Mathematical Physics* 9.12 (1968), pp. 2001–2006 (cit. on p. 56).
- [Lig52] Michael James Lighthill. "On sound generated aerodynamically I. General theory". In: *Proceedings of the Royal Society A* 211.1107 (1952), pp. 564–587 (cit. on p. 4).
- [Lig54] Michael James Lighthill. "On sound generated aerodynamically II. Turbulence as a source of sound". In: *Proceedings of the Royal Society A* 222.1148 (1954), pp. 1–32 (cit. on p. 4).
- [MF53] P.M. Morse and H. Feshbach. *Methods of Theoretical Physics*. Vol. Vol.I. McGraw-Hill Book Company Inc., 1953 (cit. on p. 55).
- [MI68] P. M. Morse and K. U. Ingard. *Theoretical Acoustics*. 1st. New York, NY: McGraw-Hill Book Company, 1968 (cit. on p. 2).
- [MN08] Steffen Marburg and Bodo Nolte, eds. *Computational Acoustics of Noise Propagation in Fluids - Finite and Boundary Element Methods*. Springer, 2008 (cit. on p. 15).
- [Moo90] F. Richard Moore. *Elements of Computer Music*. Prentice-Hall, Inc., 1990 (cit. on p. 28).
- [Olv+10a] F. W. J. Olver, D. W. Lozier, R. F. Boisvert, and C. W. Clark, eds. *NIST Handbook of Mathematical Functions*. Print companion to [NIST:DLMF]. New York, NY: Cambridge University Press, 2010 (cit. on p. 40).
- [Olv+10b] Frank W. J. Olver, Daniel W. Lozier, Ronald F. Boisvert, and Charles W. Clark. *NIST Handbook of Mathematical Functions*. 1. Cambridge University Press, 2010 (cit. on p. 12).
- [Pie91] A. D. Pierce. *Acoustics, An Introduction to its Physical Principles and Applications*. Acoustical Society of America, 1991 (cit. on pp. 4, 25).
- [Pig+15] N.J. Pignier, C.J. O'Reilly, and S. Boij. "A Kirchhoff approximation-based numerical method to compute multiple acoustic scattering of a moving source". In: *Applied Acoustics* 96 (2015), pp. 108–117 (cit. on p. 30).
- [Pol77] H.F. Pollard. *Sound Waves in Solids*. Law Book Co of Australasia, 1977 (cit. on p. 24).
- [PS02] R. Pike and P. Sabatier, eds. *Scattering: Scattering and Inverse Scattering in Pure and Applied Science*. Academic Press, 2002 (cit. on p. 30).
- [PT92] Allan D. Pierce and R.N. Thurston, eds. *High Frequency and Pulse Scattering*. Vol. XXI. Physical Acoustics. Academic Press, 1992 (cit. on p. 26).
- [Pul01a] Ville Pulkki. "Localization of Amplitude-Panned Virtual Sources I: Stereophonic Panning". In: *Journal of Audio Engineering Society* 49.9 (2001), pp. 739–752 (cit. on p. 28).
- [Pul01b] Ville Pulkki. "Spatial Sound Generation and Perception by Amplitude Panning Techniques". PhD thesis. Helsinki University of Technology, 2001 (cit. on p. 28).
- [Pul97] Ville Pulkki. "Virtual Sound Source Positioning Using Vector Base Amplitude Panning". In: *Journal of Audio Engineering Society* 45.6 (1997), pp. 456–466 (cit. on p. 28).

- [Roe05] H. Roemer. *Theoretical Optics: An introduction*. Wiley, 2005 (cit. on p. 23).
- [Rum01] Francis Rumsey. *Spatial Audio*. Focal Press, 2001 (cit. on p. 28).
- [SA10] S. Spors and J. Ahrens. "Analysis and Improvement of Pre-Equalization in 2.5-dimensional Wave Field Synthesis". In: *Proc. of the 128th Audio Eng. Soc. Convention*. London, 2010 (cit. on pp. 53, 60).
- [Sch16] Frank Schultz. "Sound Field Synthesis for Line Source Array Applications in Large-Scale Sound Reinforcement". PhD thesis. University of Rostock, 2016 (cit. on pp. 53, 60).
- [Sch92] S. H. Schot. "Eighty Years of Sommerfeld's Radiation Condition". In: *Sitoria Mathematica* 19 (1992), pp. 385–401 (cit. on p. 5).
- [SH11] Ivar Stakgold and Michael Holst. *Green's Function and Boundary Value Problems*. Third. Wiley, 2011 (cit. on p. 11).
- [SM93] B.Z. Steinberg and J.J. McCoy. "Marching acoustic fields in a phase space". In: *J. Acoust. Soc. Am.* 93.1 (1993), pp. 188–204 (cit. on p. 38).
- [Spo] S. Spors. "An Analytic Secondary Source Selection Criterion for Wavefield Synthesis". In: *in 33rd German Annual Conference on Acoustics (DAGA)* (cit. on p. 45).
- [Spo+08] S. Spors, R. Rabenstein, and J. Ahrens. "The Theory of Wave Field Synthesis Revisited". In: *Proc. of the 124th Audio Eng. Soc. Convention*. Amsterdam, 2008 (cit. on pp. 45, 52).
- [Spo05] S. Spors. "Active Listening Room Compensation for Spatial Sound Reproduction Systems". PhD thesis. Friedrich-Alexander-Universität Erlangen-Nürnberg, 2005 (cit. on pp. 8, 15, 44).
- [Spo07] S. Spors. "Extension of an Analytic Secondary Source Selection Criterion for Wave Field Synthesis". In: *Proc. of the 123rd Audio Eng. Soc. Convention*. New York, 2007 (cit. on p. 45).
- [SS14] F. Schultz and S. Spors. "Comparing Approaches to the Spherical and Planar Single Layer Potentials for Interior Sound Field Synthesis". In: *Acta Acus. Utd. With Acust.* 100 (2014), pp. 900–911 (cit. on pp. 19, 43, 55, 56).
- [SS16] F. Schultz and S. Spors. "On the Connections of Wave Field Synthesis and Spectral Division Method Plane Wave Driving Functions". In: *Proc. of 42nd DAGA*. Aachen, Germany, 2016 (cit. on p. 60).
- [Sta97] E.W. Start. "Direct sound enhancement by wave field synthesis". PhD thesis. Delft University of Technology, 1997 (cit. on pp. 51, 53).
- [TM05] I. Tinkelman and T. Melamed. "Local spectrum analysis of field propagation in an anisotropic medium. Part I. Time-harmonic fields". In: *Journal of Optical Society of America* 22.6 (2005), pp. 1200–1207 (cit. on pp. 37, 38).
- [Tra+14] E.R. Tracy, A.J. Brizard, A.S. Richardson, and A.N. Kaufman. *Ray tracing and beyond: Phase Space Methods in Plasma Wave Theory*. Cambridge University Press, 2014 (cit. on p. 62).
- [Tsa+00] L. Tsang, J.A. Kong, and K. Ding. *Scattering of Electromagnetic Waves: Theory and Applications*. Wiley and Sons, 2000 (cit. on p. 29).
- [Ver97] E.N.C. Verheijen. "Sound Reproduction by Wave Field Synthesis". PhD thesis. Delft University of Technology, 1997 (cit. on pp. 51, 53).

- [Vor07] A.G. Voronich. "Tangent Plane Approximation and Some of Its Generalizations". In: *Acoustical Physics* 53.3 (2007), pp. 298–304 (cit. on p. 29).
- [Vor99] A.G. Voronich. *Wave Scattering from Rough Surfaces*. 2nd. Vol. Springer Series on Wave Phenomea. Springer, 1999 (cit. on p. 29).
- [Wat15] K. Watanabe. *Integral Transform Techniques for Green's Function*. Second Edition. Springer, 2015 (cit. on p. 12).
- [WB89] C.P.A. Wapenaar and A.J. Berkhout. *Elastic Wave Field Extrapolation*. 2nd edition. Elsevier, 1989 (cit. on p. 17).
- [Wie14] H. Wierstorf. "Perceptual Assessment of Sound Field Synthesis". PhD thesis. Technischen Universitat Berlin, 2014 (cit. on p. 43).
- [Wil99] E. G. Williams. *Fourier Acoustics: Sound Radiation and Nearfield Acoustical Holography*. 1st. London: Academic Press, 1999 (cit. on pp. 1, 2, 5, 7, 8, 10, 11, 15, 16, 18, 32, 40, 56, 57).
- [Wu10] Sean F. Wu. "Techniques for Implementing Near-Field Acoustical Holograph". In: *SOUND & VIBRATION* 44.2 (2010), pp. 12–16 (cit. on p. 15).
- [Zio95] L. J. Ziomek. *Fundamentals of Acoustic Field Theory and Space-Time Signal Processing*. Boca Raton, 1995 (cit. on p. 4).
- [Zot09] F. Zotter. "Analysis and Synthesis of Sound-Radiation with Spherical Arrays". PhD thesis. Institute of Electronic Music, Acoustics University of Music, and Performing Arts, 2009 (cit. on pp. 10, 55).
- [ZS13] F. Zotter and S. Spors. "Is sound field control determined at all frequencies? How it is related to numerical acoustics?" In: *Proc. of the AES 52nd International Conference*. Guildford, UK, 2013 (cit. on pp. 19, 45, 55).